2015

# Short Wave Infrared Imaging System for Night and Day Long Range Facial Recognition and Surveillance

Robert B. Martin

# Short Wave Infrared Imaging System for Night and Day Long Range Facial Recognition and Surveillance

**Robert B. Martin**

**Thesis submitted**
**to the Benjamin M. Statler College**
**of Engineering and Mineral Resources**
**at West Virginia University**

**in partial fulfillment of the requirements for the degree of**

**Master of Science in**
**Electrical Engineering with Electronics and Photonics Concentration**

**Jeremy Dawson, Ph. D., Chair**
**Lawrence Hornak, Ph. D.**
**Thirimachos Bourlai, Ph. D.**
**Brian Lemoff, Ph. D.**

**Department of Electrical Engineering**

**Morgantown, West Virginia**
**2015**

**Keywords: SWIR, Biometrics, Facial Recognition, Surveillance**

# ABSTRACT

## Short Wave Infrared Imaging System for Night and Day Long Range Facial Recognition and Surveillance

**Robert B. Martin**

The capability to detect, observe, and positively identify people at a distance is important to numerous security and defense applications. Traditional solutions for human detection and observation include long-range visible imagers for daytime and thermal infrared imagers for night-time use. Positive identification, through computer face recognition, requires facial imagery that can be repeatably matched to a database of visible spectrum facial mug shots. Nighttime identification at large distances is not possible with visible imagers due to lack of light, or with thermal infrared imagers due to poor correlation with visible facial imagery. An active-SWIR imaging system was developed that is eye-safe, invisible, and capable of producing close-up facial imagery at distances of several hundred meters and full body images to thousands of meters, even in total darkness. The SWIR images correlate well to the visible spectrum allowing for biometric facial recognition and long range target detection either day or night. The process of researching existing technologies, establishing requirements of a suitable system, design process, and hardware implementation will be discussed in great detail. Once the system is assembled, it will be used to acquire data not yet produced by any existing technology. The results will be examined and a discussion made into future work.

## Acknowledgements

I would like to thank my committee members Dr. Jeremy Dawson, Dr. Lawrence Hornak, Dr. Thirimachos Bourlai, and Dr. Brian Lemoff for the mentoring and direction they provided during my post graduate work. I would like to especially thank Dr. Dawson for the extra guidance given during this process. His contribution means more than he probably will ever know. Without Dr. Lemoff's strong dedication to his work, I would not have this opportunity of furthering my education. And for that, I am deeply grateful.

I would like to thank my colleagues at the West Virginia High Technology Foundation Consortium. Specifically, I would like to thank staff members Robert Ice, Mikhail Sluch, William McCormick, Kris Kafka and Jason Stanley for their efforts on the project. Without them, my portion of work would not be possible. I would also like to thank Jordan Martin and Andrew Dolby for their work. While their time on the project was much shorter, their contributions were just as crucial to the completed task. I would like to thank the MorphoTrust USA team and Aces & Eights in the collaboration efforts. I would also like to thank the Foundation's CEO Jim Estep for giving me this unique opportunity and supporting me as an employee/student.

This research was performed under contract N00014-09-C-0064 from the Office of Naval Research, with funding from the Deployable Force Protection Science and Technology Program, and with additional support from a subcontract from West Virginia University Research Corporation through Award No. 2010-DD-BX-0161 awarded by the National Institutes of Justice.

Lastly, I would like to thank my family for being with me through this process. My life has changed immensely since it started and they have kept me strong throughout. My mother most of all gets my deepest gratitude.

# Table of Contents

# List of Figures

# List of Tables

# 1 Introduction

## 1.1 Background

Long range imaging is a valuable tool for many surveillance applications. Detection and identification of humans and other targets of interest with maximum standoff distances is normally favorable. Agencies in defense, law enforcement, and private security often times require systems to operate 24 hours a day which produces the challenge of imaging under night time light levels or otherwise dark conditions. A robust system is favorable that will allow the user to detect, identify, and track a target of interest under any atmospheric condition, whether day or night, and at the maximum possible distance while remaining completely undetected.

When discussing imaging, the first manner that comes to mind is the visible spectrum where the human eye has sensitivity. These visually pleasing color images are in the wavelength range of between 380nm and 800nm depending on the individual's eye. Equipment for acquiring these images is very inexpensive and readily available as it is widely used anywhere from cell phone cameras to normal closed circuit television (CCTV) surveillance systems. For adequate acquisition, one of two lighting options must be utilized when operating during night time conditions. First, local illumination such as street lamps can be used as passive source. The need for illumination limits the operator as to where the system can be positioned. The target, if desiring to go undetected, will be avoiding the well-lit areas. The second method for imaging under low light conditions is producing an active illumination. This is typically seen as the flash on normal cameras or constant spotlight originating near the imager. This method has two main draw backs. To ensure the target is not harmed during imaging, illuminating with an eye safe amount of light must be done at all times. This limits the distance in which a visible spectrum, actively illuminated system can function. Also, when the source is producing a large amount of light, the system cannot go undetected.

Many systems exist that utilize near infrared (NIR) technology. Operation is typically accomplished in the 800nm to 900nm range. Typical silicon imagers are sensitive in this range; however, the human eye cannot detect this illumination. This band has its advantages because it can use the inexpensive imaging technology while remaining covert to the unaided human eye. Also, as wavelength increases past the visible band, the amount of illumination intensity allowable while remaining eye safe also increases. This in turn increases the sensor standoff distance. Typical illumination sources come in the form of a light emitting diode (LED) array. The close proximity to the visible band also produces imagery that is very recognizable to the operator.

Increasing in wavelength, short wave infrared (SWIR) is the next band of interest. It spans from approximately 1.0 μm to 1.7 μm. Images start to deviate from their appearance in the visible band, but are still recognizable with little experience. Passive SWIR imaging is very useful for outdoor surveillance when looking at wide angles of view[1]. Ambient solar glow proves to be sufficient on clear to partly cloudy nights to produce an adequate scene view. However, on cloudy nights or when dealing with narrow angles of view, supplemental illumination needs to be provided. Illuminating at this band again has a great advantage as it is even further from the human eye's sensitivity band allowing for a much greater intensity while maintaining eye safety.

Focal plane technology also increases in cost within this band. Typical silicon arrays are completely insensitive here requiring the use of the much more expensive InGaAs technology. An actively illuminated system operating in this band can be considered completely covert. This system would be invisible to typical cameras and even night vision goggles (NVG).

Long wave infrared (LWIR) or "thermal" infrared is the next band in increasing wavelength used for imaging. Applications in this region are typically implemented between 7.0 μm and 14 μm. In opposition to the previous bands discussed, thermal imaging relies on the emissions from the target. Thermal imaging is very good for the detection of people and other objects of large temperature differential from the background such as vehicles. Table 1 illustrates the comparison between each band.

**Table 1 Imaging Technology Comparison**

**A tabulated assessment of imaging spectral bands versus a four main design constraints.**

| Wavelength | Human Eye Sensitivity | Conventional Camera Sensitivity | NVG Sensitivity | Relative Technology Cost |
|---|---|---|---|---|
| **Visible** | Fully Visible | With illumination | Visible | Low |
| **NIR** | Dull Red | With illumination | Visible | Low |
| **SWIR** | Invisible | Invisible | Invisible | High |
| **LWIR** | Invisible | Invisible | Invisible | Med |

Standoff distance greatly affects what is acquired by the operator. Image quality degrades as distance increases. This is due to many factors such as the system's resolution. As with any optical system, objects will reduce in size as the target distance increases. This means each object will occupy fewer pixels on the detector and thereby losing key features as distance increases. To combat this, optical systems implement zoom. While increasing feature size is beneficial for object detection, it also decreases the amount of light collected due to the smaller acceptance angle. This unfortunately decreases the signal-to-noise ratio again degrading the image. Atmospheric conditions also play a part in standoff imaging. The greater the distance between the object and the detector means a greater chance of interferences. These interferences may be humidity, precipitation, and turbulence that may spoil the image.

Facial recognition systems operating in the visible spectrum have become a very robust technology. These systems are used in many areas such as military and law enforcement to make initial identification of unknown targets. Typical functionality includes an input probe image to be submitted or matched to a pre-populated gallery of mug shots. Facial recognition is also being used in consumer level projects such as photograph organization for sorting individuals into folders.

Facial recognition becomes difficult when you move outside of the visible spectrum. Most typical applications require the input image from your sensor to be matched against an existing gallery of persons' of interest. This operation outside of the visible spectrum requires the matching of two images that do not look the same in some ways to operator. Operation in the NIR, however, is not greatly challenging. Here images simply look like the grayscale version of the same visible spectrum individual. The operator can make manual matches based on the strong correlation between the NIR image they are acquiring and the visible image they are used to seeing.

Facial recognition performed in the SWIR band is not an established field. The human face begins to take on different characteristics when compared to the same individual viewed from the visible band. Certain features such as the large amount of skin absorption, lack of pupil, and high reflection of the human hair make a familiar individual unrecognizable to an untrained operator. Similarly, matching SWIR probe images against a visible spectrum gallery in a commercially available facial recognition system will give poor results. Figure 1 illustrates facial imagery in the visible, NIR, and SWIR bands.

**Figure 1 Multi-Band Imaging.**

**Photographs of the same individual acquired in the visible, NIR (850nm), SWIR (>1,400nm), and LWIR (7.5µm-15µm) bands respectively.**

Facial recognition in the LWIR band proves to be the most difficult of those discussed. To date, very little research has been performed to match thermal images to a gallery composed of visual spectrum mug shots. Despite the fact that thermal images already differ greatly from their visible counterpart, they also suffer from variability due to atmospheric conditions and the individual's mood[2]. This means the same person can be imaged multiple times, under different conditions, and give vastly diverse signatures. This proves difficult for repeatable facial recognition.

With these considerations in mind, an actively illuminated SWIR system is the best option to detect, identify, and track at long standoff distances. Operation in the SWIR band will allow for completely covert operation unlike visible and NIR bands. The active illumination tackles the issue of darkness while maintaining a higher amount of eye safety when compared to the visible spectrum. Although larger and more expensive than most thermal infrared imaging systems, this SWIR unit will produce narrow angle images that will give greater detail of objects. It will also give suitable facial recognition imagery without atmospheric or individual mood variability.

## 1.2 Research Goals

The focus of this research is to test SWIR facial recognition. Gathering information about the technology and existing systems is essential to developing a starting point. If it is discovered that no platform currently exists that can produce such imagery, one will have to be developed. The main task will be to construct an actively illuminated SWIR imaging platform that will give the operator the ability to detect, identify, and track a person at a standoff distance. The system should be able to make a positive identification via facial recognition at a distance of up to 400 meters at both day and night. The system should also be able to detect a person at a range of up to 3,000 meters at night and past that distance during the day. While performing these tasks, a useful system will also need to exhibit many other characteristics such as being covert and maintaining the greatest distance between the operator and the

target. The system must be robust both in hardware and the ability operate under varying environmental conditions. The system must be portable and easy to use. It must be safe; both for the operator and for the target of interest. Once the system is developed, it will be necessary to test its functionality and methods for implementation in multiple applications will be explored.

## 1.3 Research Tasks

The first step in this process is to research existing technologies. Can a system be purchased to meet the aforementioned goals? If not, planning is needed to produce a system capable of accomplishing this task. Then production of this imagery is initiated by the identification of each necessary component used to assemble the imaging platform. Researching established techniques for typical camera lenses, automatic motion systems, and military deployable systems drive many of the design considerations. First, a lens system is needed. This is accomplished through optical modeling and collaboration with a lens manufacturer. Once received, the lenses will need to be mounted and put into motion. Solid modeling is implemented in this step to conceptualize the parts before fabrication. The models can then be submitted for manufacture. Supporting functions must be defined and the electronic devices capable of these tasks must be purchased. Software must be developed that will control everything including lens motion, supporting electronics, facial recognition, and post processing. All parts must then be combined into a man-portable, environmentally protected system.

The hardware system will then be tested through data collections and field demonstrations. Facial recognition performance can then be tested. The results will be compared to commercially available products. Any improvements necessary will be implemented accordingly.

## 1.4 Completed Tasks

Along with other team members from the West Virginia High Technology Consortium Foundation (WVHTCF), a system was produced to meet the aforementioned goals. Throughout this paper it will be designated with the proper name the "System." Personally, my contributions to this project were:

- Task 1: Research, design, and model. I gathered data about the problem and researched whether any existing technologies would fulfill these tasks. I received the lens model and created a mounting scheme that satisfied all specifications. Through solid model design, I was able to design and submit for manufacture parts of the System.
- Task 2: System fabrication and assembly. Once received, I was able to assemble the parts, troubleshoot, and make the proper changes to produce a working laboratory prototype. I found and purchased many devices to be placed into the system that allowed all functions to be performed. I produced a software program that was the first step in the development of an autonomous system. I was then able to audit this system and decide where improvements could be made in size, weight, and performance. I was able to develop the hardware of a complete second generation system. This unit became smaller, man-portable, user friendly, and environmentally sealed.
- Task 3: System Testing and Optimization. I have taken both units offsite to many exercises for the purpose of gathering data. These results have been used both in-house and shared with partners for system optimization. Conference presentations have been made to share the knowledge gained by this research effort[3,4,5,6,7].

# 2 Theory

## 2.1 Gaussian Beam Optics

One of the many components that will go into the assembly of a system capable of producing SWIR imagery for facial recognition is the required illumination. While the discusion of the selection of an actual illumination source will be covered in Section 3.2.1, here the assumption will be made that a highly coheret, laser-like source will be used. For this reason, a general understanding was necessary for the design and assembly of the required components.

The source chosen and discused in Section 3.2.1 is fiber coupled and at many points exibits the traits of a Gausian beam. Specifically that means the beam power is concentrated tightly around the optical axis, the profile of the beam is symetrical about the optical axis, there is a minimum size (waist) at which the beam gradually increasing on either side, and the wavefront normals have the minimum value allowed by the wave equation. This Gausian profile is of most interest at the free space filter. Here, the orginal source is launced from the single mode fiber, directed through a band pass filter, and then refocused onto a single mode fiber.

The complex amplitude of a Gausian beam is characterized by the expression below and from it many important evaluations can be drawn.

$$U(r) = A_0 \frac{W_0}{W(z)} \exp\left[-\frac{\rho^2}{W^2(z)}\right] \exp\left[-jkz - jk\frac{\rho^2}{2R(z)} + j\zeta(z)\right] \qquad (1)$$

$W_0$ and $z_0$ are two variables applicable to the illuminator design. As later discussed, a broad spectrum source will be selected where a narrow band will be necessary. For this reason, a filter must be employed. Where filtering options are available for fiber coupled systems, launching into free space, filtering, and re-coupling to a fiber is a quick and cost effective alternative. Given these factors, this option was chosen.

It would be desired to launch the illumination from the fiber in such a way that after passing through a lens system it is collimated. At this point, the understanding of the Gaussian beam comes into play. According to the following two equations and the subsequent illustration, the beam will have a minimum size called the waist. It is dependent on wavelength and focus length called the Rayleigh range.

$$W(z) = W_0\sqrt{1 + \left(\frac{z}{z_0}\right)^2} \qquad (2)$$

$$W_0 = \sqrt{\frac{\lambda z_0}{\pi}} \qquad (3)$$

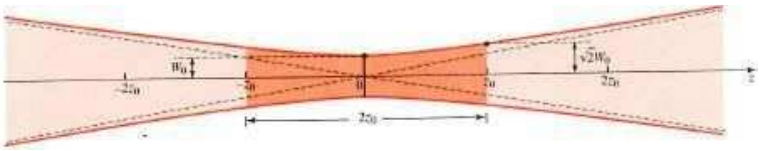

**Figure 2 Depth of Focus of a Gaussian Beam[8].**

Calculations can then be performed to calculate the Rayleigh range with a given spot size. This is important in this application because the collimated beam will then need to be re-focused back into another fiber after filtering. The depth of focus is considered two times the Rayleigh range. A sample calculation is shown below with a corresponding collimating graded index (GRIN) collimator. Figure 3 gives specific characteristics of this collimator with the "beam diameter" being of most interest.

| GENERAL SPECIFICATIONS | | INDIVIDUAL SPECIFICATIONS | | PAIR SPECIFICATIONS | |
|---|---|---|---|---|---|
| CENTRAL WAVELENGTH | 1550 nm | BEAM DIAMETER | 0.5mm | WORKING DISTANCE | 15 +/-5 mm |
| COLLIMATOR BANDWIDTH | ± 30 nm | BEAM DIVERGENCE | 0.25° | | |
| MAX. TENSILE LOAD | 5 N | INSERTION LOSS | <0.1 dB** | | |
| OPERATING TEMPERATURE | -5 to 60°C | MIN. RETURN LOSS** | 60 dB | PAIR INSERTION LOSS* | <0.2 dB** |
| STORAGE TEMPERATURE | -40 to 85°C | MAX. OPTICAL POWER (CW) | 300 mW | | |
| | | RAYLEIGH LENGTH (TYP.) | 779mm | | |

**Figure 3 GRIN Collimator[9].**

The depth of focus is shown to be 1.013 meters. This can be found via a simple calculation given a wavelength of interest of 1,550 nm. This value is obviously much greater than necessary for the length of the filter assembly and will prove to be a more than adequate design constraint. However, if the waist was chosen to be that of the fiber at 10µm, it is seen that the depth of focus of 405.4µm is insufficient. This illustrates the necessity of the external optics.

$$2z_{0=}\frac{2\pi W_0^2}{\lambda} \qquad (4)$$

$$2z_{0=}\frac{2\pi 500\mu m^2}{1.55\mu m} = 1.013m$$

$$2z_{0=}\frac{2\pi 10\mu m^2}{1.55\mu m} = 405.4\mu m$$

## 2.2 Facial Recognition

As previously mentioned in Section 1.2, one of the main goals of the System is to acquire remote identifications of targets via facial recognition. This type of identification would match a single SWIR probe image against a pre-populated, visible spectrum gallery or database. Traditionally, the probe image is searched to find landmarks such as the eyes, nose, lips, jaw, or ears. These points are then saved and compared to the gallery where the points have already been extracted. The highest likely matches are the ones corresponding to greatest corresponding number of points to the gallery image. However, there are more complicated factors such as obstructions, head tilts and angles, and skin textures that force algorithms to adapt and become much more complex.

As discussed in Section 1, matching SWIR images to a database populated of visible band images, or "cross spectral matching," has its challenges. In Pan's paper[10], they put a value to the penetration depth of human skin as imaged at different wavelength. Optical penetration is shown as[10]:

$$1/\sqrt{3\mu_a\mu'_{s'}} \qquad (5)$$

where $\mu_a$ is and $\mu'_s$, are the absorption coefficient and reduced scattering coefficient of human tissue respectively. The decreased reflectance as wavelength increases matches with the dark skin tones seen in the SWIR human imagery.

Bourlai[11] describes using photometric normalization algorithms traditionally used for illumination variations to combat these cross spectral challenges. In his work, he describes in detail five specific methods: contrast limited adaptive histogram equalization (CLAHE), single scale retinex with logarithmic transformation (SSRlog), single scale retinex with arc-tangent transformation (SSRatan), SSRlog followed by CLAHE, and SSRatan followed by CLAHE. Once these preprocessing methods were applied, face and eye detection algorithms were used as described further by Bourlai's colleague Kalka[12]. Matching was accomplished using both commercially available and research produced facial recognition software packages and compared the results.

Chang[13] describes their research to fuse visible spectrum images to thermal band infrared images for the purpose of facial recognition. This method uses a discrete wavelet transform (DWT) that involves manipulating weighted coefficients depending on lighting conditions. During low light conditions, higher priority is given to the coefficients corresponding to the thermal band imagery and visa-versa for adequate lighting with respect to the visible band imagery. While this fusion is not directly applicable to the SWIR, the visible band cross spectral matching is of interest in this paper. It should be noted that their results conclude imagery with high-frequency content produced the highest rank matches. Looking back to the Bourlai and Kalka research and in particular the imagery comparing the preprocessing methods, this seems to coincide with their results also.

While the development of this type of software in-house is possible as described in Kalka's paper with the local binary patterns (LBP) and local ternary patterns (LTP), many commercial mature systems exist. One such package is called ABIS® System FaceExaminer[14] from MorphoTrust USA. This commercial of-the-shelf (COTS) package matches typical visible spectrum probe images against visible spectrum gallery images. A plugin was designed by MorphoTrust that applies pre-processing to the SWIR images produced by the System imager to match against the visible gallery.

Typical functionality of the System face recognition portion would be to submit a user defined number of probe SWIR images to be matched against the visible gallery. The software initially searches for eyes in each of the probes. If none are found or are improperly located, the user can manually input the proper locations. The matching is then initiated where each probe is compared against the gallery and given a match score. The results of all probes are then combined in a fusion scheme based on the highest scores. Finally, the most likely matches are ranked by scores from highest to lowest.

## 2.3 Laser Illumination Speckle

### 2.3.1 Speckle Background

Using narrow band lasers for illumination has advantages. Chromatic aberration can almost completely be neglected allowing for a much simpler and lighter lens design. However, the narrow band does produce one major disadvantage, speckle. Speckle is defined as the generation of a random intensity

distribution, called a speckle pattern, when light from a highly coherent source, such as a laser, is scattered by a rough surface or inhomogeneous medium[15].

Facial recognition relies heavily on landmark detection of the human face. When speckle is present, false positives are given usually resulting in improper placement of the eye markers. This has to be minimized for proper system operation. Figure 4 illustrates the highly coherent incident illumination with speckle very noticeable.

**Figure 4 Speckle.**

**Facial imagery showing the effects of highly coherent incident illumination distortion or "speckle."**

### 2.3.2 Types of Speckle

There are two main types of speckle that will be discussed in this section. First, the type of most concern to facial recognition is caused by the modal interference patterns of the multimode fiber (MMF). The second type is an interference pattern caused by imaging stationary targets.

#### *2.3.2.1 Multimode Fiber Induced Speckle*

Multimode fiber induced speckle is represented in Figure 4 as the large "blotchy" areas of high and low intensities. The interference pattern here is caused by the coherence of the modes of the fiber source. Any slight movement of the illumination fiber causes large displacement of these "blotches" on the image. This may seem like a problem, but later it will be described how to take advantage of this property.

As can be seen from the Figure 4 image, facial features become hard to distinguish. One eye has ample illumination while the other is very dark. Also, the nose and the lips are almost indistinguishable. The areas of high intensity prove problematic when trying to maintain the highest possible signal levels. These are the areas that will be limited by the eye safety constraints. If there is a large amount of speckle present, the intensity increases only in these certain areas. This will require the operator to reduce the output power to maintain the eye safety limits.

#### *2.3.2.2 Stationary Target Induced Speckle*

Stationary target induced speckle is produced when illuminating a stationary object. Here, coherent reflections interfere inhibiting the imager from resolving details below a certain size. This is illustrated in Figure 5. The USAF target is illuminated in the first picture with a continuous spectrum halogen lamp. The second image shows the same target being illuminated by a narrow band source. It can be seen that features below approximately 3 mm cannot be resolved with the exact same imaging equipment.

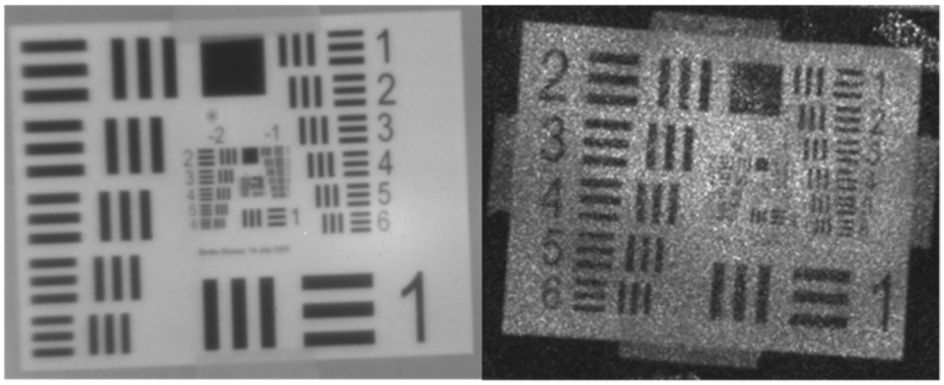

**Figure 5 USAF Target.**

**(left) Illuminated with an incandescent lamp. (right) Illuminated with a narrow band source.**

For the facial recognition application, this type of speckle is of no concern. The subjects of the System will always be in sufficient motion and have feature sizes much greater than those illustrated above.

### 2.3.3 Literature Review of Speckle Reduction

When approaching speckle reduction, most techniques will fall into one of the following categories[16]:

A. Control of spatial coherence
B. Control of temporal coherence
C. Spatial sampling
D. Spatial averaging
E. Digital signal processing

Parts A and B will also be evaluated experimentally in later sections. Spatial averaging and digital signal processing will not be discussed in this paper.

#### *2.3.3.1 Control of Spatial Coherence*

Control of spatial coherence involves controlling the signal at the source. As previously mentioned, small perturbations of the illuminator multimode fiber cause great effects on the output interference patterns. If one can perform this operation fast enough, i.e. greater than the frame rate of the imaging device, the modal speckle can be reduced.

This can be mechanically implemented in many ways, three of which are illustrated in Figure 6.

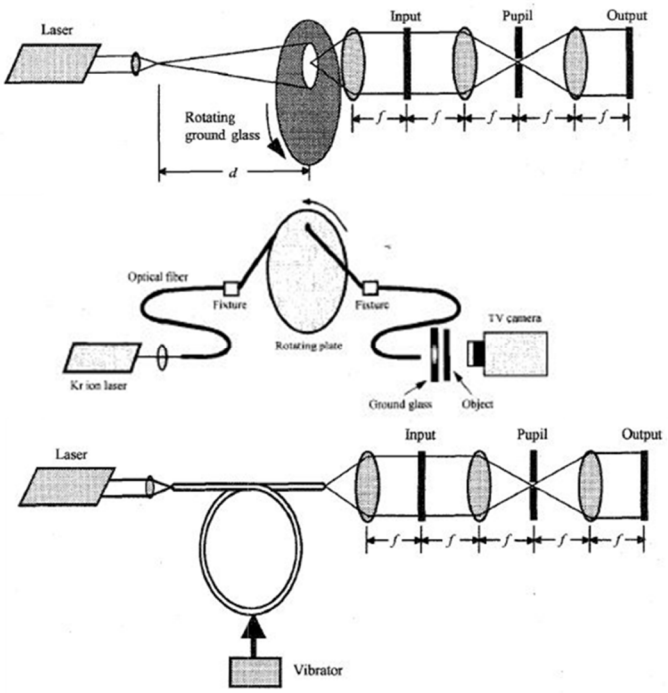


**Figure 6 Three Techniques for Spatial Coherence Control[11]**

**(top) Free space launch and rotation of an interference filter. (middle) Rotation of fiber. (bottom) Vibration of fiber.**

These techniques may seem crude or rudimentary, however there are industry standards using the vibrator method. For instance, IEEE 802.3aq and FOTP 203 call for mechanical vibration of three "figure-of-eight" elements. A commercially available unit can be purchased to comply with these standards[17].

#### *2.3.3.2 Control of Temporal Coherence*

Like the aforementioned method, control of temporal coherence involves manipulating the source. Alternatively, this method involves varying the illumination wavelength with respect to time. This method basically integrates time average of multiple speckle patterns giving a virtual speckle reduction. Temporal coherence is more so a function of swept spectral width and less sweep frequency. This means the wider the band, the smaller amount of speckle will be present. A sweep frequency much greater than the imager frame rate is necessary to decrease the coherence received by each pixel.

#### *2.3.3.3 Spatial Sampling*

Unlike the previous two methods, spatial sampling can be implemented at the image plane. Multiple independent speckle patterns are produced by rotating circular aperture or random mask at the Fourier transform plane. Speckle reduction is then accomplished by the time average of these patterns. It has been claimed that through these methods the stationary target induced speckle discussed in Section 2.3.2.2 can be completely reduced[16].

As mentioned, this type of speckle is not an issue for the System; however, future applications may dictate this implementation to be necessary. While retrofitting the system with a rotating aperture or 4f optical system may not be difficult, it would add mechanical motion near the imager producing unwanted vibrations. Figure 7 illustrates an example of the 4f system with rotating aperture.

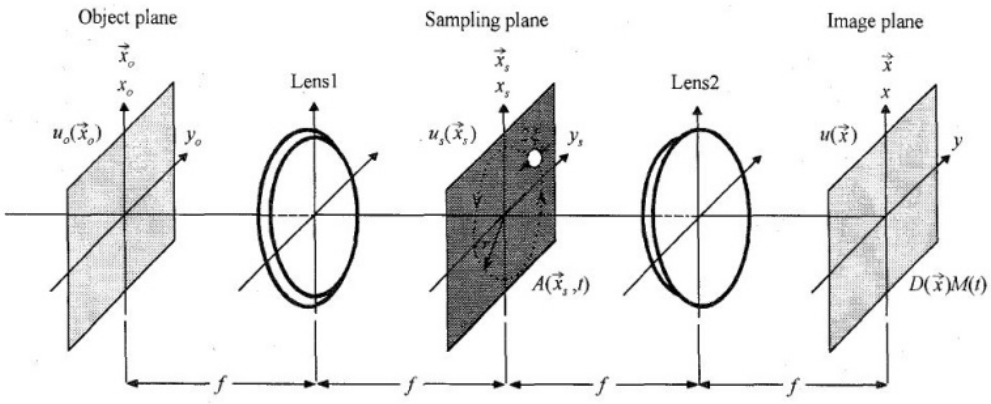


**Figure 7 4f Optical System with Rotating Aperture[11].**

## 2.4 Eye Safety

Anytime human subjects are involved it is very important to maintain their absolute safety. The System produces diverging laser illumination. For this reason, it is necessary to know exactly what the allowable intensity is to maintain eye safety. As defined in the ANSI Z136 and IEC 60825 laser eye safety standards[18,19], the System must maintain Class 1M specifications at the output lens and Class 1 at the target at all times. Class 1M states that there is no hazard to the naked eye. However, there does exist a potential hazard if magnifying optics are used. Typically binoculars or scopes are the optics of concern. Class 1 illumination is safe even under optical magnification up to seven times.

Calculations can be performed at any given wavelength to find the allowable intensity levels. The calculations below will illustrate the advantages of moving as far away from the visible spectrum as possible. Three tables are necessary from the IEC 60825 to find the allowable intensity levels. These can be found in Appendix 6.1.1 and in the text below.

For example, the following is the process to find the allowable intensity level at a wavelength of 800 nm and at the Class 1M level. The first step in this process is finding the aperture size that represents both the wavelength and classification of interest. This information can be found in Figure 8 (Table 11 of the eye safety standards).

**Table 11 – Measurement aperture diameters and measurement distances for the default (simplified) evaluation**

| | Condition 1<br>*applied to collimated beam where e.g. telescope or binoculars may increase the hazard* | | Condition 2<br>*applied to diverging beam where e.g. magnifying glasses, microscopes may increase the hazard* | | Condition 3<br>*applied to determine irradiation relevant for the unaided eye and for scanning beams* | |
|---|---|---|---|---|---|---|
| Wavelength<br>nm | Aperture stop<br>mm | Distance<br>mm | Aperture stop<br>mm | Distance<br>mm | Aperture stop/ limiting aperture<br>mm | Distance<br>mm |
| < 302,5 | – | – | – | – | 1 | 0 |
| ≥ 302,5 to 400 | 25 | 2 000 | 7 | 70 | 1 | 100 |
| ≥ 400 to 1 400 | 50 | 2 000 | 7 | 70 | 7 | 100 |
| ≥ 1 400 to 4 000 | 7 × condition 3 | 2 000 | 7 | 70 | 1 for $t \leq 0{,}35$ s<br>1,5 $t^{3/8}$ for 0,35 s < $t$ < 10 s<br>3,5 for $t \geq 10$ s ($t$ in s) | 100 |
| ≥ 4 000 to $10^5$ | – | – | – | – | 1 for $t \leq 0{,}35$ s<br>1,5 $t^{3/8}$ for 0,35 s < $t$ < 10 s<br>3,5 for $t \geq 10$ s ($t$ in s) | 0 |
| ≥ $10^5$ to $10^6$ | – | – | – | – | 11 | 0 |
| NOTE The descriptions below the "Condition" headings are typical cases for information only and are not intended to be exclusive. | | | | | | |

**Figure 8 Aperture Size**

**Table 11 of the IEC 60825 eye standards[19].**

The "Condition 1" column will be used since the beam will be nearly collimated at times and binoculars or telescopes would pose the greatest risk. Once this value is known, its cross-sectional area can be calculated.

$$A = \pi r^2 \qquad (6)$$

$$A = \pi * \left(\frac{50mm}{2}\right)^2$$

$$A = 1{,}963.5\ mm^2$$

The permissible power levels can then be acquired from Figure 9 with the constants coming from Figure 10. Again, these are wavelength dependent. It is also necessary to know that the System illumination source is continuous.

**Table 4 – Accessible emission limits for Class 1 and Class 1M laser products and $C_6 = 1$** [a, b]

| Wavelength $\lambda$ nm | Emission duration $t$ s | | | | | | | | | | |
|---|---|---|---|---|---|---|---|---|---|---|---|
| | $10^{-13}$ to $10^{-11}$ | $10^{-11}$ to $10^{-9}$ | $10^{-9}$ to $10^{-7}$ | $10^{-7}$ to $1{,}8 \times 10^{-5}$ | $1{,}8 \times 10^{-5}$ to $5 \times 10^{-5}$ | $5 \times 10^{-5}$ to $1 \times 10^{-3}$ | $1 \times 10^{-3}$ to 0,35 | 0,35 to 10 | 10 to $10^2$ | $10^2$ to $10^3$ | $10^3$ to $3 \times 10^4$ |
| 180 to 302,5 | $3 \times 10^{10}$ W·m$^{-2}$ | | 30 J·m$^{-2}$ | | | | | | | | |
| 302,5 to 315 | $2{,}4 \times 10^4$ W | | Thermal hazard ($t \le T_1$) $7{,}9 \times 10^{-7}$ $C_1$ J | | | | | Photochemical hazard $7{,}9 \times 10^{-7}$ $C_2$ J ($t > T_1$) | $7{,}9 \times 10^{-7}$ $C_2$ J | | |
| 315 to 400 | | | $7{,}9 \times 10^{-7}$ $C_1$ J | | | | | | $7{,}9 \times 10^{-3}$ J | | $7{,}9 \times 10^{-6}$ W |
| 400 to 450 | $5{,}8 \times 10^{-9}$ J | $1{,}0\ t^{0{,}75}$ J | $2 \times 10^{-7}$ J | | $7 \times 10^{-4}\ t^{0{,}75}$ J | | | | $3{,}9 \times 10^{-3}$ J | $3{,}9 \times 10^{-5}$ C W | |
| 450 to 500 | | | | | | | | | $3{,}9 \times 10^{-3}$ $C_3$ J and [c] $3{,}9 \times 10^{-4}$ W | | |
| 500 to 700 | | | | | | | | | $3{,}9 \times 10^{-4}$ W | | |
| 700 to 1 050 | $5{,}8 \times 10^{-9}$ $C_4$ J | $1{,}0\ t^{0{,}75}\ C_4$ J | $2 \times 10^{-7}$ $C_4$ J | | $7 \times 10^{-4}\ t^{0{,}75}\ C_4$ J | | | | $3{,}9 \times 10^{-4}$ $C_4$ $C_7$ W | | |
| 1 050 to 1 400 | $5{,}8 \times 10^{-8}$ $C_7$ J | $10{,}4\ t^{0{,}75}$ $C_7$ J | $2 \times 10^{-6}$ $C_7$ J | | | $3{,}5 \times 10^{-3}\ t^{0{,}75}$ $C_7$ J | | | | | |
| 1 400 to 1 500 | $8 \times 10^5$ W | | $8 \times 10^{-4}$ J | | | | $4{,}4 \times 10^{-3}\ t^{0{,}25}$ J | $10^{-2}\ t$ J | $1{,}0 \times 10^{-2}$ W | | |
| 1 500 to 1 800 | $8 \times 10^6$ W | | $8 \times 10^{-3}$ J | | | | | $1{,}8 \times 10^{-2}\ t^{0{,}75}$ J | | | |
| 1 800 to 2 600 | $8 \times 10^5$ W | | $8 \times 10^{-4}$ J | | | | $4{,}4 \times 10^{-3}\ t^{0{,}25}$ J | $10^{-2}\ t$ J | | | |
| 2 600 to 4 000 | $8 \times 10^4$ W | | $8 \times 10^{-5}$ J | $4{,}4 \times 10^{-3}\ t^{0{,}25}$ J | | | | | | | |
| 4 000 to $10^6$ | $10^{11}$ W·m$^{-2}$ | | 100 J·m$^{-2}$ | 5 600 $t^{0{,}25}$ J·m$^{-2}$ | | | | | 1 000 W·m$^{-2}$ | | |

NOTE Laser products that meet the requirements for classification as Class 1 by satisfying measurement conditions 1 and 2 may be hazardous when used with viewing optics having greater than ×7 magnification or objective diameters greater than those specified in Table 11.

[a] For correction factors and units, see Table 10

[b] The AELs for emission durations less than $10^{-13}$ s are set to be equal to the equivalent power or irradiance values of the AEL at $10^{-13}$ s.

[c] In the wavelength range between 450 nm and 500 nm, dual limits apply and a product's emission must not exceed either limit applicable to the class assigned.

**Figure 9 Permissible Power Level**

**Table 4 of the IEC 60825 eye standards[19].**

**Table 10 – Correction factors and breakpoints for use in AEL and MPE evaluations**

| Parameter | Spectral region nm |
|---|---|
| $C_1 = 5{,}6 \times 10^3\ t^{0{,}25}$ | 180 to 400 |
| $T_1 = 10^{0{,}8(\lambda - 295)} \times 10^{-15}$ s | 302,5 to 315 |
| $C_2 = 30$ | 180 to 302,5 |
| $C_2 = 10^{0{,}2(\lambda - 295)}$ | 302,5 to 315 |
| $T_2 = 10 \times 10^{[(\alpha - \alpha_{min})/98{,}5]}$ s | 400 to 1 400 |
| $T_2 = 10$ s for $\alpha < 1{,}5$ mrad | 400 to 1 400 |
| $T_2 = 100$ s for $\alpha > 100$ mrad | 400 to 1 400 |
| $C_3 = 1{,}0$ | 400 to 450 |
| $C_3 = 10^{0{,}02(\lambda - 450)}$ | 450 to 600 |
| $C_4 = 10^{0{,}002(\lambda - 700)}$ | 700 to 1 050 |
| $C_4 = 5$ | 1 050 to 1 400 |
| $C_5 = N^{-1/4}$ [a] | 400 to $10^6$ |
| $C_6 = 1$ | 180 to 400 and 1 400 to $10^6$ |
| $C_6 = 1$ for $\alpha \leq \alpha_{min}$ [b] | 400 to 1 400 |
| $C_6 = \alpha/\alpha_{min}$ for $\alpha_{min} < \alpha \leq \alpha_{max}$ [b] | 400 to 1 400 |
| $C_6 = \alpha_{max}/\alpha_{min} = 66{,}7$ for $\alpha > \alpha_{max}$ [b,c] | 400 to 1 400 |
| $C_7 = 1$ | 700 to 1 150 |
| $C_7 = 10^{0{,}018(\lambda - 1\,150)}$ | 1 150 to 1 200 |
| $C_7 = 8$ | 1 200 to 1 400 |

$\alpha_{min} = 1{,}5$ mrad
$\alpha_{max} = 100$ mrad

$N$ is the number of pulses contained within the applicable duration (8.3 f) and Clause A.3).

NOTE 1 There is only limited evidence about effects for exposures of less than $10^{-9}$ s for wavelengths less than 400 nm and greater than 1 400 nm. The AELs for these emission durations and wavelengths have been derived by calculating the equivalent radiant power or irradiance from the radiant power or radiant exposure applying at $10^{-9}$ s for wavelengths less than 400 nm and greater than 1 400 nm.

NOTE 2 See Table 11 for aperture stops and Table A.4 for limiting apertures.

NOTE 3 In the formulae in Tables 4 to 9 and in these notes, the wavelength must be expressed in nanometres, the emission duration $t$ must be expressed in seconds and $\alpha$ must be expressed in milliradians.

NOTE 4 For emission durations which fall at the cell border values (for instance 10 s) in Tables 4 to 9, the lower limit applies. Where the symbol "<" is used, this means less than or equal to.

[a] $C_5$ is only applicable to pulse durations shorter than 0,25 s.
[b] $C_6$ is only applicable to pulsed lasers and to CW lasers for thermal retinal limits.
[c] The maximum limiting angle of acceptance $\gamma_{th}$ shall be equal to $\alpha_{max}$ (but see 8.4 d)).

**Figure 10 Constants**

**Table 10 of the IEC 60825 eye standards[19].**

$$P = 3.9\,x\,10^{-4} C_4 C_7 \qquad (7)$$

$$P = 3.9\,x\,10^{-4} * 10^{0.002(800-700)} * 1$$

$$P = 0.618\,mW$$

Intensity is then found by dividing the power by the cross-sectional area found above.

$$I = \frac{P}{A} \qquad (8)$$

$$I = \frac{0.618}{1963.5}$$

$$I = 0.0161\,mW/mm^2$$

This means since the System needs to maintain a Class 1M eye safety rating at the optical output, the allowable intensity at a wavelength of 800 nm can only be 0.0161 $mW/mm^2$. Given that the output aperture of the system is approximately 5 inches, it can be calculated that the total power is 203 mW. To illustrate the importance of increasing in wavelength away from the visible band, 13.2 W of power is allowable at a wavelength of 1,550 nm. This represents a 65 times increase in power which is substantial for increasing the signal to noise ratio of images. A spreadsheet containing these calculations as well as those for other wavelengths can be found in Appendix 6.1.2.

## 2.5 Basic Operation

Any actively illuminated imaging system will have two primitive components: an illuminator and an imager. Considering the imager side, it was chosen that the System must operate in the SWIR band. For this reason, the focal plane array must be InGaAs based. Another requirement is light weight and man-portability. Thus, any optical system must be as simple as possible. A smaller number of lenses mean a lower weight and lessoned susceptibility to vibrational damage. One way to cut down on lens system complexity is to decrease the spectral band of interest. By doing this, chromatic aberration that typically requires many lenses for compensation is dramatically decreased. For the system to change the field of view (FOV), certain lenses will need to be placed into motion. Since a user friendly system is required, this process should be automated.

The illumination source must match the spectral band imaged on the array. Also, it should always produce a spot size at the target that matches the FOV of the imager. Therefore, the illuminator must also have optics that are motion controlled. Careful consideration must be taken when illuminating humans with any type of radiation. Eye safety must be maintained at all times. Calculations to find the allowable intensity levels were discussed in the previous section, Section 2.4.

Automatic focus is a higher level function necessary for this system. To accomplish this task, the system must first know the range of the target. While it is possible for the operator to know this value, it would be beneficial for the system to know as well. For this task, a laser range finder (LRF) should be implemented. With the known distance, the system should then correlate this with the proper lens positioning. This will be discussed in greater detail in Section 2.6.

The system must be able to report a target's location from its remote position. For this to be accomplished, the system must first know its location. This will be accomplished through the use of a global positioning system (GPS). The system will then be able to use this position and the range from the LRF to calculate the target's location. These calculations can be seen in their implemented LabVIEW form in Appendix 6.2 and particularly Figure 69.

Making for a robust system, it must be contained within an environmental enclosure. This enclosure along with associated heating and cooling must be able to operate in inclement conditions such as extreme temperature, rain, fog, or snow. The enclosures and assemblies must be capable of normal carrier transport and the abuse of every day operation.

The system must contain a control platform to govern all the functionalities previously mentioned. A normal personal computer based system will be constructed. The programming tasks will be carried out on this machine. All data will be stored on this machine as well as the operator's interactions.

## 2.6 Lookup Tables

In order for the image displayed on the System video feed to be in focus, the system will need to associate the displayed FOV with the actual one. To accomplish this, physical measurements will need to be made at select intervals of target distances. Given that the System also employs zoom, multiple FOV's will also need to be measured at each distance. At each of these increments, a correlation will be made between the imaged FOV and the physical position of the motorized lenses. The idea being the operator or automated system will request a focused image at a given distance and FOV. This is a "lookup table" approach.

Many methods of this approach were discussed or implemented, but they all have the exact same basis. One must relate the physical separation at the target to the pixel separation viewed on the screen. This is illustrated in Figure 11(a). Here, a normal 8 ½" X 11" piece of paper is imaged. Pixels are chosen at the extremities of this sheet of paper. Once the relation is drawn between pixel separation and physical space, the FOV can be calculated given that the width of the image is 640 pixels. An example of this calculation is shown in Equations 9 and 10. It is to be noted that this equation compensates for the case when the x value (column) of the pixels do not fall on the same y value (or row).

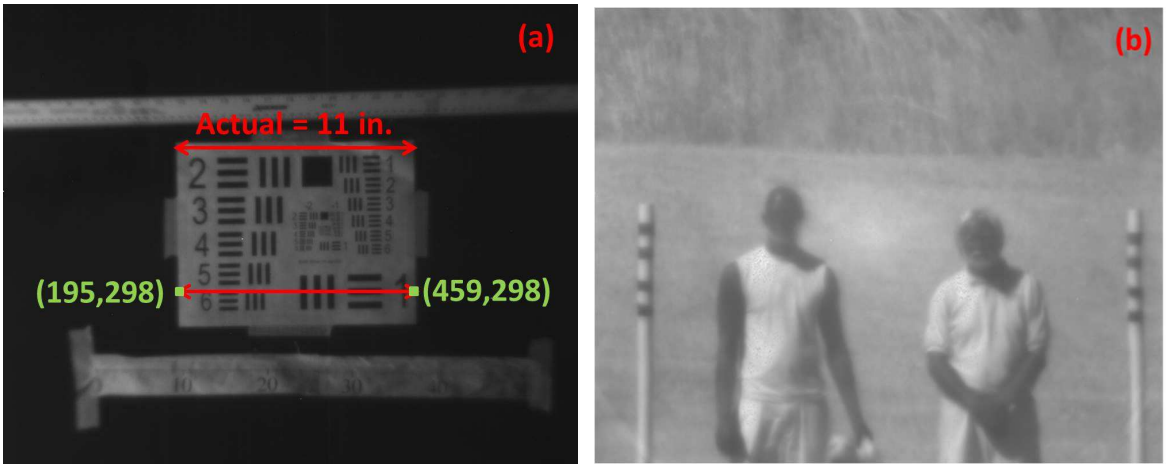


**Figure 11 Lookup Table Build Process**

**(a) USAF Resolution Test Target and comparison of true spatial measurement versus imaged pixel spans. (b) Long range lookup table measurements using poles set at a known separation to calculate FOV.**

$$\Delta_{pixel} = \sqrt{(x_2 - x_1)^2 + (y_2 - y_1)^2} \qquad (9)$$

$$\Delta_{pixel} = \sqrt{(459 - 195)^2 + (298 - 298)^2}$$

$$\Delta_{pixel} = 264\ pixels$$

$$\frac{FOV}{640\ pixels} = \frac{279.4\ mm}{264\ pixels} \qquad (10)$$

$$FOV = 677.3\ mm$$

The normal method to building this table would be to move a focus target such as the 1951 United States Air Force (USAF) Resolution Test Target pictured in Figure 11(a). Starting with the system at a narrow FOV, adjust the motion lenses until the focus is optimal. The optimal focus is a judgment made by the operator. The actual FOV is calculated in the preceding manner and the value along with the corresponding lens positions are recorded in a tabulated fashion. This process is repeated for multiple FOV's at each distance increment. It is to be noted that at each distance there exists a minimum and maximum FOV. It is very important to record a value for each of these limits. The poles shown in Figure 11(b) are used at longer distances and wider FOV to replace the paper target.

The completed lookup table has values for the distance, FOV, and lens positions. The distance increments are measured at every 10 meters from a range of 10 meters to 150 meters. Then the increment increases to 25 meters from a range of 175 meters to 300 meters. The increment then increases to 50 meters between the ranges of 400 meters to 650 meters. Values are also recorded at 800 meters and 950 meters. Once the table is completed the computer program can perform a two dimensional interpolation to produce a focus at any distance and FOV.

# 3 System Design and Assembly

To achieve the program goals of obtaining suitable imagery for long range, night time facial recognition, a hardware platform must be constructed. Many components will be required. These include an illumination source, imaging unit, motion control system for focusing at various distances and FOV's, environmental enclosures, and overall control system. The following sections present in detail these design considerations and the process of implementing each.

## 3.1 Optical Head Unit

### 3.1.1 Lens Mounting and Motion

To meet the imaging requirements of this project, the lens system will need to operate at a wavelength of greater than 1400 nm, utilize a narrow 10 nm band, produce a X10 motorized zoom, and filter out all other light. Telephoto lens systems with these specifications do not exist off the shelf. For this reason, they will need to be custom designed and manufactured. This process was completed by a WVHTCF team member. The lens design was received in the form of a Zemax file. Zemax is a very useful optical design tool that allows the user to simulate and modified one's design prior to fabrication. This design was then sent to a company for lens fabrication.

The next step is to decide how to hold the lenses. They vary greatly in both size and weight. The largest lens has a diameter of greater than 5.5 inches and weighs more than 630 grams. The smallest lens has a diameter of 6 millimeters and a weight of approximately 0.15 grams. Variations of size do not permit for a single mounting scheme throughout the system and will need to be examined on a case-by-case basis. Many mounting schemes were considered. Some were sketched by hand and others were modeled in using a modeling software package. Figure 12 illustrates two such cases for the main imager lens holders.

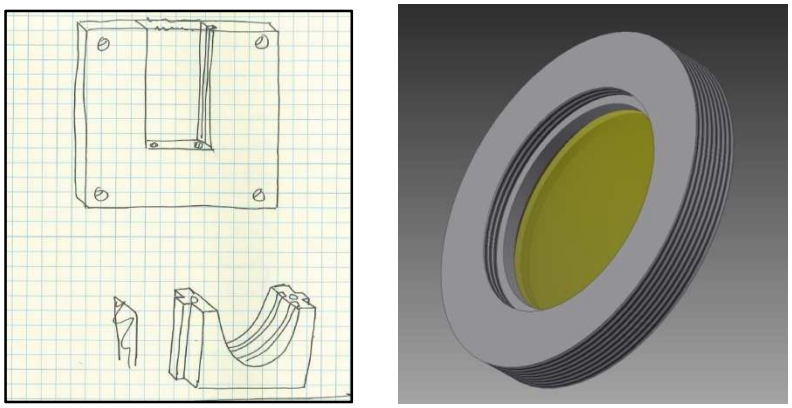

**Figure 12 Original Sketches**

**(left) Hand drawn sketch of imager doublet cart and doublet holder. (right) Solid model "sketch" of imager doublet holder.**

All mechanical design was performed using Autodesk Inventor[20]. Without prior knowledge, experience, or training in three dimensional modeling, the project required studying and research in this area. After Inventor was chosen as the design package of choice via online reviews, it was necessary to gain experience within the resources available. This meant following tutorials provided with the software suite

and online videos. Normally, arbitrary parts were modeled to familiarized oneself with both software functions and the mechanical design progression.

Many factors had to be considered when settling on a design. Some of the most important are the precision in which the lenses need to be placed, the thermal cycling in which they will be subjected, and the mechanical shocks and vibrations attributed to normal use. This led to the conclusion of a concentric design illustrated in Figure 13. The main advantage to this approach is keeping all components positioned relative to the optical axis. The mounts are made from aluminum due to its low weight, capability to be machined at high precision, low coefficient of thermal expansion, and other machinability characteristics.

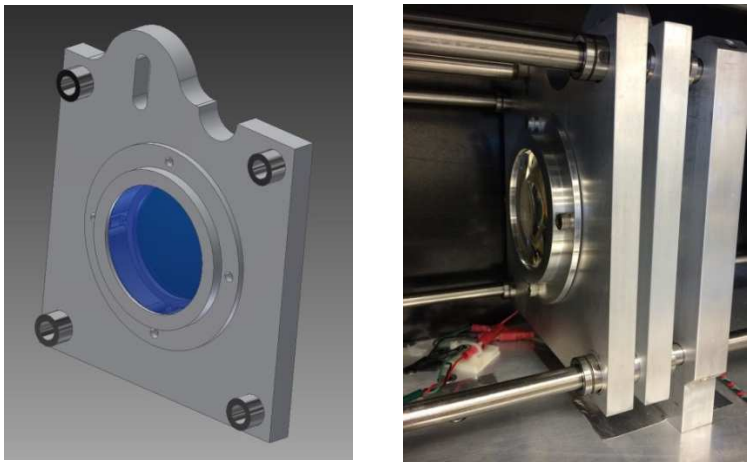

**Figure 13 Imager Doublet Cart.**

**(left) Solid model of a doublet cart and doublet holder illustrating a concentric design. (right) Implemented concentric design in the System generation 1.**

Next the decision was made on the mechanism to facilitate the lens motion. Focusing and zooming can be accomplished by manually positioning lenses; however, this would not be viable for long term use. For this reason, a motorized assembly must be designed and constructed. Again, many different methods were considered including linear stages, conventional telephoto lens tubes, and DC motor actuated units. The prototype System started by pairing a four rail system propelled with stepper motor driven, linear actuators. Figure 14 illustrates this basic configuration.

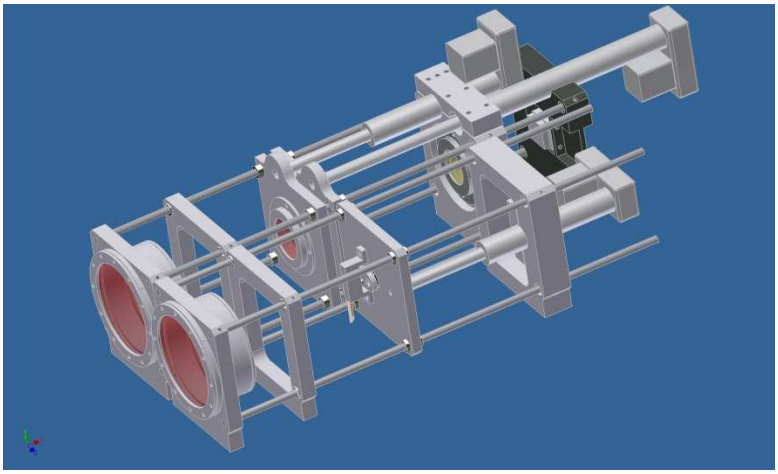

**Figure 14 System 1 Solid Model.**

**This is the solid model of the complete System 1 as designed in Autodesk Inventor.**

The parts used for this system were intentionally made larger due to the fact it was a laboratory prototype. It may possibly need to be modified at a later time. The rail system allowed for thermal cycling in a manner that kept all lenses on the optical axis. The rail system teamed with linear bearings allowed for smooth movement in the zoom direction and little movement off axis. The linear actuator provided the necessary .001 inch step resolution while producing a full zoom in less than two seconds total time. Homing switches, both magnetic and mechanical, are also included in order to locate the motion components on start up.

As previously mentioned the prototype mounts and actuators are large. The second generation system was constructed to decrease weight and improve portability. It maintained the use of the four rail system and concentric lens mounts. However, this version needed to be man portable and major improvements needed to be made in both weight and size. The linear actuators were replaced with a simple ACME screw and stepper motor system. The rails were reduced in size from 3/8 inch to 1/4 inch. The individual lens mounts were stripped of all unnecessary aluminum material. Figure 15 illustrates the transition between the systems.

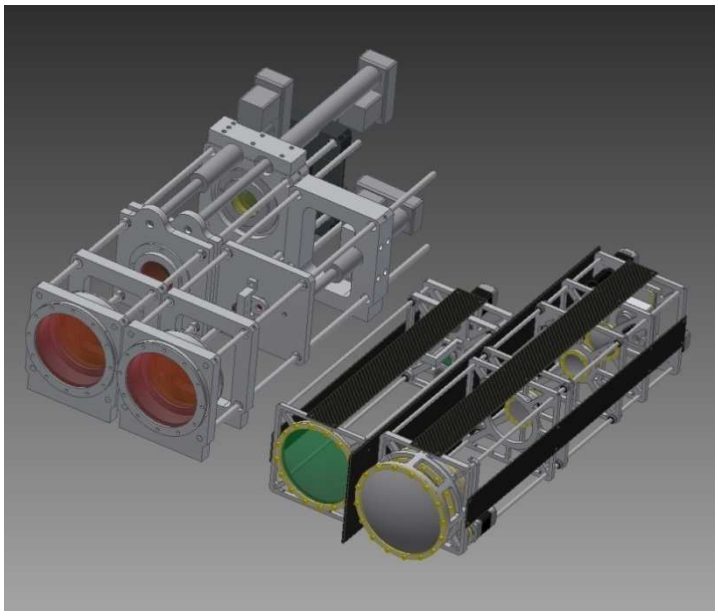

**Figure 15 Both Generation Systems**

**This solid model illustrates the size and material reduction between the first generation system on the left and second generation system on the right.**

After the successful implantation of the lens mounting scheme in the first system, it was desired to maintain the same basic concept for the second generation unit. For this reason, it was decided to decrease the size of the mounts. Instead of taking out material and hoping it will not affect functionality, each part was simulated using a finite element analysis (FEA) program called ANSYS. First, the material was removed in Inventor and then the model was transferred to ANSYS. In this program, forces were applied in the directions thought to be of concern to the real world unit. Displacements of the mounts were tracked to validate that all lens tolerances were maintained. Thermal analyses were conducted to make sure the lenses would maintain their positions and also not crack during thermal cycling. Figure 16 depicts one of the mounts as taken from the FEA program.

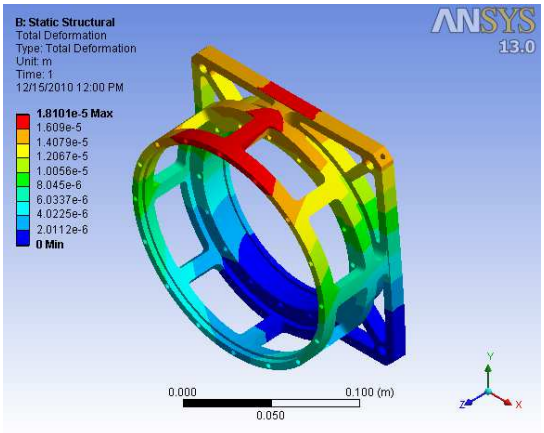


**Figure 16 Finite Element Analysis Results**

**This illustration is the resulting screenshot from a FEA experiment to test the total deformation of a lens holder under real world conditions.**

### 3.1.2 Imager

The imaging system consists of a large fixed doublet, followed by two independently moving smaller doublets, and a final fixed doublet. Also included is a large motorized iris and SWIR imager from Goodrich now UTC Aerospace. Figure 17 depicts the Zemax layout and ray tracing of the imaging system.

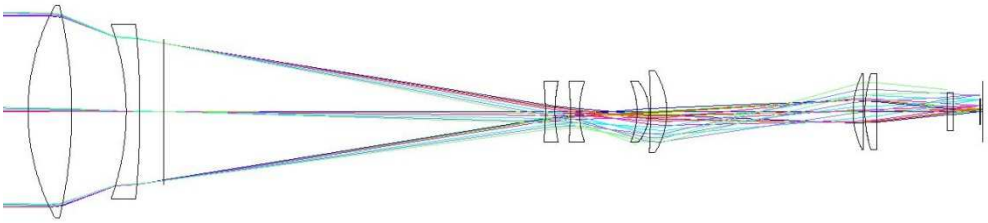

**Figure 17 Zemax Layout**

**Ray tracing and optical layout as displayed by the optical design software Zemax.**

The first generation system had the iris positioned in front of the output lens. This unit was designed and fabricated by a local machine shop. The mechanism was very large and heavy. It consisted of a 6 inch manual diaphragm, large brass gear, NEMA 17 stepper motor, and large aluminum mount. The motorized movement of this iris was slow and loud. Figure 18 depicts this unit.

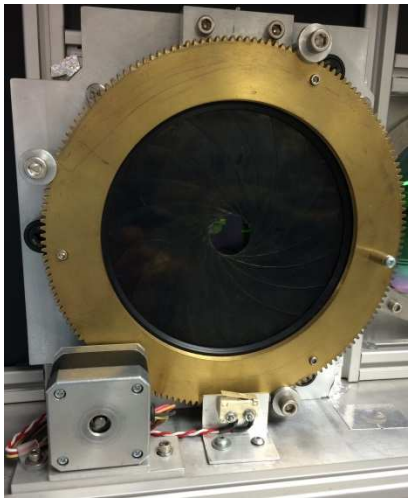

**Figure 18 Motorized Iris**

**This is the motorized iris on the first generation System. It suffers from high weight, loud actuation, and slow motion.**

It was necessary to improve the iris. A total redesign was implemented in the second system. First, it was decided by the WVHTCF team member in charge of the optical design that the iris can be moved behind the first doublet. This reduces the necessary maximum aperture from approximately 140 mm to 100 mm. Then it was decided to combine the iris and large doublet mount. The large brass gear was replaced with a thin plastic version wrapped around the diaphragm. The NEMA 17 stepper was also replaced with a smaller and lighter NEMA 14. This new design drastically reduced the size, reduced the weight, and increased the speed. Figure 19 shows this system.

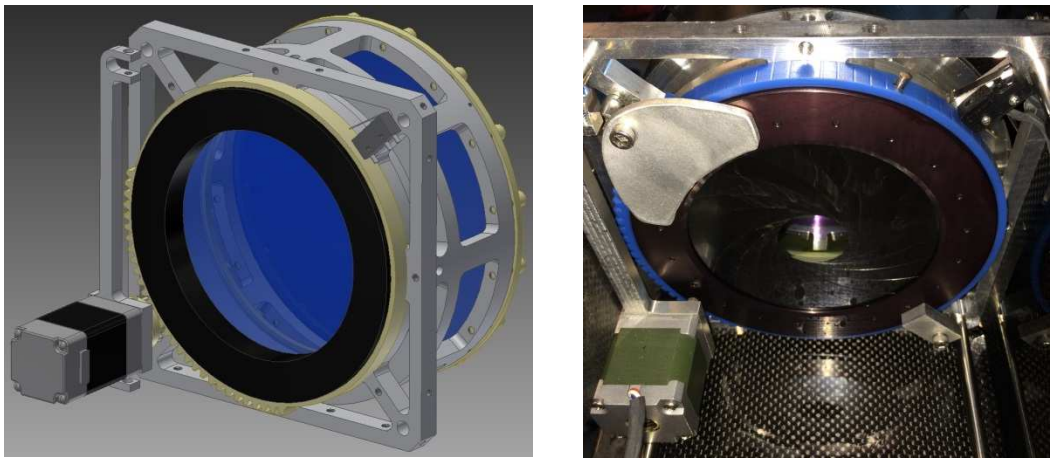

**Figure 19 Motorized Iris**

**This is the motorized iris on the second generation System. Many improvements were made between generations including changing location to decrease size and weight, using plastic where possible to decrease acoustic noise, and also significantly increase speed. (left) Solid model. (right) Actual implementation on the second generation system.**

The prototype system was paired with a COTS SWIR focal plane array from Goodrich (now UTC Aerospace). This is a 640X512, 25µm pitch, InGaAs area scan imager. It was mounted to the System imager in the same manner as the lenses within the four rail system. It also requires a frame grabber card in the control computer. Again, the aluminum mount is very large and heavy. The second generation system was initially implemented with a different focal plane array from Aerius Photonics. This unit was not commercially available but allowed for collaboration between the WVHTCF team and the manufacturer. This system is divided into three sections: the array unit, the supporting electronics, and a frame grabber or Ethernet to GigE Vision converter.

After a few months with the Aerius device, the decision was made to switch back the Goodrich imager. One of the second generation systems was retrofitted with an adapter that would mount to the existing Aerius support and accept the first generation System Goodrich unit. This had limitations such that it was impossible to align the center pixel of the array with the optical axis. For the most part, this is not a huge problem. The result was a simple shifting center of the image from full to minimum zoom. A completely new Goodrich unit was purchased with better specifications and meeting Mil standards. A total redesign was then accomplished on the focal plane array mount. This unit was fabricated and installed with the new Goodrich unit into the other second generation system.

### 3.1.3 Illuminator

Projecting light from the System should involve an illumination source and diverging optics. The source itself could be collocated with the imaging optics, but this would prove to be a very heavy option. Fiber coupling with the source located at some distance away will dramatically reduce weight. This was the path taken for this system.

The System illuminator is a multimode fiber coupled system. The objective of this system is to adjust the divergence of the illumination to always match the field of view of the imager. The full angle divergence of the system must adjust from a minimum of 0.07° and maximum of 5.7°. The first generation system consisted of a large output doublet, a motorized small lens, and fiber mount. The mounts were again left

very large for potential modification. The large motion mechanism was driven by the same linear actuators used in the imager. Figure 20 shows both the Zemax layout of the initial illuminator lens design and also the solid model of the complete system.

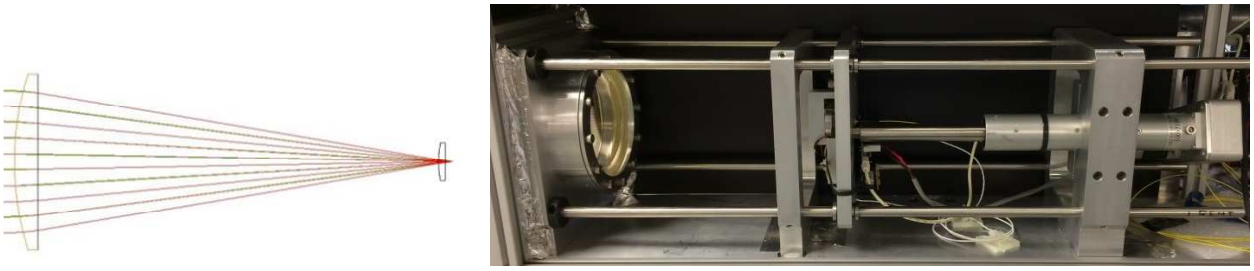

**Figure 20 Illuminator**

**(left) Zemax layout and ray tracing of original illuminator. (right) Hardware implementation of first generation illuminator.**

The motion for the small lens is controlled by a very small piezoelectric screw actuator. This tiny device is a COTS system called a "Squiggle" motor from New Scale Technology. At the time of first implementation, this unit made for a very small and effective system. However, longevity proved to be a an issue with the Squiggle motor. The screw would continue to stall under very low and normal load. After multiple replacements, it became evident that it would not be a sufficient design to transition to the second generation system. Figure 21 depicts the first generation small lens motion system.

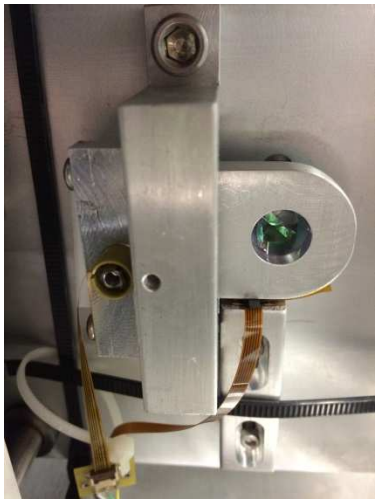

**Figure 21 Small Lens Motion System (Generation 1)**

**This is the hardware implementation of the small lens motion system on the first generation System including Squiggle motor and supporting mounts.**

The small lens motion on the second generation system employs the same stepper motor and ACME screw function as the larger parts. A NEMA 8 motor, the smallest commercially available, and accompanying mount requires at least four times the space compared to the Squiggle system. It also weighs approximately four times more; however, it is easily capable of moving the small lens accurately and reliably. Figure 22 depicts this new configuration.

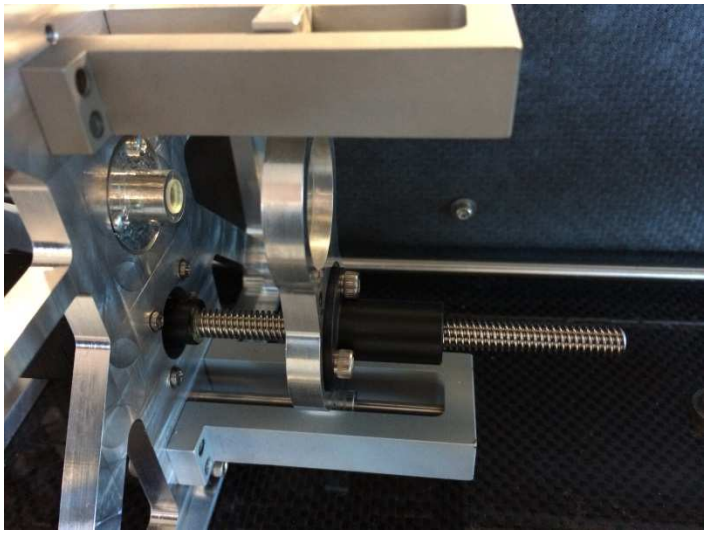

**Figure 22 Small Lens Motion System (Generation 2)**

**This is the hardware implementation of the small lens motion system on the second generation System.**

### 3.1.4 Electronics

To control lens zoom motion and other hardware and software tasks, a computer program must first be developed. Since the first generation unit was designed to be a laboratory system, a higher level programming suite could be employed. For this reason, the first generation system was completely implemented via National Instruments LabVIEW products. This allowed for quick installation and constant modifications. Within the head unit is a large driver box for each stepper motor and one large breakout box. These items are pictured in Figure 23.

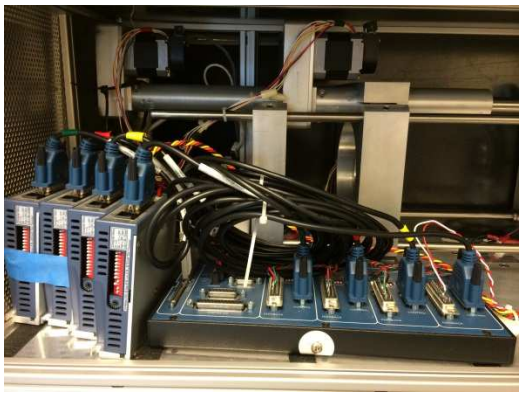

**Figure 23 Motion Control Electronics**

**These are the required National Instruments electronics to drive the linear actuators in the System 1.**

Also within the head unit is an electronic compass from Ocean Server Technology Incorporated. This one inch by one inch printed circuit board, 3-axis tilt compensated compass unit provides the System with an azimuth to calculate the target's location. All electronics in this system are combined into one umbilical cable and connected to the computer. This large bundle is not ideal for mobilization because of the lack of modularity.

Many more tasks were desired to be implemented within the second generation system. Accordingly, the amount of electronics contained within it was also significantly increased. The Goodrich imager is a CameraLink based system. Connections are made via a large, high density, ribbon cable. Carrying high speed digital signals, the length of this cable is very limited. For this reason, the CameraLink cable is connected to a GigE Vision converter allowing for a tenfold increase in length between the imager and computer. The large National Instruments stepper drives were replaced by very small 1.6 inch by 1.6 inch units from All Motion. The control input to these drives is typical serial communications. Here again, cable length is very limited. For this reason, the WVHTCF team decided it would be beneficial to convert these signals to TCP/IP via a serial to Ethernet converter.

Initial research was conducted by the WVHTCF team in the implementation of automatic target tracking. Through later market searches, it was found that a few mature, COTS systems exist that provide many video processing features. One such unit was chosen and purchased from Sightline Applications. This product contains many functions useful to the System including the CameraLink to Ethernet conversion, image stabilization, moving object detection, and target tracking. An ordinary Gigabit Ethernet switch is also contained within the head unit for combining all Ethernet cables into one.

The compass has been temporarily removed from the second generation system. Due to interferences from the motion drivers, stepper motors, thermal electric cooler, and environmental enclosure, repeatable accuracy cannot be obtained from the current electronic compass. Azimuth can be obtained through an alternative method that adds complexity during the system set up process. If the sensor location is known, the user can look at the video screen and point to a known calibration point at the greatest distance away possible. Using these two GPS points an initial heading can be calculated. A sample of this calculation can be seen in its implemented form in Appendix 6.2 and particularly Figure 69. Once the initial azimuth is known, the position of the PTU unit can be tracked for subsequent values.

For accurate target position reporting and image focus, the System must have an accurate assessment on the range. For this reason, the second generation system is equipped with a LRF. Initially a relatively inexpensive COTS unit was purchased from Newcon Optik. This system allowed for quick integration but had two major limitations. The first drawback of this unit is the fact its operation wavelength is 905 nm. This means while remaining covert to the naked eye, the System is now detectable by NVG's and conventional silicon imagers. Secondly, the typical maximum detection distance was limited to 1,000 meters. Once it was realized that the target distance would far surpass this range, an upgrade became necessary. The System was then retrofitted with a unit from Instro Precision Limited. This model increased the detection range past 3,000 meters. Another great advantage to this system is its operating wavelength. At 1550 nm, this LRF is out of the sensitivity range of NVG's and silicon imagers making the System now completely covert.

### 3.1.5 Environmental Enclosure

As previously mentioned, the parts on the original System were intentionally over built to allow for later modifications. This was also the case for the baseplate in which this system rests and mounts to the pan/tilt unit (PTU). This supporting structure weighs in excess of 30 pounds itself. When it was required that this system be mobilized, a member of the WVHTCF team designed and assembled an environmental enclosure. This consisted of an 80/20 Inc. aluminum extrusion frame and black plastic panels. This did not allow for moisture repulsion but was sufficient to operate the system outside in fair weather or under

shelter. Cooling was provided by piping in cooled air. The entire head unit weighed well over 90 pounds.

The second generation system needed to be field deployable to acquire data away from the WVHTCF location and be able to operate in almost any conditions. This required a sealed system that did not allow air transfer from outside to inside due to moisture concerns. If the environment inside the box became humid, the probability of condensation building up on the lenses would be greatly increased. Thermal electric cooling (TEC) and heating is a simple solution to this problem. In TEC systems, no air is passed through the border. Heat is transferred through the walls via conduction through a metallic wall. COTS TEC cooler/heaters are available. However, they are a fixed size and cannot be modified to fit the space available on the optics head unit. For this reason, a custom unit was designed and implemented. First, calculations were made in order to find out how much heat transfer would be required. It was decided to allow the optics head unit to vary in temperature from 70°F to 100°F. All attempts were made to maintain 70°F; however, it required too many Peltier units. A ceiling temperature of 100°F was chosen because all devices within the optics head can easily function here. Calculations were made with the range, heat developed within the box, and contribution from the ambient environment in mind. Four Peltier units proved to be sufficient for this application. Figure 24 illustrates the TEC unit.

**Figure 24 Thermal Electric Cooler**

**(left) Solid model of the TEC device for System 2. (right) Actual implementation of the TEC unit on the System 2.**

Serious weight reduction was needed on the aluminum baseplate. For the second generation system many solid and composite materials were examined for this task. A unique product from Dragon Plate was chosen that consisted of 1/4" rigid foam sandwiched between two layers of carbon fiber. This material holds many advantages in that it is lightweight, relatively rigid, does not suffer from thermal expansion, easily machinable, and the foam core offers a small amount of insulation.

An enclosure “lid” was then designed and fabricated to protect the entire optical head unit during outdoor use. Maintaining a lightweight design is very important. For this reason, carbon fiber was again the ideal building material. The concept was developed in house and then the solid model was sent to Dragon Plate for basic manufacture. Once this was received, it was modified to accept the remaining

components. The front of the system was fitted with large, anti-reflection coated optical flats. These windows can easily be cleaned of dust or water and can be replaced if badly damaged. The inside is lined with insulation and heat reflective barrier to minimize thermal transfer. The TEC unit is mounted to the back along with a panel of Mil Spec connectors to interface with the umbilical cord. Finally an aluminum rail system is welded and glued inside the enclosure to mount to the baseplate. While the natural black color of the carbon fiber finish is beneficial for night time operation, it is not ideal for staying cool in sunny and hot weather. For the reason, a large white cover was assembled with additional insulation and a visor to shade the input/output windows. This visor can be emplaced or removed quickly and easily with the attached Velcro. Figure 25 illustrates the second generation optical head unit. The resulting assembly dropped the weight from 90 pounds on the first generation system to approximately 30 on the second generation unit.

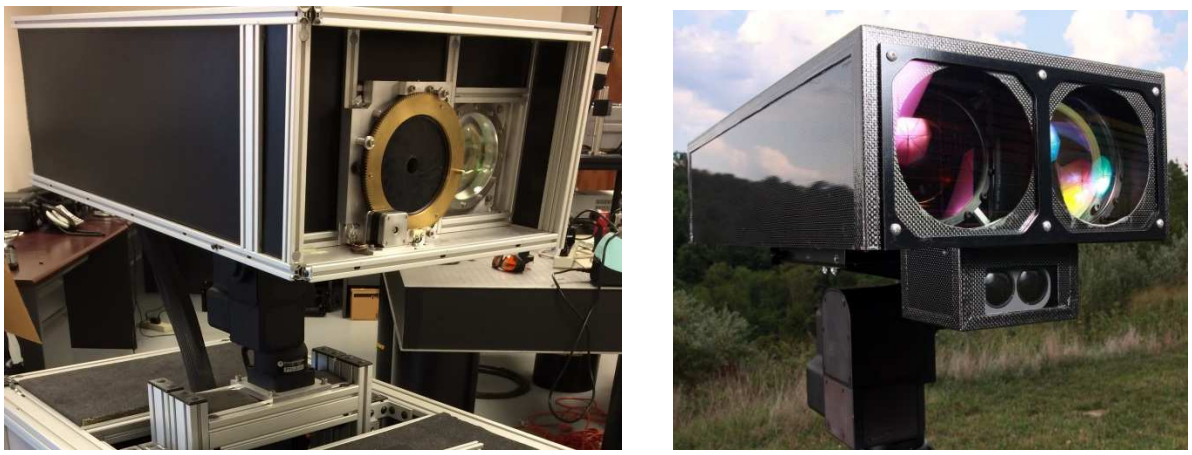

**Figure 25 The System Optical Head Unit**

**(left) System 1 optical head unit weighing approximately 90 pounds. (right) System 2 optical head unit weighing approximately 30 pounds.**

## 3.2 Electronics Enclosure

### 3.2.1 Illumination Source

The first generation System was paired with a high power, narrow band laser diode from SemiNex Corporation. This is a multimode fiber coupled device. A very simple drive circuit was constructed consisting of a variable voltage, bench-top DC power supply and TEC driver. Whenever it was desired to run the illuminator, the operator would need to manually power on the supply and adjust the voltage to achieve the desired optical power output. The output fiber was then connected to a "shaker" unit. The definition and purpose of the shaker will be described in Section 4.2.2.1 and was also briefly mention in Section 2.3.3.1. From the shaker, the fiber was then connected to the optical head.

The WVHTCF team was not convinced that the laser source was the best option for the second generation system. The main concern was the sharp and narrow peaks in the optical spectrum. It was decided that filling the narrow illumination band as evenly as possible would greatly reduce the laser speckle (also discussed in Section 4.2.2.2). For this reason, other source options were explored. Since two generation systems were to be built, each unit was outfitted with a different source. First was a swept wavelength source. This unit had a very narrow peak of approximately 1-2 nm. The idea was to quickly sweep the

wavelength within the System imaging band to reduce the reflective coherence. This unit proved to be unreliable due to many reasons greatest of which was maintaining the sweep within the designated spectral band.

The second and preferred configuration begins with a superluminescent light emitting diode (SLED) as a source. As with any other LED, the spectrum is relatively broad and low in intensity. For this reason, the single mode fiber coupled SLED needs to be filtered and then amplified. Finding a narrow band pass fiber filter is very unlikely. However, a WVHTCF team member was able to find a conventional one inch dielectric filter. A mounting system was then designed and fabricated which consisted of COTS fiber collimators, COTS gimbal mounts, and custom parts. This system is depicted in Figure 26.

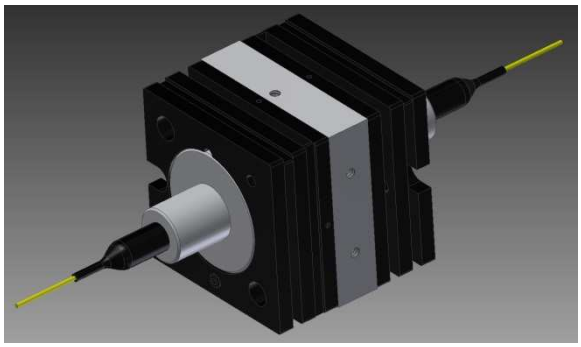

**Figure 26 Free-Space/Fiber Optic Filter**

**This is a solid model of the assembly used to filter the fiber coupled SLED to the appropriate spectral window.**

From the filter, the fiber is then connected to an erbium doped fiber amplifier from Manlight. This unit is remotely controlled via traditional serial commands. It can be cued for many system statuses and set the output power from 10 dBm to 37 dBm. Exiting the amplifier, the fiber is single mode and will need to be converted to multimode. A WVHTCF team member found a mode conditioning cable from Fiberdyne that offsets a 10 µm single mode fiber with a 62/125µm multimode fiber. From here, the fiber is then sent to a shaker system and then off to the optical head. Figure 27 is a block diagram of the entire illumination system.

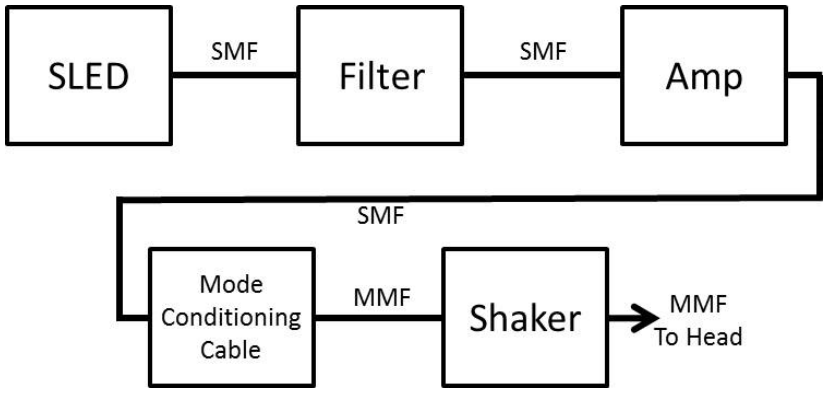


**Figure 27 Illumination Source**

**This is a block diagram of the second generation system illumination source showing each hardware component. Both types of connecting fibers are also depicted: single-mode fiber (SMF) and multi-mode fiber (MMF).**

### 3.2.2 Electronics

Due to the simplicity of the first generation system, very few electronics are contained within the enclosure outside of the illumination parts. Initially, the second generation system was powered with DIN rail mounted supplies. The control board for the optical head TEC is contained within the box. The enclosure also has a GPS unit, serial to Ethernet converter, Ethernet switch, and a remotely controlled relay. Later the DIN rail supplies were replaced by smaller and lighter solid state versions.

### 3.2.3 Environmental Enclosure

As the first generation system was never meant to leave the laboratory, it initially did not have a cabinet dedicated to housing the electronics system. Once it became evident that it would be mobilized, a member of the WVHTCF team designed and fabricated a large wheeled base unit as an enclosure. The cabinet was constructed of 80/20 Inc. aluminum extrusions and was not environmentally sealed. This is a very heavy unit and is not man portable. It requires a large van and ramps for transport.

For the second generation system to be tactical, the individual system components had to be of adequate size and weight for personnel transport. Initially, the electronics enclosure was a plastic, ruggedized computer rack unit. All individual components are packaged within 4U sever computer chassis including the computer. This unit was still relatively heavy and required at least a two person lift. Also, cabling was run through a rubber grommet in the case making it not completely weather tight. A decision was then made to remove the computer from the electronics unit and reduce the enclosure's size. A model from EIC was chosen with a paired TEC unit. Once Mil Spec connectors were added to the side of the enclosure, the unit became completely sealed and able to function in all weather conditions.

## 3.3 Computer

### 3.3.1 Software

As previously mentioned, the first generation System was a National Instruments LabVIEW based system for the purpose of quick implementation and small amount of software background needed. All automation was controlled via their pictorial based programming. Lens motion is one such automation. In order for the five motion axes to be in the correct place, it was decided that the System would focus given a known distance. A lookup table approach was taken where the system would be manually calibrated at given interval distances. This approach was discussed in detail in Section 2.6. Once the operator choses a target distance, the software will check the table and move the linear actuators, iris stepper, and squiggle motor to the correct position. Video is displayed with the assistance of the LabVIEW Video Toolkit. All video functions can be controlled via this interface including exposure and toggling the automatic gain control (AGC). The PTU interface is another control programmed into the LabVIEW front panel. This unit accepted serial commands which were sent when either the direction arrows were clicked or a position on the video screen was selected. The System interface also had a button that started a new encounter in the facial recognition system. A complete file structure was developed for this purpose. Figure 28 shows the first generation System user interface.


**Figure 28 System 1 GUI**

**This is the main interface to control the System 1 including zoom, focus, pan/tilt, and face recognition initialization.**

The complete LabVIEW code developed for this system can be found in Appendix 6.2.

With the increased functionality required for the second generation system, LabVIEW control would be a poor choice as a programming platform. A full time programmer was added to the WVHTCF team and most software tasks were turned over to him. The only remaining responsibilities of software concern were designing the user interface (not implementing) and initial software support of hardware devices such as the LRF and compass.

### 3.3.2 Hardware

The first generation system was controlled with a Dell workstation running Windows XP. LabVIEW and the facial recognition software were installed on this machine. Given that only still images were stored on this machine a large hard drive capacity was not required.

The second generation system is able to record all video making it a requirement for a large amount of memory. Also, the system must be accessible to multiple users at any given time. For this reason, a server based machine was assembled. Individual computer parts were specified and purchased. Then a member of the WVHTCF team mounted them into a 4U server chassis. Once it was decided to remove the computer from the electronics box, a web search was conducted to find a more rugged standalone unit. A system was chosen from Sterling Computers. This system met all the hardware specifications and came in a semi-rugged case with integral keyboard and mouse.

As the system is network connected, additional users can login via Windows "Remote Desktop Connection." From this interface, the user can monitor the system and view the live System feed. If remote operation is desired, a user can control all functionalities from this connection. The network connection can be both wired and wireless. However, video view frame rate is dependent on the wireless network's connection speed. Figure 29 depicts the System operation on a Windows based wireless tablet.

**Figure 29 Tablet System Operation**

**The System application running on an Acer Windows 8 based tablet over a WiFi network.**

## 3.4 Complete System

The basic structure of the system is comprised of three components: the optical head unit, the electronics enclosure, and the computer control unit. Figure 30 is a conceptual illustration of the main elements of the system.

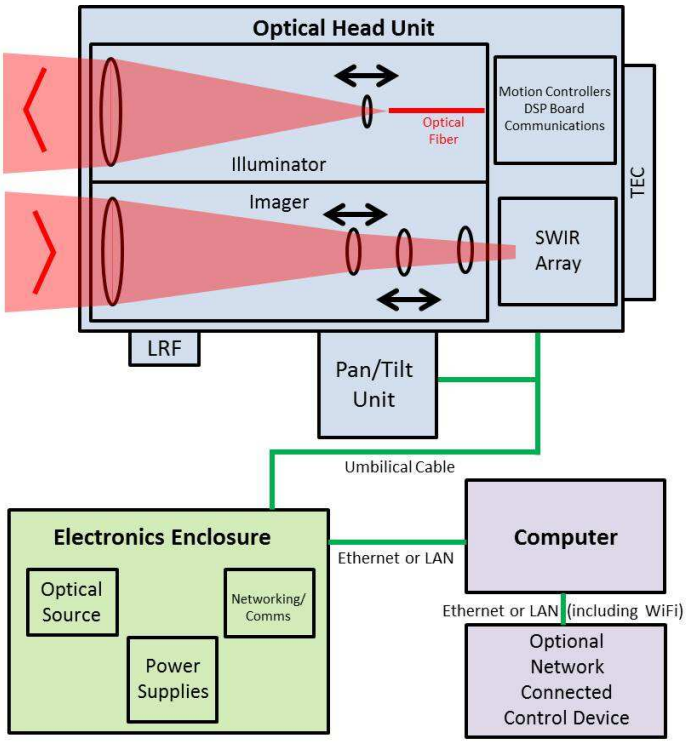


**Figure 30 System 2**

**Block diagram of the complete second generation System.**

To date, two versions of the System have been implemented. First was a proof-of-concept laboratory unit. It is to be noted, however, that this unit was modified to leave the indoor environment when it

became required for outdoor and offsite demonstration. The second generation system is a smaller, environmentally sealed, and more tactical system used for hands on evaluation by existing and potential customers. Two second generation systems were produced. Figure 31 shows both of these systems.

**Figure 31 System Generation Comparison**

**(left) Actual System 1. (right) System 2.**

# 4 Experimental Results

## 4.1 Data Collection

Prototype systems need to be trained and tested before their operational deployment. This is the case for the System. For various reasons, data will need to be acquired to calibrate, improve, and characterize system behavior. Below is a list of three such data collections. These will give insight into the design and implementation process.

### 4.1.1 Initial SWIR Data Collection

As discussed in previous sections, there are both advantages and disadvantages to the potential illumination wavelengths. Characteristics can be calculated and speculated upon, but in many instances it is beneficial to actually experiment with multiple options. One of the first steps of the System design process was to make this wavelength decision. The team members in charge of the design narrowed it down to two: less than 1000 nm and a wavelength greater than 1400 nm.

To aid in the selection process, a data collection was conducted with a certain number of human subjects. Both wavelengths were tested in this exercise. Since the original System had yet to be developed, an illumination and imaging apparatus would need to be designed and constructed. It had already been decided to use the Goodrich imager in the final system. One was purchased ahead of time with an evaluation lens. It could be used out of the box in a short range setup. Fiber coupled laser diodes in butterfly packages were used as the less than 1000 nm and greater than 1400 nm illumination sources.

These were paired with simple bench top DC power supplies and free space optics to control divergence. Along with the visible spectrum Canon camera, these items can be seen in Figure 32.

**Figure 32 Imaging Equipment**

**This is the experimental setup for the May 2009 data collection. Top center is a typical visible spectrum digital camera and in the center is a SWIR imager and lens. To the left and right of the SWIR imager are the fiber coupled sources.**

The participants were first asked to pose for a visible spectrum mug shot with normal light illumination. The Canon camera as illustrated above was remotely controlled via facial recognition enrollment software supplied by an outside source. As the image was acquired it was checked to ensure it met certain criteria such as being properly centered, containing enough resolution, and meeting a metric termed "faceness." Two of these frontal, neutral expression images were taken. Two images were then taken with the subject talking making "a" and "e" sounds. Once this was accomplished, images were acquired with the subject looking both left and right with their faces at 20° angles.

The room lights were then turn off and the IR images were acquired. As mentioned above, the Goodrich imager and evaluation lens were used for this exercise. The imager was controlled via a custom LabVIEW program. The same six images were then acquired with both the less than 1000 nm and greater than 1400 nm illumination sources. In total, 18 images were acquired from all 56 participants.

The images acquired from this exercise were run through the facial recognition software. The visible spectrum images were submitted as the gallery images. The IR images were then individually inputted as probes to be matched against that gallery. A rough comparison was then made between the two wavelength results. As expected, the lower had a higher successful match rate. This stems from the fact these images better resemble their visible spectrum counterparts. Even given this fact, the higher allowable power at the greater than 1400 nm band still proved to be the most important benefit.

### 4.1.2 Indoor, Long Range Data Collection

At this date, the first generation System had been fully assembled. However, the wavelength had not been chosen with one hundred percent certainty. Members of the System lens design team were able to make the lens system hardware switchable. A second data collection was then accomplished.

As before visible spectrum mug shots were acquired. Only frontal neutral expression images were necessary for this portion. The IR images were acquired at two ranges of 50 meters and 106 meters in a completely dark hallway. During week one, the less than 1000 nm images were taken. The participants were asked to pose in 14 shots at each distance. These poses were:

- two frontal neutral expressions
- two frontal talking
- left and right ten degree pose angles talking and neutral pose angles
- left and right twenty degree pose angles talking and neutral pose angles
- left and right ninety degree neutral pose angles

They were then asked to repeat the process at the second distance. In all, 59 participants were imaged. The hardware was then changed to operate at greater than 1400 nm. The process was then repeated with the 59 participants.

### 4.1.3 WVU/WVHTCF Data Collection

The second generation system was tested in a third data collection. In collaboration, WVU and the WVHTCF conducted a large collection on the Evansdale campus (Morgantown, WV). One main objective was to acquire outdoor imagery at much longer distances. Both organizations needed data from this exercise, so it was necessary to tailor the program to meet both requirements. WVU would provide the indoor controlled environment for visible spectrum acquisition and WVHTCF would provide the System.

Once a site was chosen for the System to be positioned, three locations were selected each having a clear line of sight to the sensor. The three distances were 100 meters, 200 meters, and 350 meters all within the student recreation center's parking lot. Figures 33 and 34 show both the aerial view and the true view of the experimental placement. It should be noted the illustrations are displayed during daylight hours but the experiment is conducted under total darkness.

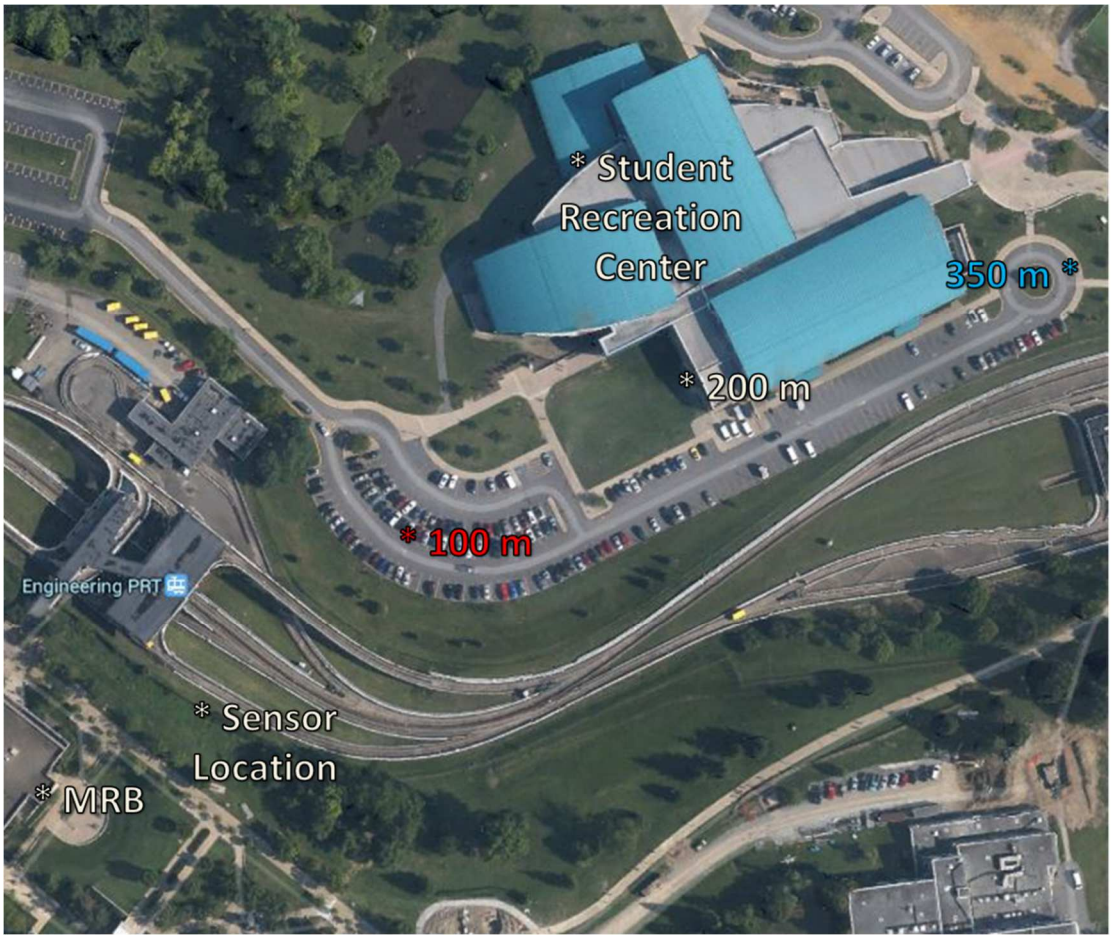


**Figure 33 WVU Data Collection Aerial View**

**This aerial view of the WVU data collection shows the sensor location, three target locations, and major campus landmarks.**

**Figure 34 WVU Data Collection Ground View**

**This is the view taken from the sensor location. It should be noted that this image was taken during the day for the purpose of illustration where all data was collected under complete darkness.**

Each subject would be required to pose for high resolution, visible spectrum images in the WVU laboratory conducted by graduate students. Here they were also assigned a number and then ushered to the 100 meter mark.

Considering the second generation System is able to record video and has a large storage capacity, it is no longer limited to single image acquisition. At thirty frames per second, ample data will be available for post processing. Four different scenes were performed at each distance by every subject. First the system was set to its narrowest zoom level. This corresponds to a FOV of approximately 640 mm. The subject was then asked to look towards the imager with a neutral expression. After a two second video clip is acquired, the subject was then instructed to rotate 360 degrees, pause, and then rotate the opposite direction a full turn. For the third clip, a piece of tinted glass was put in front of the subject again with the neutral expression. The fourth clip is conducted with the imager zoomed out. The subject is then instructed to walk approximately ten feet perpendicular to the FOV, perform the two 360 degree rotations, and walk back to the starting position. This exercise is capable of acquiring both gate and full body rotations for person detection cascades.

The subjects, typically in groups of ten, were then asked to proceed to the 200 meter mark and the routine was repeated. Once completed, they were then ushered to the 350 meter and final range. In all, 104 subjects were collected over a six month span. Figure 35 depicts the wide angle imagery at all three distances.

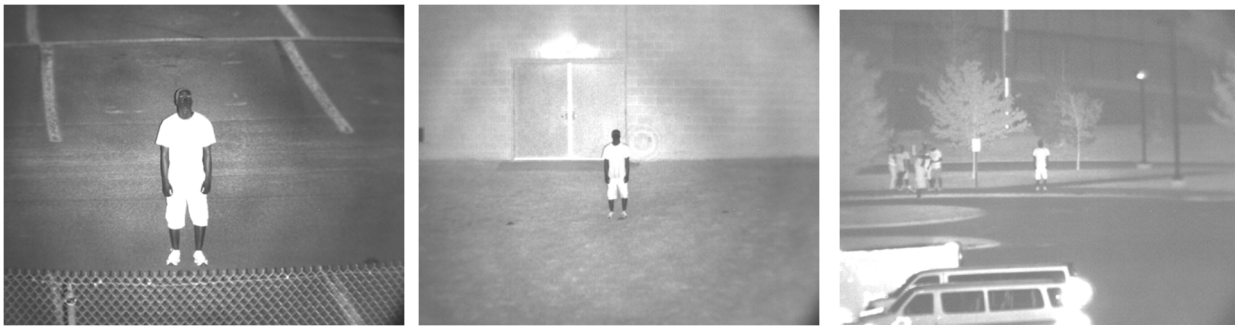

**Figure 35 SWIR, Night Time, Long Range Imagery**

**This is sample imagery taken from the WVU data collection under complete darkness. (left) Range of 100 meters. (center) Range of 200 meters. (right) Range of 350 meters.**

Appendix 6.4 contains the public release and consent forms used during this data collection. Sample high resolution, visible imagery taken in the WVU laboratory is also found there.

## 4.2 Speckle Reduction

### 4.2.1 Speckle Metric

To judge the strength of each speckle reduction method described in Section 2.3, a set of standards needs to be produced. This should allow for objective comparison. There are many developed techniques for the quantification of speckle noise[21]; however, for this application, a ratio of standard deviation to mean will be used. The metric will be applied over the whole image, down each column, or can be run on a single row. A MATLAB program was developed to perform these tasks and can be found in Appendix 6.3.

### 4.2.2 Experimental Results

#### *4.2.2.1 Control of Spatial Coherence*

The vibrating technique will be examined in this exercise. The experimental setup is sourced by multimode fiber coupled laser diode operating at a wavelength greater than 1400 nm. The fiber is then vibrated with a rotational counterbalance motor. This "shaker" unit is assembled to match other COTS fiber shakers found with a web search. Figure 36 illustrates the illumination spot with the vibrator off and vibrator on. It also denotes the resulting standard deviation scores (lower value indicates better speckle reduction).

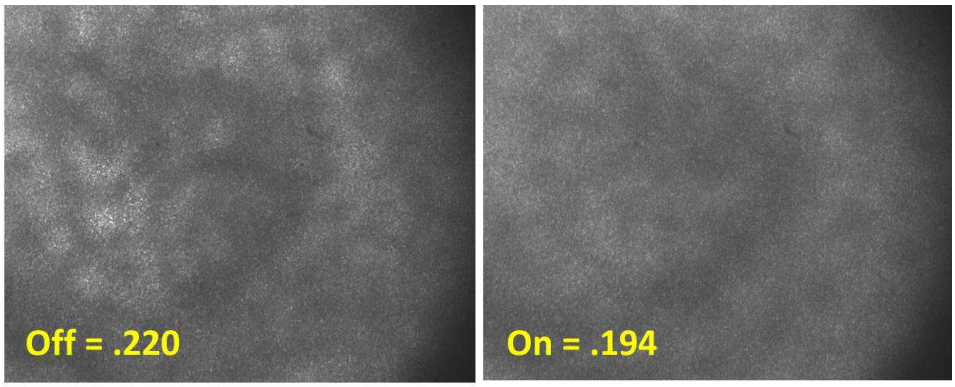


**Figure 36 Laser Speckle**

**(left) Vibrator off. (right) Vibrator on.**

#### *4.2.2.2 Control of Temporal Coherence*

This experimental setup consists of an OEQuest swept wavelength laser[22] and a Manlight amplifier [6]. Since both the source and the amplifier are single mode fiber devices, they were passed through a mode conditioning patch cord. This device converts the single mode signal to multimode by implementing a small offset of fiber alignment. Once multiple modes are present, the multimodal vibration necessary for speckle reduction can be accomplished. Figure 37 illustrates a "no sweep" single wavelength, a 1 kHz sweep, and 1 kHz sweep and vibration combination.


**Figure 37 Swept Laser**

**(left) No Sweep. (center) Sweep. (right) Vibrate and sweep.**

### 4.2.3 Results Analysis

Substantial improvements can be seen with both of the aforementioned techniques analyzed. However, due to the small spectral range of the second generation System, the swept laser cannot be used alone. Mechanical vibrations will also need to be applied for adequate speckle reduction. Also, the metric seems to be useful for a low level measurement within very controlled environment. However, comparing two separate illumination sources seems to be difficult. Other techniques will be explored in future work.

## 4.3 SWIR Signatures

### 4.3.1 Signatures Background

While the primary goal of the System is to detect and identify people, the unique signatures produced in its imagery can offer the user a valuable tool in accessing and averting threats. There are many signatures that differ from the visible and thermal infrared bands. A few of these along with facial recognition statistics will be presented in the following sections.

### 4.3.2 Facial Signatures

As discussed in Section 4.1.3, the data collection conducted at WVU produced a data set of 104 individuals at three distances performing in various scenes. Figure 38 illustrates two of these individuals. These are the frontal, neutral poses typically acquired by the System for use in facial recognition. All three distances are displayed along with the associated visible-spectrum mug shot.

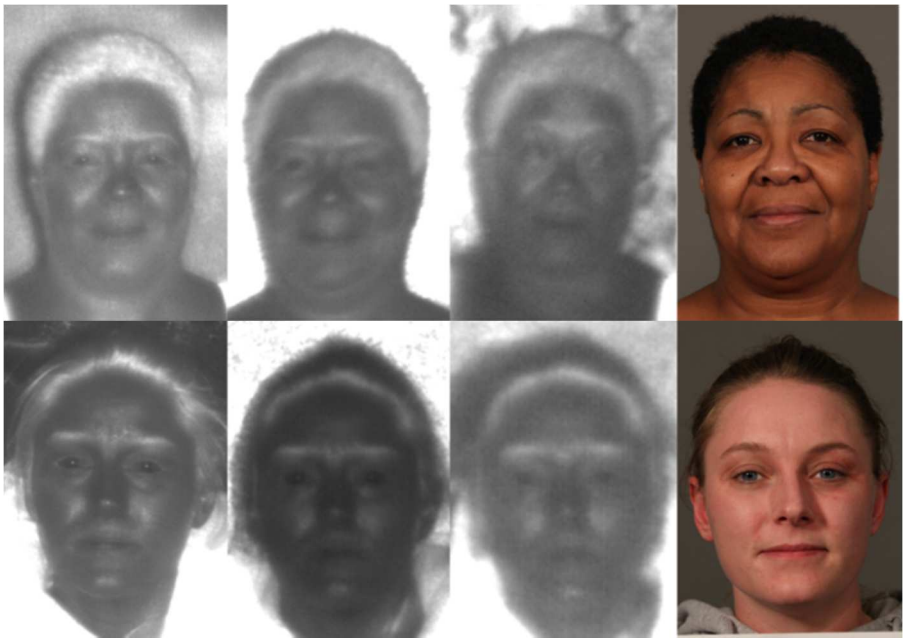

**Figure 38 System SWIR Facial Images**

**Target ranges of 100, 200, and 350 meters in complete darkness followed by their associated visible-spectrum mug shots.**

### 4.3.3 Full Body Signatures

As previously mentioned, facial recognition is conducted at distances of up to 400 meters. Beyond this point, the System still produces very useful imagery. Typical applications in this range are person detection, tracking, and manually recognized object identification. Figure 39 illustrates such imagery with data acquired in the fall of 2012 at Camp Roberts, California. At ranges of 1,000 meters, 1,700

meters, and 3,000 meters, all three images are taken in complete darkness. As can be seen with the first image, some facial features are still present including the target's mustache and glasses. His automatic assault rifle is also clearly identified. As can be expected, the resolution and signal to noise level decreases as distance increases. However, images (b) and (c) still provide ample information into the targets' actions and location.

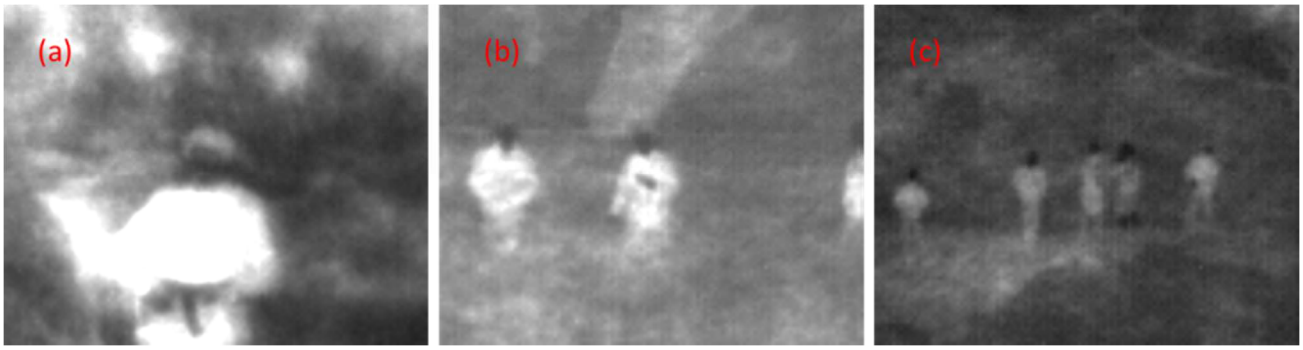


**Figure 39 System human imagery**

**All images were taken under complete darkness at ranges of (a) 1,000 meters (b) 1,700 meters (c) 3,000 meters.**

### 4.3.4 Water Signatures

Within the SWIR band, the absorption coefficient of water is three orders of magnitude higher than the visible band[23]. This produces a very unique characteristic for imaging water structures. Figure 40 illustrates this effect. A snow pile looks bright white as it is typically seen in the visible spectrum. However, when viewed in the SWIR band, it is completely black. This could prove useful in situations where a person is clothed in white camouflage and is concealing themselves in areas of snow. They would appear bright white with a completely black surrounding. Also, a person in wet clothing would stand out when in front of lighter backgrounds.

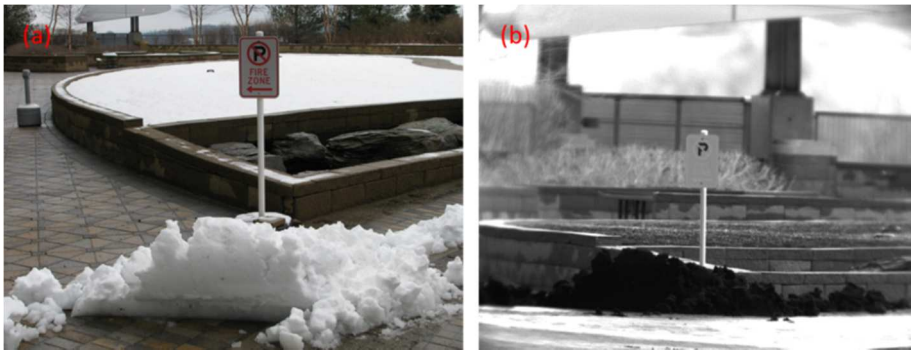


**Figure 40 SWIR Snow Signature**

**(a) Visible Spectrum image of snow pile. (b) SWIR imagery of snow pile.**

### 4.3.5 Clothing Signatures

The fibers used to make clothing produce a very unique signature when viewed through the System. Color as typically viewed is well outside of the SWIR band. It has no influence on the imaged intensity. However, the type of fibers used for the clothing play a large role. Figure 41 illustrates a few scenes involving clothing types. Images (a) and (b) show the same black, 100% cotton pullover sweatshirt. They are, however, imaged at two different contrast levels. Images (b) and (c) share the same contrast

level. However, the shirt worn in (c) is a synthetic blend. This is very interesting because the large signal produced from the cotton shirt gives a stark contrast to the vegetation in the background.

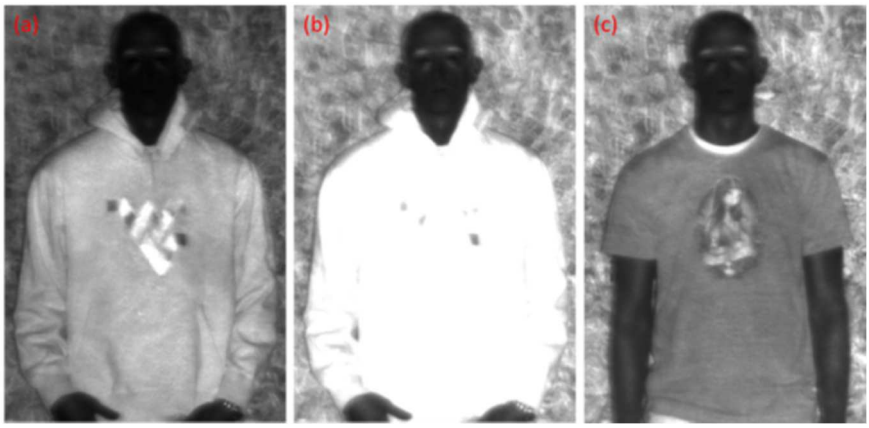


**Figure 41 SWIR Clothing Signature**

**(a) Black, 100% cotton sweatshirt (b) Same image as image "a" but with contrast level to match image "c" (c) Synthetic blend t-shirt**

Person detection of someone in camouflage is again a viable option for this technology. While thermal infrared imaging is an excellent tool for person detection, the System has a great advantage over this technology given the fact it can produce more details of the target. Figure 42 illustrates this point where a simulated sniper can be seen crawling in the prone position at a distance of 393 meters in complete darkness. Visible spectrum imagery during daylight hours would produce a scene that would be very difficult to distinguish the sniper and would be impossible at night without giving up the imager's location. However, the System produces imagery that even gives details of the potential threat such as the two-way radio attached to his belt.

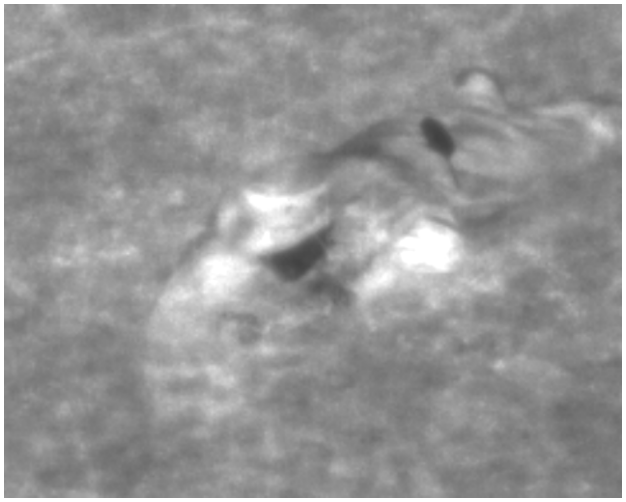

**Figure 42 Simulated Sniper**

**Simulated sniper crawling into position in total darkness at a distance of 393 m.**

### 4.3.6 Retro Reflection

Snipers go to great lengths to conceal themselves in order to reach their firing position. Typically they cover themselves in native foliage or wear ghillie suits. Another simulated sniper, this one wearing a ghillie suit, is shown in Figure 43. These images were acquired at a range of 1,815 meters in complete darkness. Here again the large contrast between the vegetation background and synthetic fibers can be seen.

One advantage the System has over passive systems is the ability to take advantage of the back scatter caused by the illuminator. Images (b) and (c) of Figure 43 show the retro reflection seen when the illumination spot is pointed towards optics. The target's binoculars and rifle scope produce pixel saturation points where there are very small signal levels elsewhere. This very easily gives up the target's location.

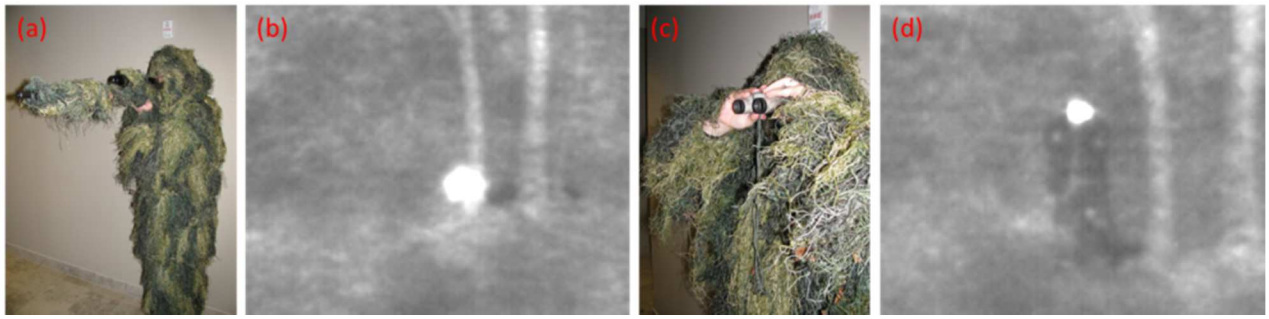


**Figure 43 Ghillie Suit / Retro Reflection**

**(a) Target with sniper rifle and wearing ghillie suit. (b) Target wearing ghillie suit in prone position behind tree looking at the System with rifle scope at a distance of 1,815 meters in total darkness. (c) Target with binoculars and wearing ghillie suit. (d) Target wearing ghillie suit standing beside tree looking at the System with binoculars at a distance of 1,815 meters in total darkness.**

## 4.4 Facial Recognition Data Analysis

### 4.4.1 Partner Analysis

The facial imagery generated by the System is of interest not only to the WVHTCF but other groups as well. The second collection dataset was shared with two research groups[6,7] at WVU to train and test face recognition algorithms they generated in house. In his paper, Kalka describes pre-processing the SWIR images before submission using MorphoTrust's FaceIt G8. He was able to acquire a 90% rank 1 positive match rate with the 50 meter data and 80% success rate for the 106 meter images. Similar results were described in Zuo's paper. Here a false acceptance rate of 0.1%, a correct response rate of 85% at 50 meters and 74% at 106 meters were achieved.

Similarly, all datasets have been given to MorphoTrust to generate, train, and test their pre-processing SWIR algorithms. This work directly relates to the plugin they supply to the System. Figure 44 illustrates the results of this work when testing against the second data collection images. This is a plot of the receiver operator characteristics (ROC) of the 50 meter and 106 meter data. The submissions include the fusion of nine images of each person. They submitted three frontal images with neutral expressions, two images with the subject speaking, and four images containing a ten degree pose angle. The gallery consisted of the entire second data collection's visible spectrum mug shots. At a false acceptance rate of 1%, a correct acceptance rate of 70% was achieved for both the 50 and 106 meter data.

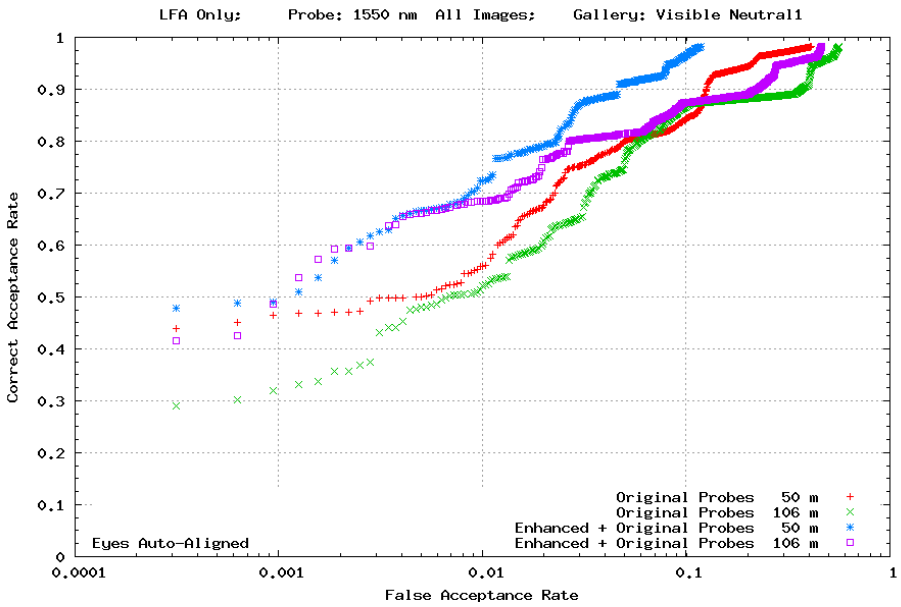


**Figure 44 Receiver Operating Characteristic**

**Receiver operating characteristic generated by MorphoTrust USA using the System images of 56 test subjects at 50-m and 106-m range in total darkness. Correct Acceptance Rate of roughly 70% was achieved with False Acceptance Rate of 1% at both distances.**

### 4.4.2 In-House Analysis

Figure 45 depicts two screenshots of the System facial recognition standalone GUI. These are two successful Rank 1 matches at ranges of 200 meters and 350 meters taken from the third data collection in complete darkness. The gallery used for this exercise contains greater than 1,600 people. The imagery is taken from the video files replayed at the time of analysis. From the figures below, many traits of the facial recognition system can be seen. First, the red crosses on the top left image represent eye location. The system tries to identify them automatically first for facial orientation. If none are found, the operator can input them manually. Eight of the eleven probe images were "good" faces where the system found correct eye position for the 200 meter images. As for the 350 meter case, nine of the eleven images were correctly marked. The top right image is the Rank 1 or most likely candidate after matching. The smaller faces below are the lower ranks in descending order. Their scores can be displayed by hovering the mouse.

**Figure 45 Facial Recognition Screenshots**

**Example screen shots showing the System face recognition video under dark nighttime conditions at distances of (*left*) 200 m and (*right*) 350 m. In both cases, the correct individual was chosen from a database containing visible-spectrum images of more than 1,600 people.**

At the time of the following study, the third data collection was only approximately one half complete. Only 42 participants were included. Figure 46 illustrates a cumulative match characteristics (CMC) curve of the 100 meter images. This curve illustrates the probability that the system will obtain a correct match at a given rank or better. The database used here is closed meaning each SWIR subject has a corresponding visible spectrum gallery image. There are no outside images contained within the gallery making the size 42. Fifteen probe images were submitted. There were five non-sequential video frames with three post-processed contrast levels for each. The score was then recorded. This process was conducted for each of the 42 individuals. As can be seen from the figure, 63% of the individuals tested received a top matching rank.

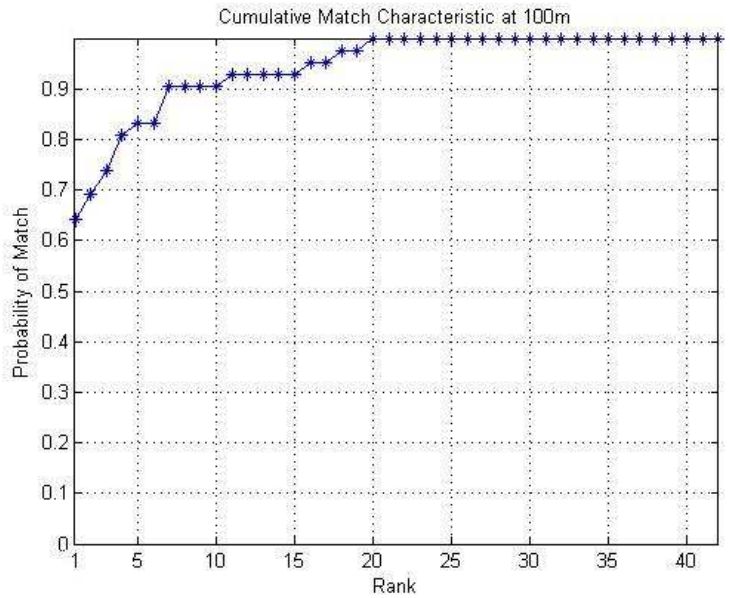


**Figure 46 100 meter Cumulative Match Characteristics Plot**

**Facial data collected at 100 meters in total darkness with a database size of 42 people. Note that for this experiment the Rank 1 probability is 63%, indicating that the correct person from the 46 person database was chosen 63% of the time.**

Appendix 6.5 contains the Matlab code and details used to generate the data and the plot above.

## 4.5 Additional Imagery

Over its lifetime of operation, the System has produced a large amount of interesting data. The following are images acquired by the system that did not fall within the previous sections. It should be noted that these images are not a qualitative measure of the system in any way. They will only illustrate interesting imagery that can be seen by the System in various situations.


**Figure 47 Shinnston Water Tower**

**At a range of 2,550 meters, this set of water towers is typically used for calibration as it is easily viewable from the WVHTCF research center. (left) Medium FOV daylight. (center) Medium FOV nighttime. (right) Narrow FOV nighttime. Notice personnel ladder and radio antenna.**

**Figure 48 Radio Tower and Wind Turbines**

**These are collected during passive, daylight illumination. The radio tower is at a range of 6.1 km from the WVHTCF research building in Fairmont, WV. The wind turbines are at a range of 48 km and located east of Morgantown, WV.**

**Figure 49 Whitetail Deer**

**Acquired at a range of approximately 400 meters in complete darkness.**

**Figure 50 Cigarette Signature**

**Flames produce a large signal.  Acquired at a range of 100 meters in complete darkness.**

**Figure 51 Pronghorn**

**Acquired at Fort Huachuca, Arizona during daylight passive illumination and at a range of approximately 300 meters.**

**Figure 52 Through Glass Viewing**

**The active illumination gives the System the advantage of looking into cars were passive systems would not have the available light. (left) 60 meter range, daylight. (right) 300 meter range, nighttime.**

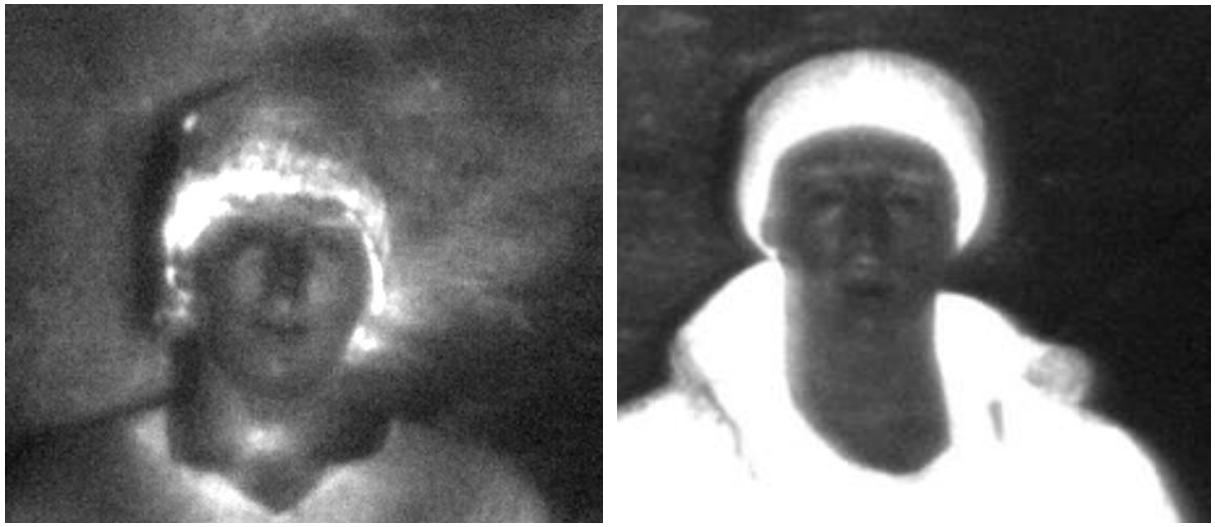

**Figure 53 Heavy Rain**

**These images were taken at night, through very heavy rain, and 70 mph wind gusts. (left) 314 meter range. (right) 297 meter range.**

# 5 Discussion and Future Work

Current technology such as visible-spectrum high resolution imaging and thermal infrared show weaknesses in night time operation and feature preservation respectively. Research was conducted to design and construct a system capable of long range, night time facial recognition. The aforementioned system has very much bridged this gap. The mobile and rugged system is shown below in Figure 54.

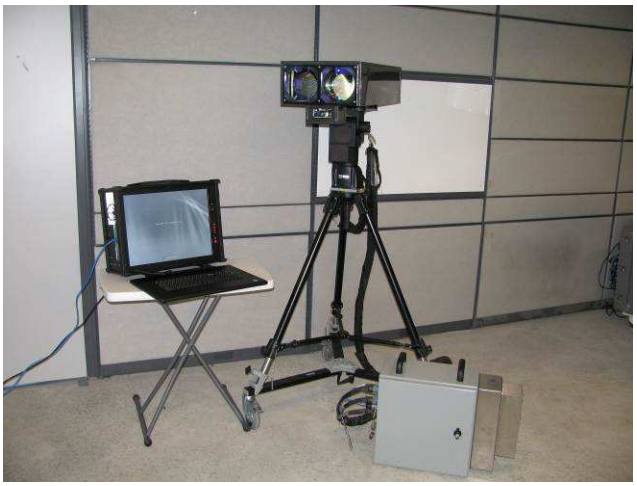

**Figure 54 System 2.**

Although matching SWIR facial imagery to a database of visible-spectrum mug shots still holds its challenges, the System achieves repeatable results to distances of 400 meters. Beyond that mark, the imagery is very good for object tracking, behavior monitoring, and wide area surveillance out to distances of 3,000 meters in complete darkness. Figure 55 shows both successful facial recognition at 350 meters with a database of over 1,600 people and also long range person detection of over 3,000 meters.

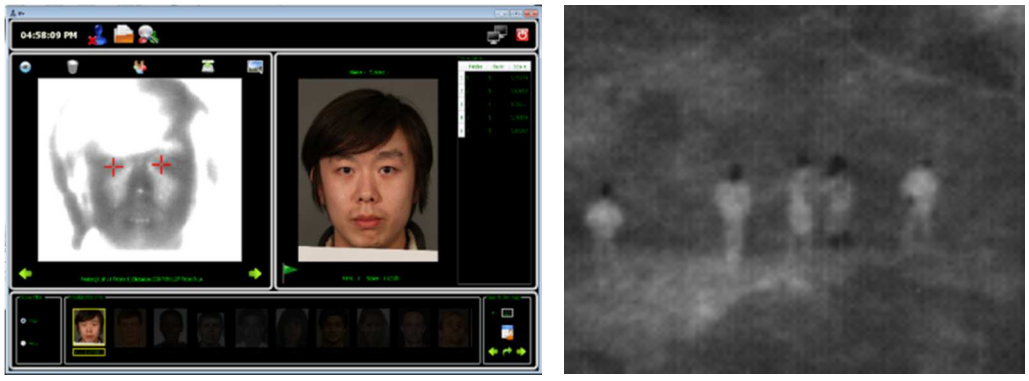


**Figure 55 System Screenshots**

**(left) Example screen shot of the System face recognition video under nighttime conditions at a distance of 350 meters. The correct individual was chosen from a database containing visible-spectrum images of more than 1,600 people. (right) Person detection under complete darkness at a range of over 3,000 meters.**

The tasks involved in this project span from basic research to hardware development. An initial scan of technologies was conducted to see if a system could be purchased to suit these needs. Once this was

proven to be impossible, researching each individual component necessary to produce the system was performed. Many models were designed and simulated to validate performance. Figure 56 illustrates the complexity of the solid models used to design each piece of the system.

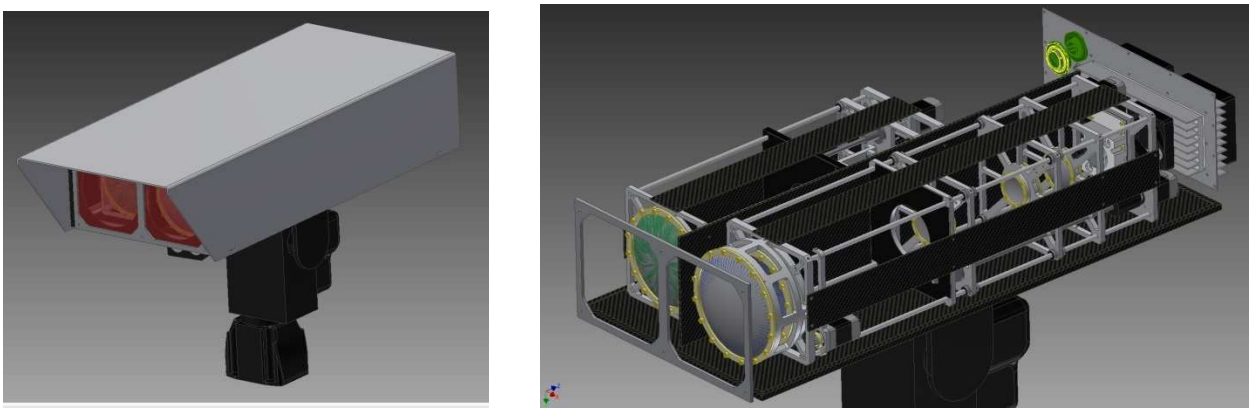

**Figure 56 The System Solid Model**

**(left) System 2 with environmental enclosure and sun visor. (right) System 2 interior components.**

Ultimately, all components were fabricated and brought together into a functioning system. These units have made their way across the country functioning in all conditions from California to Louisiana and including points in between. In each situation, the system has brought about imagery that has never been produced by any other device.

Currently the usability of the system is being improved upon. Whereas tracking to date is mostly manually controlled, the process is being automated. The system will detect any movement and decide whether it is human activity. The system would then zoom in on the head and check for a high quality face for recognition. These images will then be matched against the gallery and the user will be alerted if a high confidence match has been made. The implementation of these features will minimize the user's involvement in the system's activity freeing him/her to tend to more important tasks.

Facial recognition scoring schemes are also being improved upon. With current funding, methods are being developed to again get the user out of the loop. This involves achieving a better understanding of the current facial matching system and the relation between the SWIR and visible images. Once this occurs, scoring methods to discard false positives and spurious results can be implemented to achieve higher confidence matches.

# 6 Appendix

## 6.1 Eye Safety Data

### 6.1.1 Eye Safety Tables

**Table 4 – Accessible emission limits for Class 1 and Class 1M laser products and $C_6 = 1$ [a, b]**

| Wave-length $\lambda$ nm | Emission duration $t$ s | | | | | | | | | | |
|---|---|---|---|---|---|---|---|---|---|---|---|
| | $10^{-13}$ to $10^{-11}$ | $10^{-11}$ to $10^{-9}$ | $10^{-9}$ to $10^{-7}$ | $10^{-7}$ to $1{,}8 \times 10^{-5}$ | $1{,}8 \times 10^{-5}$ to $5 \times 10^{-5}$ | $5 \times 10^{-5}$ to $1 \times 10^{-3}$ | $1 \times 10^{-3}$ to 0,35 | 0,35 to 10 | 10 to $10^2$ | $10^2$ to $10^3$ | $10^3$ to $3 \times 10^4$ |
| 180 to 302,5 | $3 \times 10^{10}$ W·m$^{-2}$ | | 30 J·m$^{-2}$ | | | | | | | | |
| 302,5 to 315 | $2{,}4 \times 10^4$ W | | Thermal hazard ($t \le T_1$) $7{,}9 \times 10^{-7}$ $C_1$ J | | | | | Photochemical hazard $7{,}9 \times 10^{-7}$ $C_2$ J ($t > T_1$) | $7{,}9 \times 10^{-7}$ $C_2$ J | | |
| 315 to 400 | | | $7{,}9 \times 10^{-7}$ $C_1$ J | | | | | | $7{,}9 \times 10^{-3}$ J | | $7{,}9 \times 10^{-6}$ W |
| 400 to 450 | $5{,}8 \times 10^{-9}$ J | $1{,}0\ t^{0{,}75}$ J | $2 \times 10^{-7}$ J | | $7 \times 10^{-4}\ t^{0{,}75}$ J | | | | $3{,}9 \times 10^{-3}$ J | | $3{,}9 \times 10^{-5}$ C W |
| 450 to 500 | | | | | | | | | $3{,}9 \times 10^{-3}$ $C_3$ J and [c] $3{,}9 \times 10^{-4}$ W | | |
| 500 to 700 | | | | | | | | | $3{,}9 \times 10^{-4}$ W | | |
| 700 to 1 050 | $5{,}8 \times 10^{-9}$ $C_4$ J | $1{,}0\ t^{0{,}75}$ $C_4$ J | $2 \times 10^{-7}$ $C_4$ J | | $7 \times 10^{-4}\ t^{0{,}75}$ $C_4$ J | | | | $3{,}9 \times 10^{-4}$ $C_4$ $C_7$ W | | |
| 1 050 to 1 400 | $5{,}8 \times 10^{-8}$ $C_7$ J | $10{,}4\ t^{0{,}75}$ $C_7$ J | $2 \times 10^{-6}$ $C_7$ J | | | $3{,}5 \times 10^{-3}\ t^{0{,}75}$ $C_7$ J | | | | | |
| 1 400 to 1 500 | $8 \times 10^5$ W | | $8 \times 10^{-4}$ J | | | | $4{,}4 \times 10^{-3}\ t^{0{,}25}$ J | $10^{-2}\ t$ J | $1{,}0 \times 10^{-2}$ W | | |
| 1 500 to 1 800 | $8 \times 10^6$ W | | $8 \times 10^{-3}$ J | | | | | $1{,}8 \times 10^{-2}\ t^{0{,}75}$ J | | | |
| 1 800 to 2 600 | $8 \times 10^5$ W | | $8 \times 10^{-4}$ J | | | | $4{,}4 \times 10^{-3}\ t^{0{,}25}$ J | $10^{-2}\ t$ J | | | |
| 2 600 to 4 000 | $8 \times 10^4$ W | | $8 \times 10^{-5}$ J | $4{,}4 \times 10^{-3}\ t^{0{,}25}$ J | | | | | | | |
| 4 000 to $10^6$ | $10^{11}$ W·m$^{-2}$ | | 100 J·m$^{-2}$ | $5\,600\ t^{0{,}25}$ J·m$^{-2}$ | | | | | 1 000 W·m$^{-2}$ | | |

NOTE Laser products that meet the requirements for classification as Class 1 by satisfying measurement conditions 1 and 2 may be hazardous when used with viewing optics having greater than ×7 magnification or objective diameters greater than those specified in Table 11.

[a] For correction factors and units, see Table 10

[b] The AELs for emission durations less than $10^{-13}$ s are set to be equal to the equivalent power or irradiance values of the AEL at $10^{-13}$ s.

[c] In the wavelength range between 450 nm and 500 nm, dual limits apply and a product's emission must not exceed either limit applicable to the class assigned.

**Figure 57 Permissible Power Level**

**Table 4 of the IEC 60825 eye standards.**

**Table 10 – Correction factors and breakpoints for use in AEL and MPE evaluations**

| Parameter | Spectral region nm |
|---|---|
| $C_1 = 5{,}6 \times 10^3\ t^{0{,}25}$ | 180 to 400 |
| $T_1 = 10^{0{,}8(\lambda - 295)} \times 10^{-15}$ s | 302,5 to 315 |
| $C_2 = 30$ | 180 to 302,5 |
| $C_2 = 10^{0{,}2(\lambda - 295)}$ | 302,5 to 315 |
| $T_2 = 10 \times 10^{[(\alpha - \alpha_{min})/98{,}5]}$ s | 400 to 1 400 |
| $T_2 = 10$ s for $\alpha < 1{,}5$ mrad | 400 to 1 400 |
| $T_2 = 100$ s for $\alpha > 100$ mrad | 400 to 1 400 |
| $C_3 = 1{,}0$ | 400 to 450 |
| $C_3 = 10^{0{,}02(\lambda - 450)}$ | 450 to 600 |
| $C_4 = 10^{0{,}002(\lambda - 700)}$ | 700 to 1 050 |
| $C_4 = 5$ | 1 050 to 1 400 |
| $C_5 = N^{-1/4}$ [a] | 400 to $10^6$ |
| $C_6 = 1$ | 180 to 400 and 1 400 to $10^6$ |
| $C_6 = 1$ for $\alpha \leq \alpha_{min}$ [b] | 400 to 1 400 |
| $C_6 = \alpha/\alpha_{min}$ for $\alpha_{min} < \alpha \leq \alpha_{max}$ [b] | 400 to 1 400 |
| $C_6 = \alpha_{max}/\alpha_{min} = 66{,}7$ for $\alpha > \alpha_{max}$ [b,c] | 400 to 1 400 |
| $C_7 = 1$ | 700 to 1 150 |
| $C_7 = 10^{0{,}018(\lambda - 1\,150)}$ | 1 150 to 1 200 |
| $C_7 = 8$ | 1 200 to 1 400 |

$\alpha_{min} = 1{,}5$ mrad
$\alpha_{max} = 100$ mrad

$N$ is the number of pulses contained within the applicable duration (8.3 f) and Clause A.3).

NOTE 1 There is only limited evidence about effects for exposures of less than $10^{-9}$ s for wavelengths less than 400 nm and greater than 1 400 nm. The AELs for these emission durations and wavelengths have been derived by calculating the equivalent radiant power or irradiance from the radiant power or radiant exposure applying at $10^{-9}$ s for wavelengths less than 400 nm and greater than 1 400 nm.

NOTE 2 See Table 11 for aperture stops and Table A.4 for limiting apertures.

NOTE 3 In the formulae in Tables 4 to 9 and in these notes, the wavelength must be expressed in nanometres, the emission duration $t$ must be expressed in seconds and $\alpha$ must be expressed in milliradians.

NOTE 4 For emission durations which fall at the cell border values (for instance 10 s) in Tables 4 to 9, the lower limit applies. Where the symbol "<" is used, this means less than or equal to.

[a] $C_5$ is only applicable to pulse durations shorter than 0,25 s.
[b] $C_6$ is only applicable to pulsed lasers and to CW lasers for thermal retinal limits.
[c] The maximum limiting angle of acceptance $\gamma_{th}$ shall be equal to $\alpha_{max}$ (but see 8.4 d)).

**Figure 58 Constants**

**Table 10 of the IEC 60825 eye standards.**

**Table 11 – Measurement aperture diameters and measurement distances for the default (simplified) evaluation**

| | Condition 1<br>*applied to collimated beam where e.g. telescope or binoculars may increase the hazard* | | Condition 2<br>*applied to diverging beam where e.g. magnifying glasses, microscopes may increase the hazard* | | Condition 3<br>*applied to determine irradiation relevant for the unaided eye and for scanning beams* | |
|---|---|---|---|---|---|---|
| Wavelength<br>nm | Aperture stop<br>mm | Distance<br>mm | Aperture stop<br>mm | Distance<br>mm | Aperture stop/ limiting aperture<br>mm | Distance<br>mm |
| < 302,5 | – | – | – | – | 1 | 0 |
| ≥ 302,5 to 400 | 25 | 2 000 | 7 | 70 | 1 | 100 |
| ≥ 400 to 1 400 | 50 | 2 000 | 7 | 70 | 7 | 100 |
| ≥ 1 400 to 4 000 | 7 × condition 3 | 2 000 | 7 | 70 | 1 for $t \leq 0{,}35$ s<br>$1{,}5\ t^{3/8}$ for 0,35 s < $t$ < 10 s<br>3,5 for $t \geq 10$ s ($t$ in s) | 100 |
| ≥ 4 000 to $10^5$ | – | – | – | – | 1 for $t \leq 0{,}35$ s<br>$1{,}5\ t^{3/8}$ for 0,35 s < $t$ < 10 s<br>3,5 for $t \geq 10$ s ($t$ in s) | 0 |
| ≥ $10^5$ to $10^6$ | – | – | – | – | 11 | 0 |
| NOTE The descriptions below the "Condition" headings are typical cases for information only and are not intended to be exclusive. | | | | | | |

**Figure 59 Aperture Size**

**Table 11 of the IEC 60825 eye standards.**

## 6.1.2 Eye Safety Calculation Spreadsheet

**Table 2 Eye Calculation Spreadsheet**

**This spreadsheet shows the calculations of permissible power levels at both the Class 1 and Class 1M limits at multiple wavelengths.**

| | | | | |
|---|---|---|---|---|
| 400nm-1400nm Condition III | 7 | | class 1 M aperture (400-1400) | 38.48451 |
| 1400nm-4000nm Condition I | 24.5 | | class 1 aperture (1400-4000) | 471.4352 |
| 1400nm-4000nm Condition III | 3.5 | | class 1 M aperture (1400-4000) | 9.621128 |
| | | | 5" diameter | 12667.69 |
| Permissible Powers | [mW] | | 1m diameter | 785398.2 |
| 800nm | 0.618 | | | |
| 980nm | 1.42 | | | |
| 1064nm | 1.95 | | | |
| 1550nm | 10 | | | |
| | | | | |
| **Class 1 M @ 5" Output** | | | | |
| | Permissible Intensity [mW/mm2] | Power [mW] | Intensity at 1 m Spot Size [mW/mm2] | |
| 800nm | 0.016058409 | 203.422898 | 0.000259006 | |
| 980nm | 0.036897962 | 467.4118367 | 0.000595127 | |
| 1064nm | 0.050669737 | 641.8683673 | 0.000817252 | |
| 1550nm | 1.03937922 | 13166.53061 | 0.016764147 | |
| | | 28979.59184 | | |
| | | | | |
| **Class 1 @ 1 meter Spot** | | | | |
| | Permissible Intensity [mW/mm2] | Power [mW] | Equivalent Intensity at 5" Output [mW/mm2] | |
| 800nm | 0.000314745 | 247.2 | 0.019514218 | |
| 980nm | 0.0007232 | 568 | 0.044838493 | |
| 1064nm | 0.000993127 | 780 | 0.061573988 | |
| 1550nm | 0.021211821 | 16659.72511 | 1.315135521 | |

## 6.2 System 1 LabVIEW Source Code

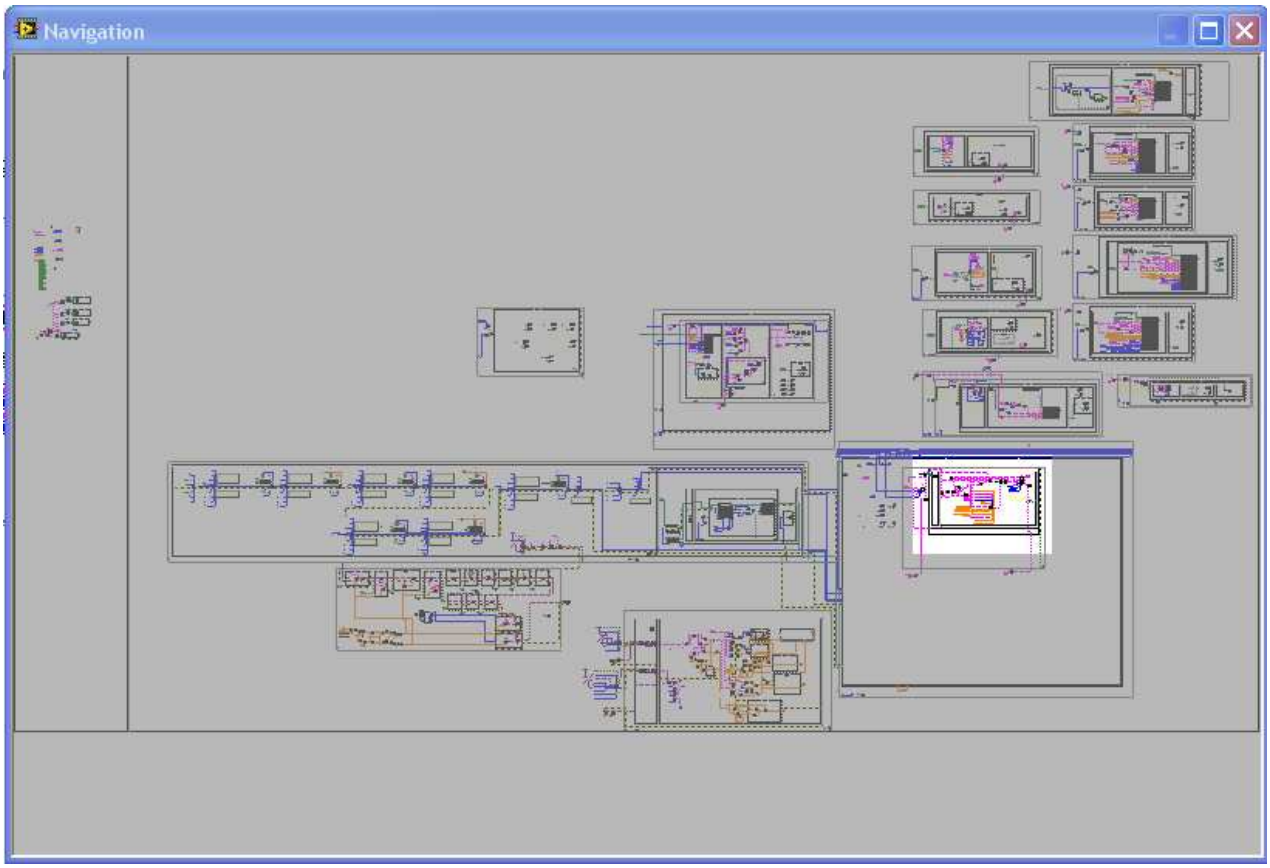


**Figure 60 System 1 LabVIEW Navigation Pane**

**This window shows a zoomed-out view of the entire System 1 LabVIEW program.**

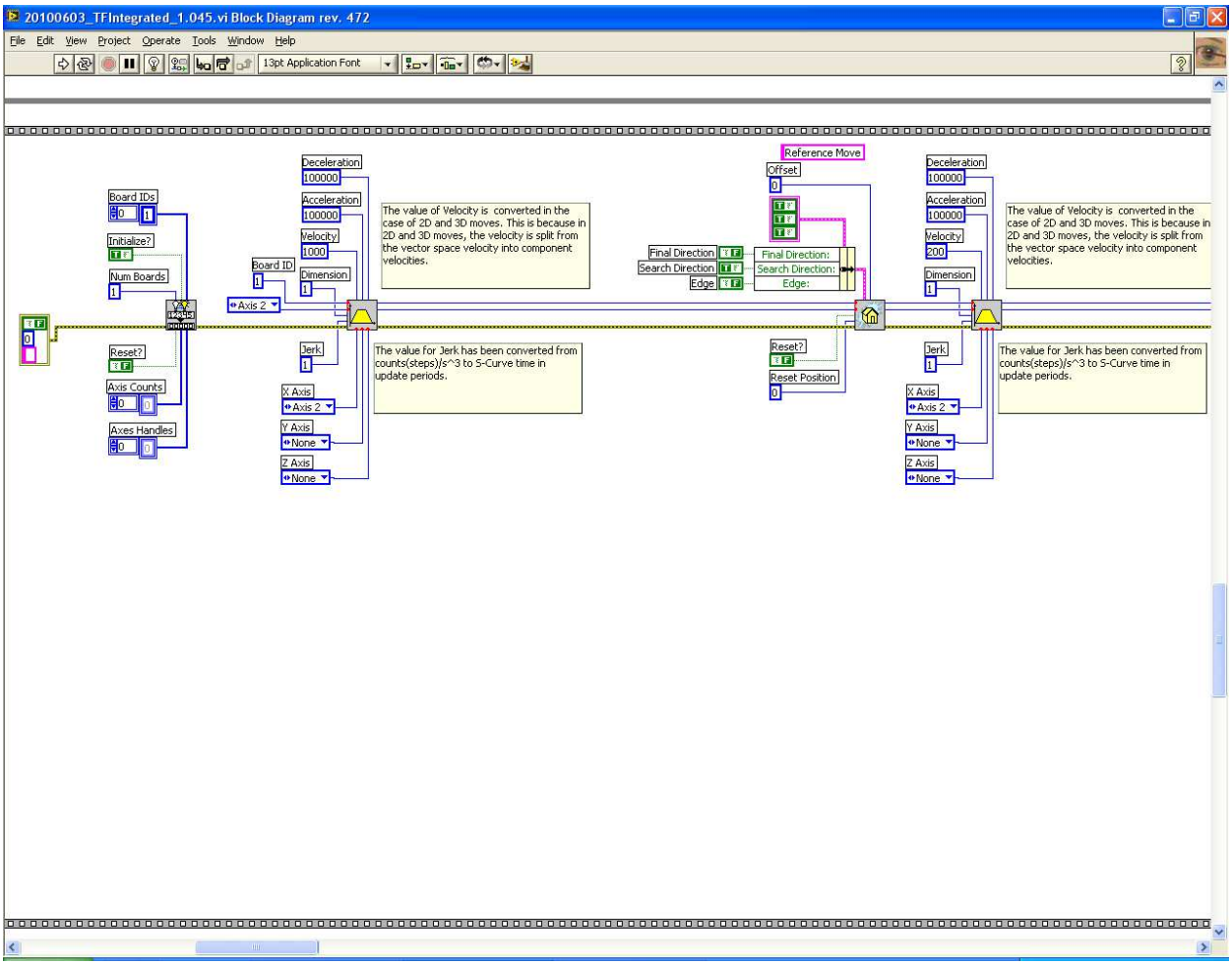


**Figure 61 Initialization Process**

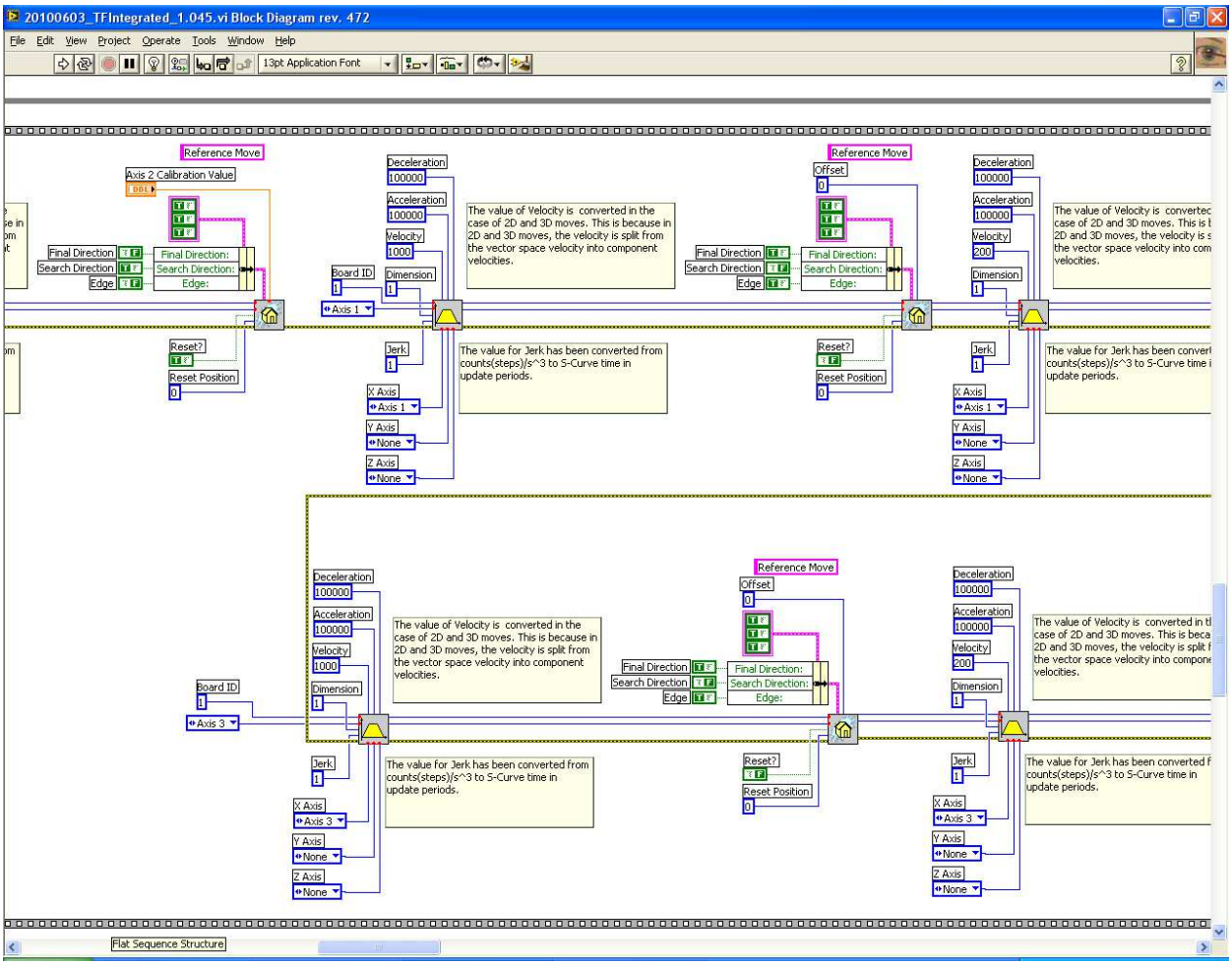


**Figure 62 Initialization Process**

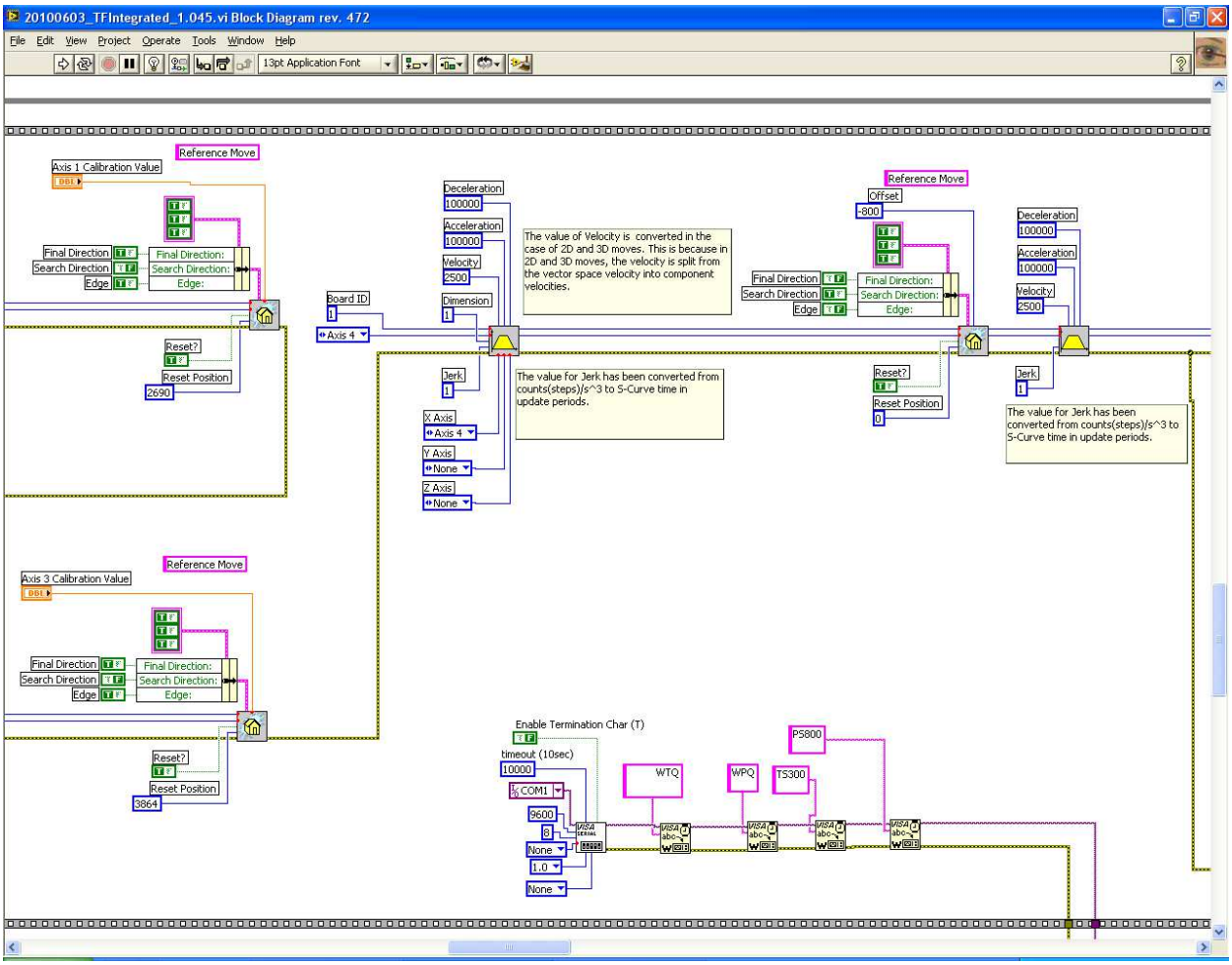


**Figure 63 Initialization Process**

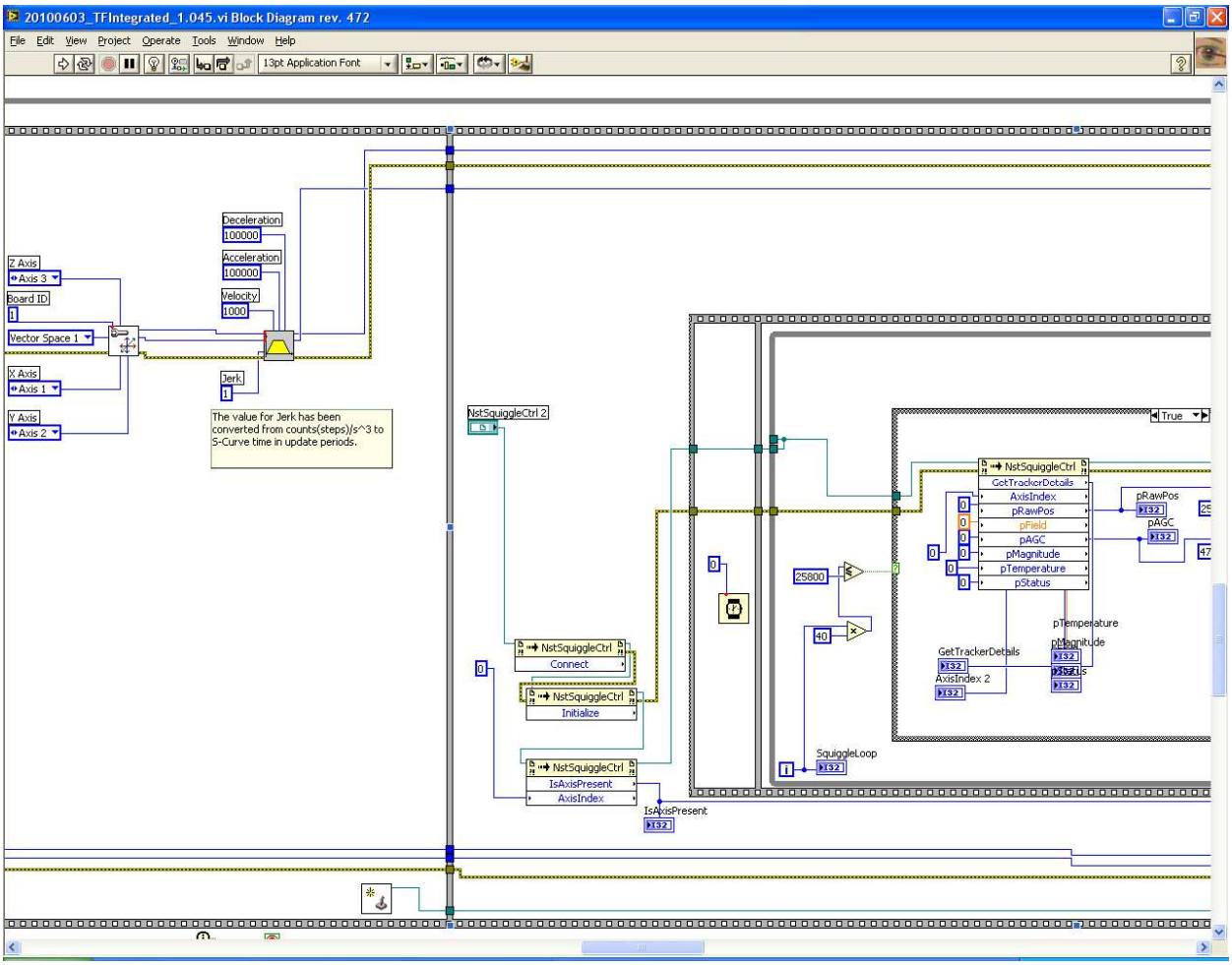


**Figure 64 Initialization Process**

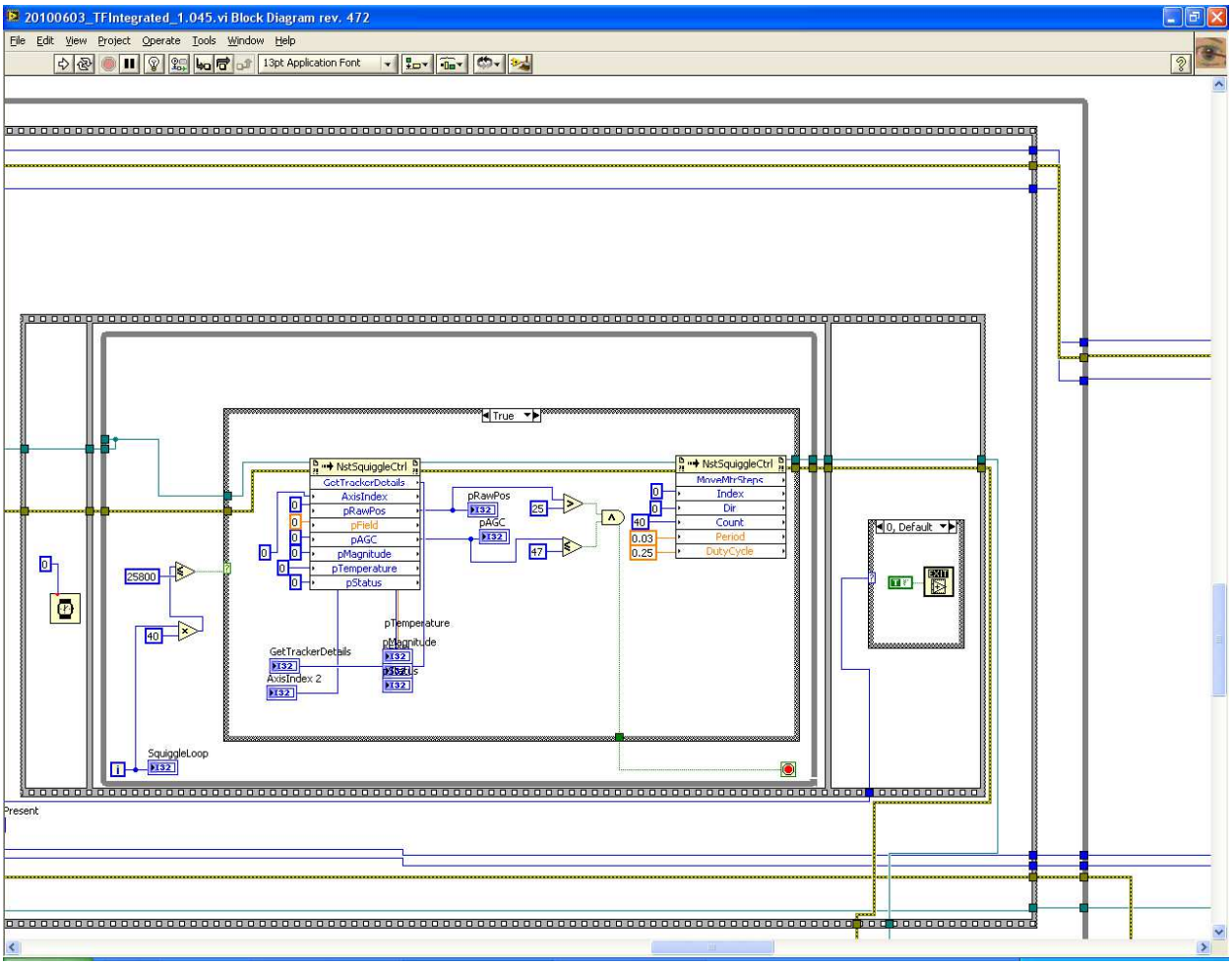


**Figure 65 Initialization Process**

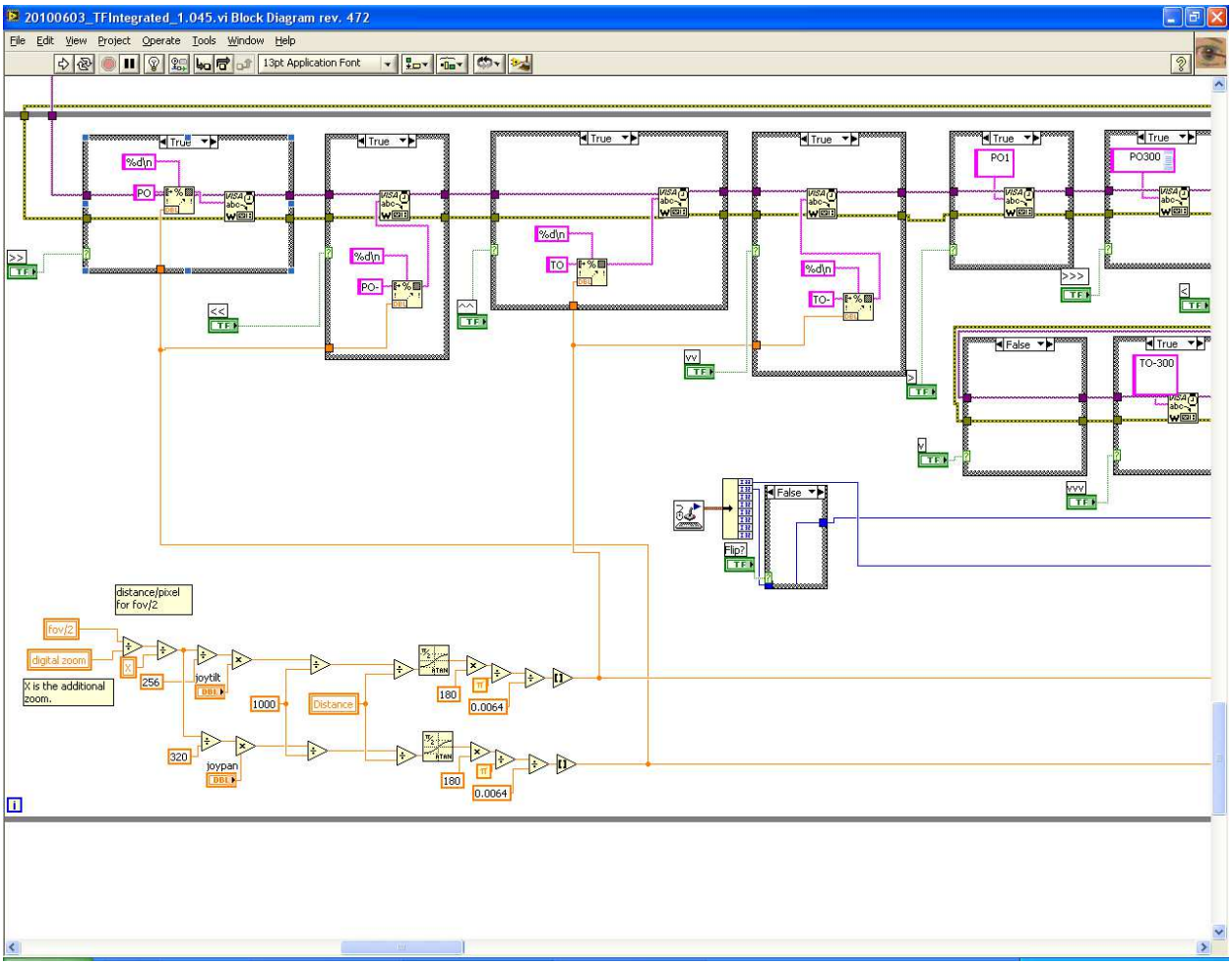


**Figure 66 Calculate Zoom and Set Lens Positions**

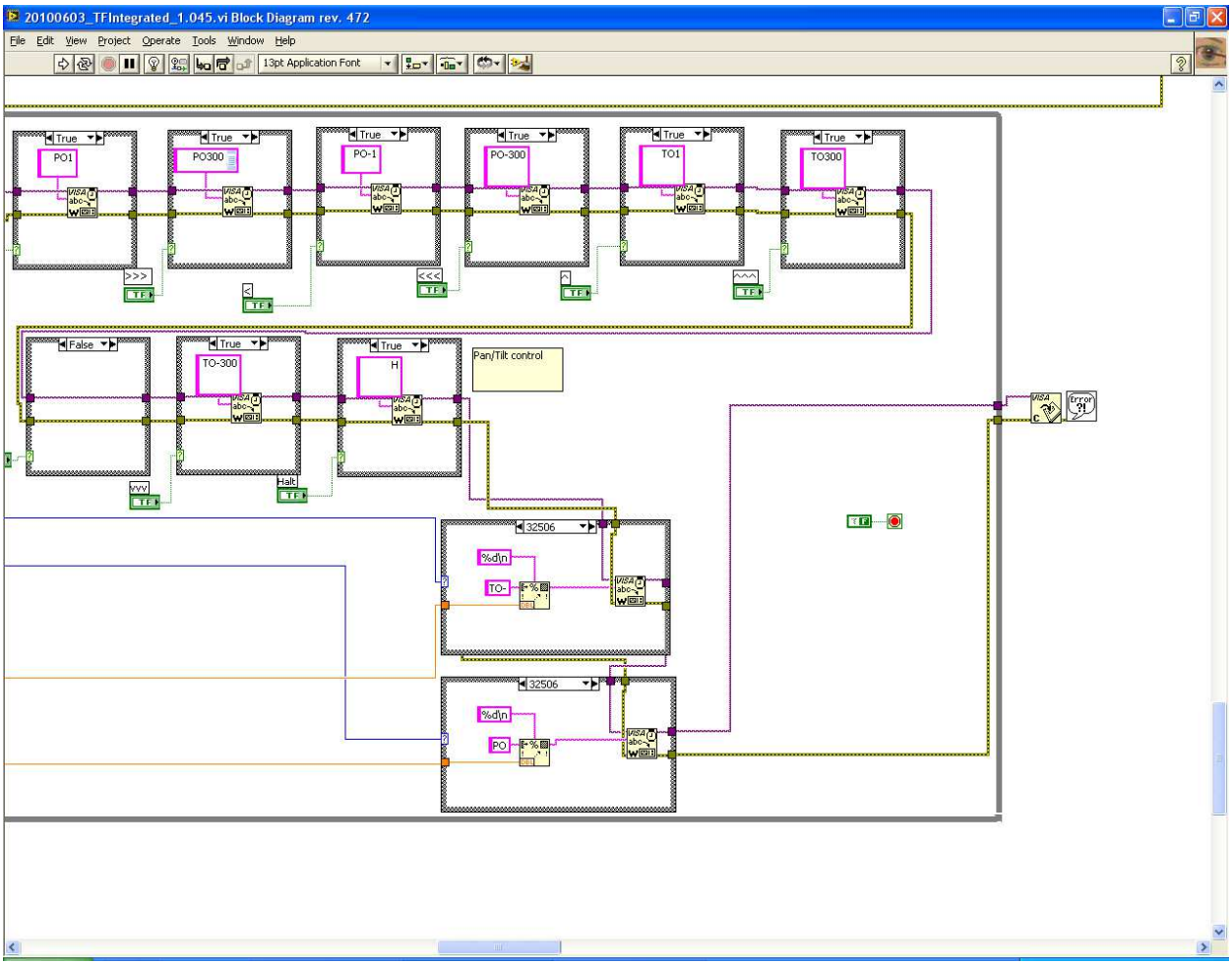


**Figure 67 Set Lens and PTU Position**

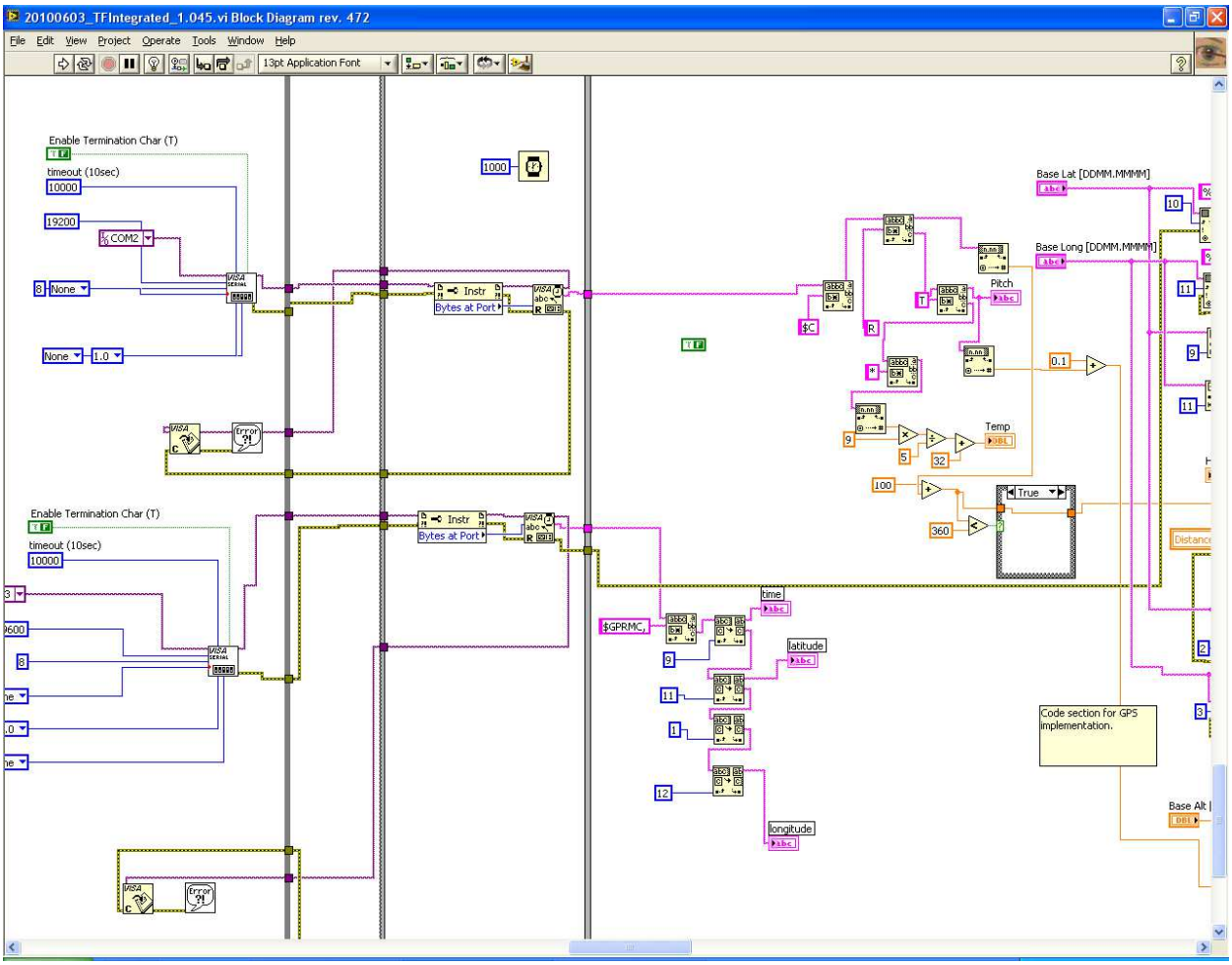


**Figure 68 Initialize Main Loop and Serial Ports**

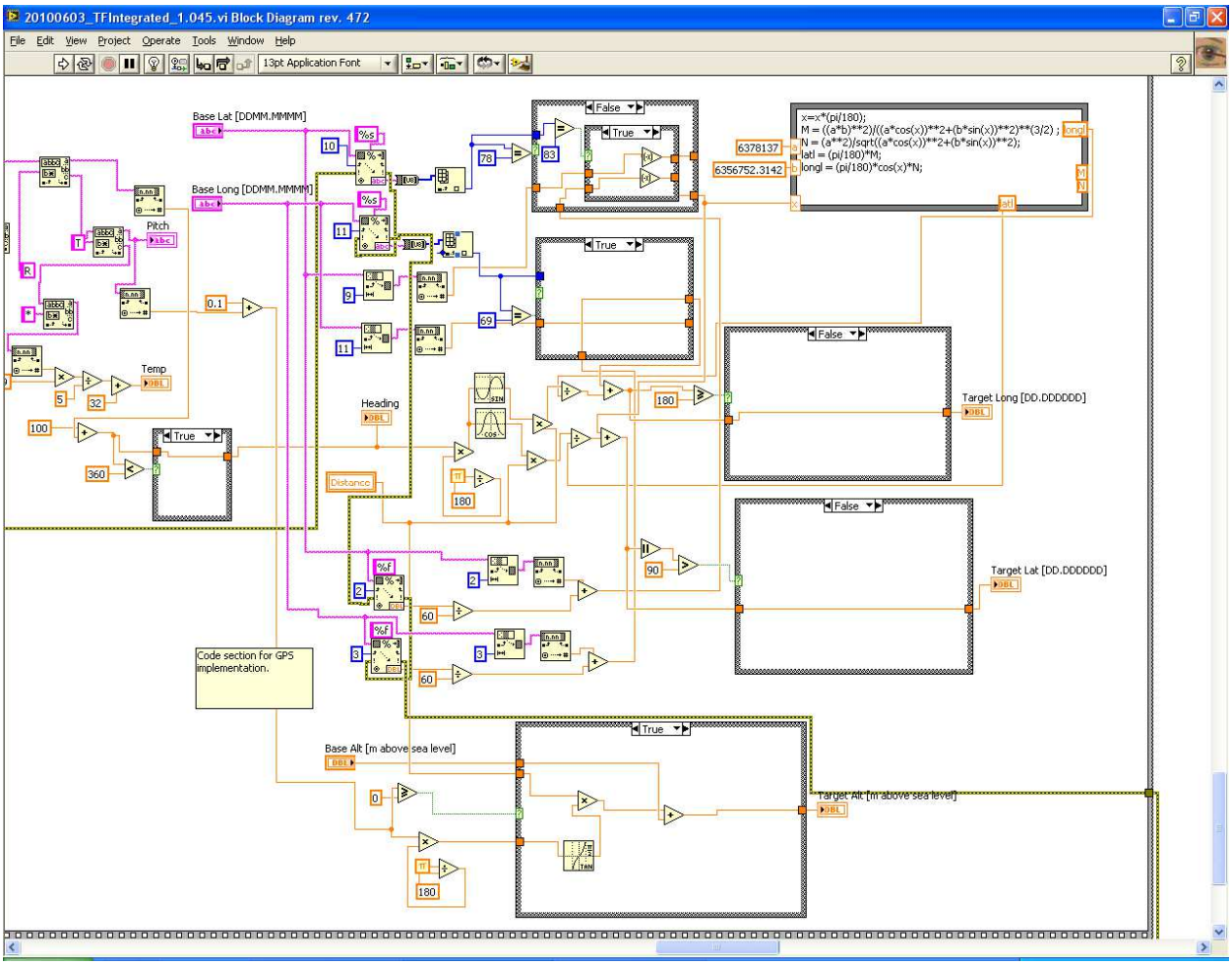


**Figure 69 Calculate Target Position**

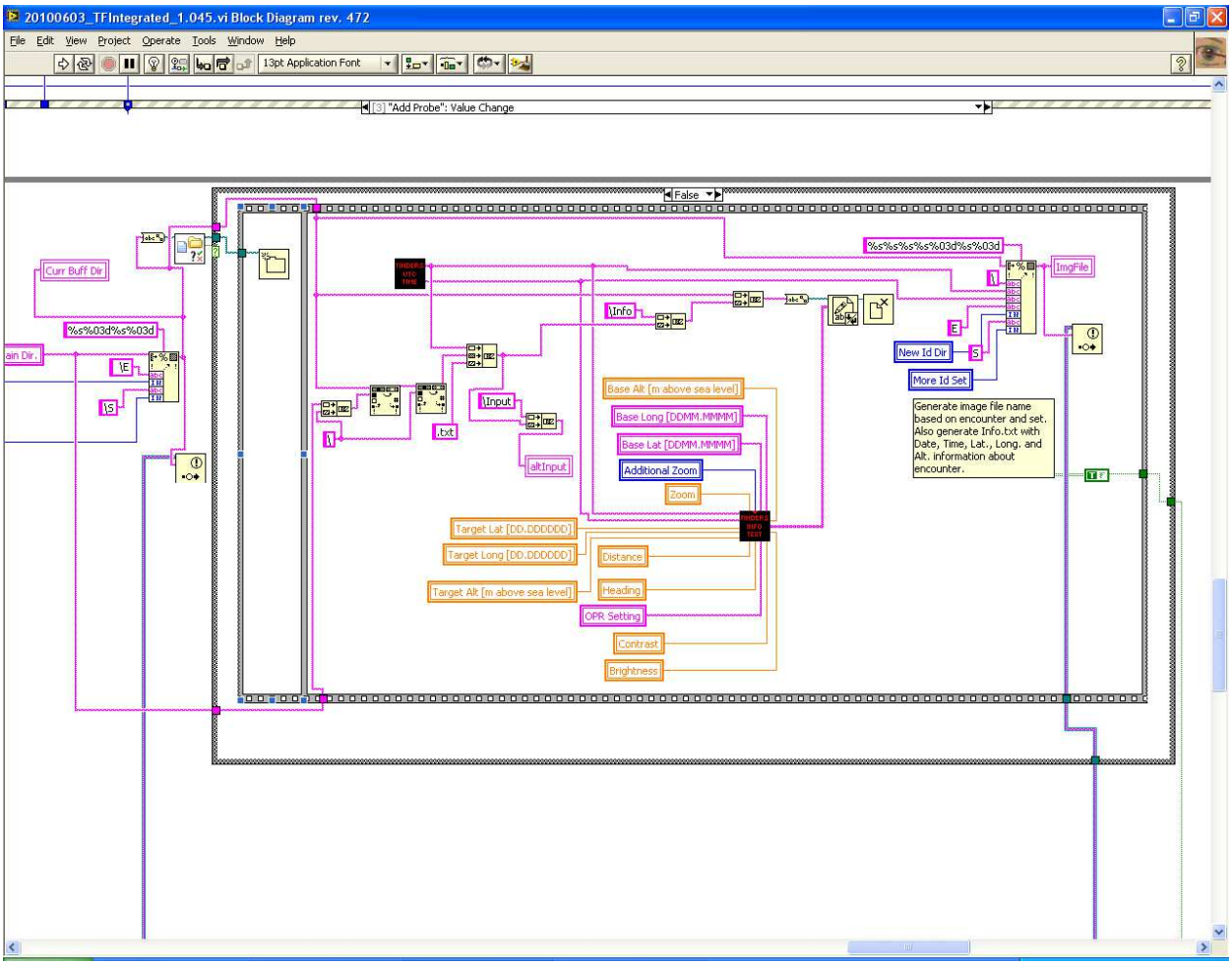


**Figure 70 Generate Filename and Text File for "Add Probe"**

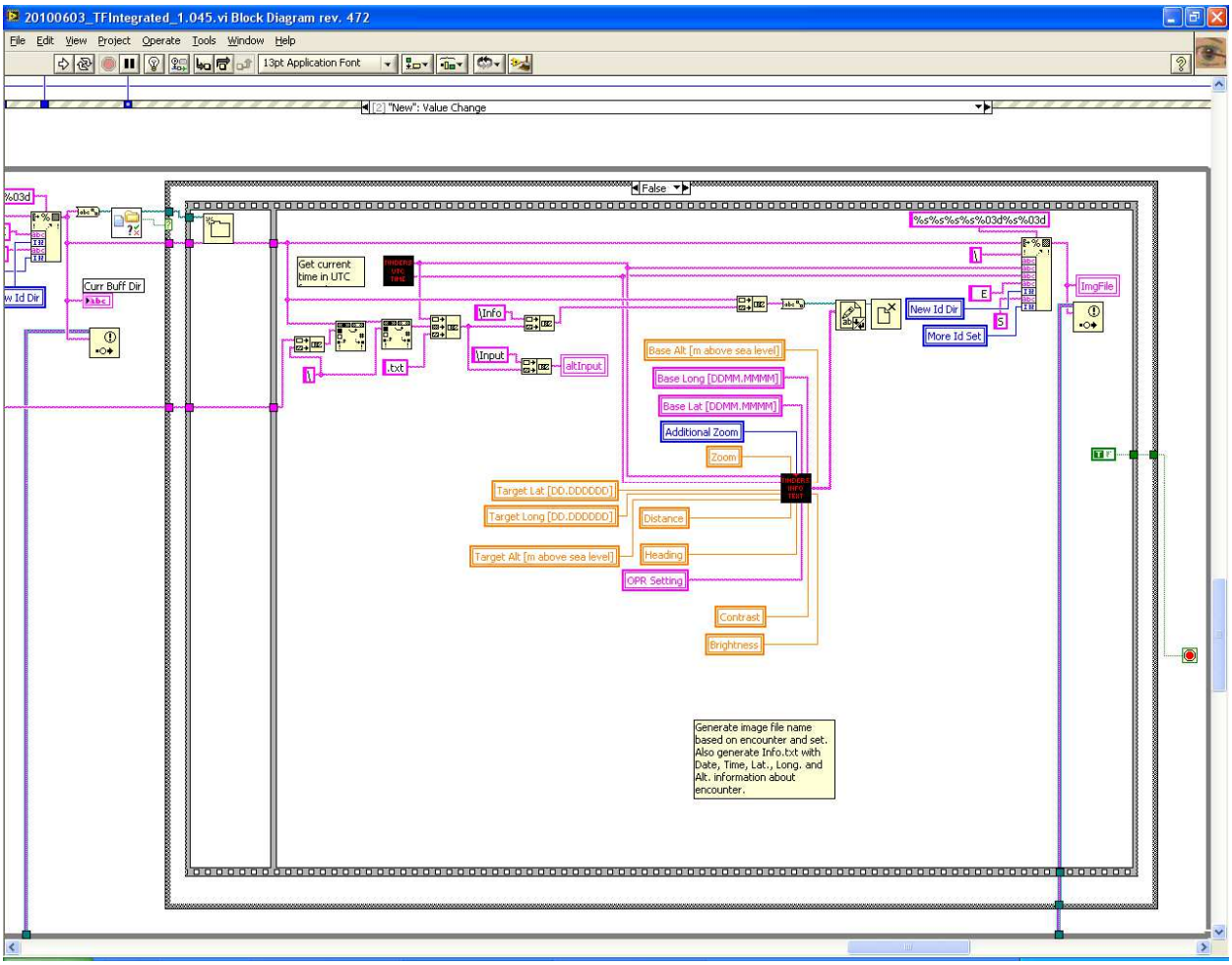


**Figure 71 Generate Filename and Text File for "New Encounter"**

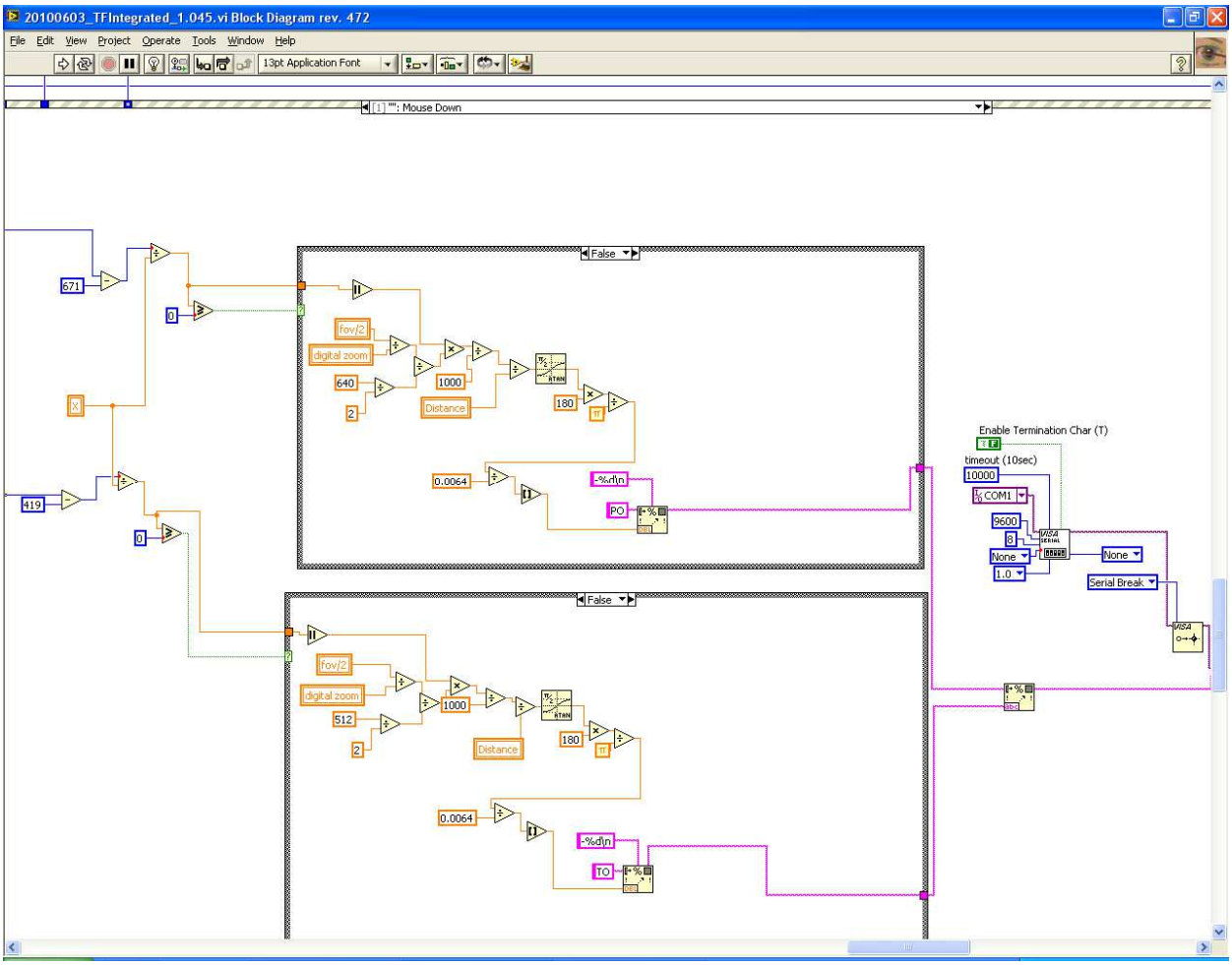


**Figure 72 PTU Commands**

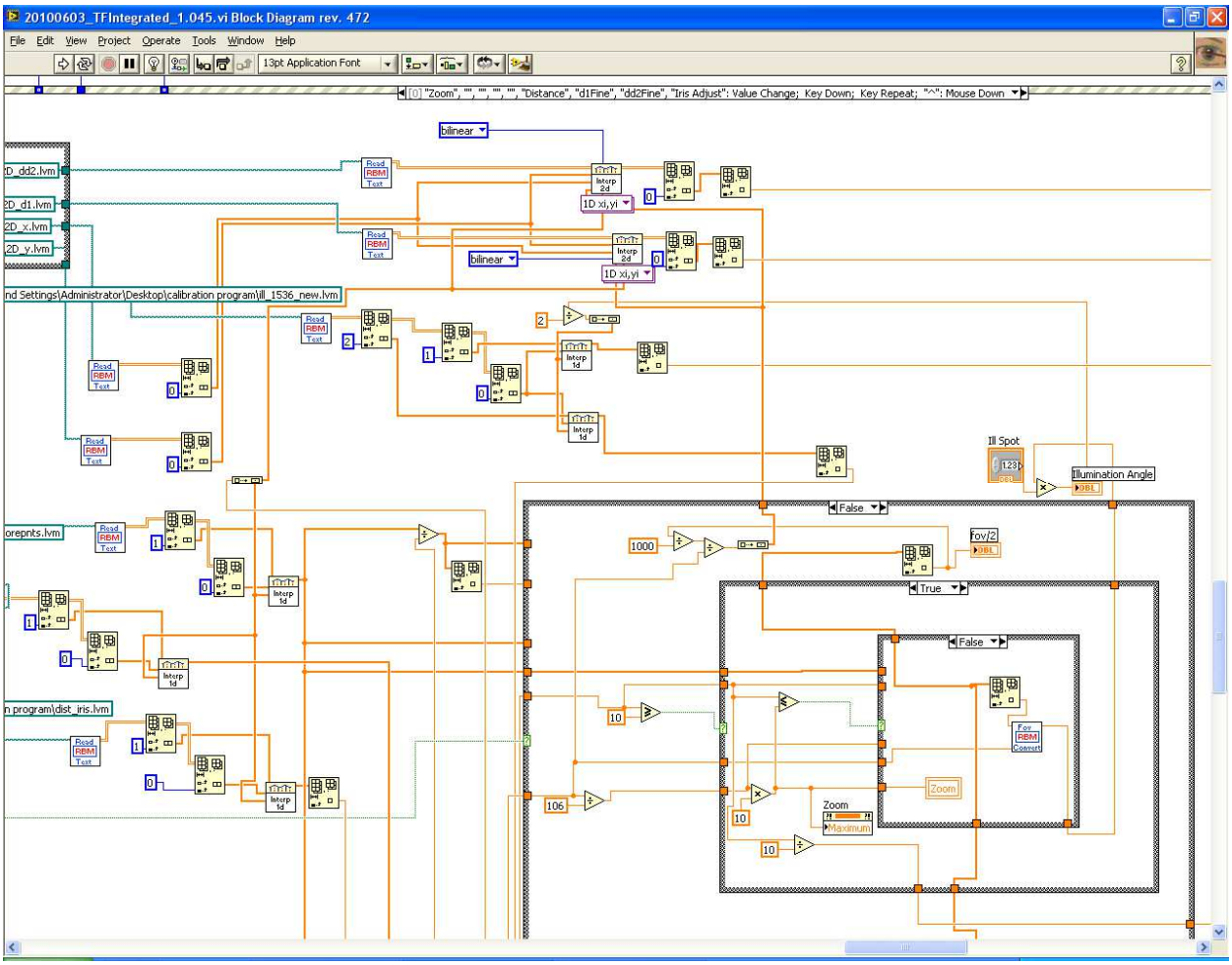


**Figure 73 Lookup Table Interpolation**

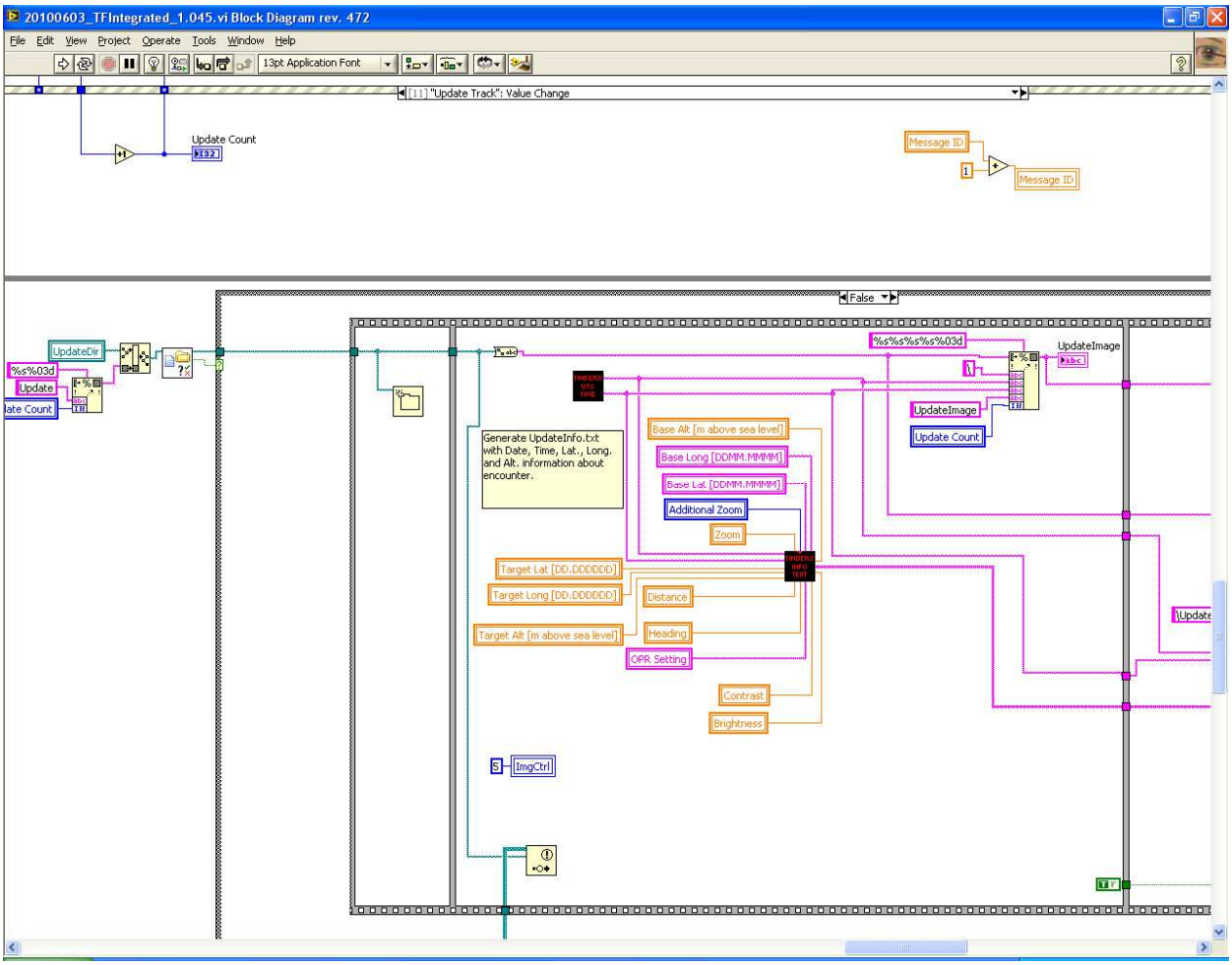


**Figure 74 Generate Filename and Text File for "Update Track"**

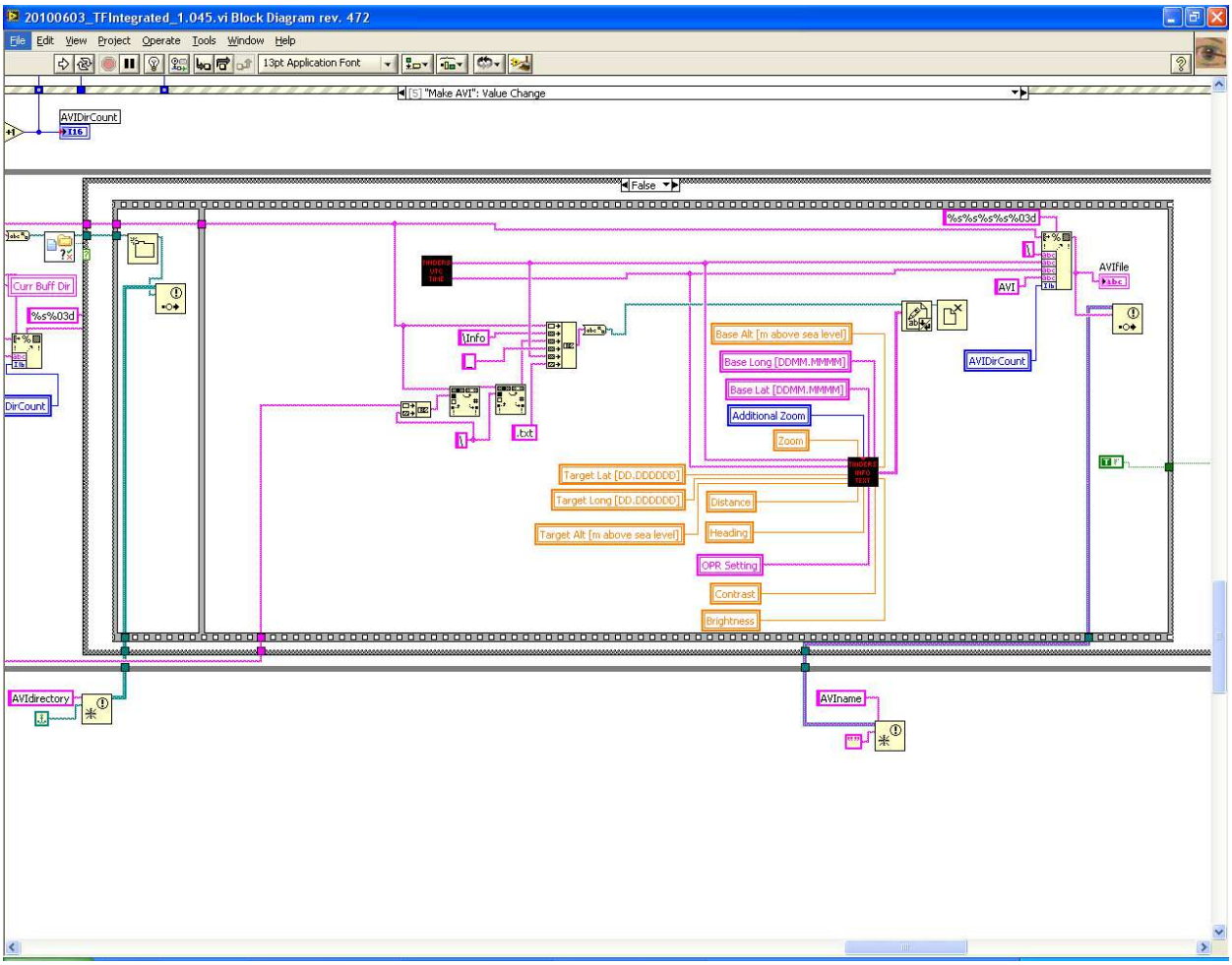


**Figure 75 Generate Filename and Text File for "Make AVI"**

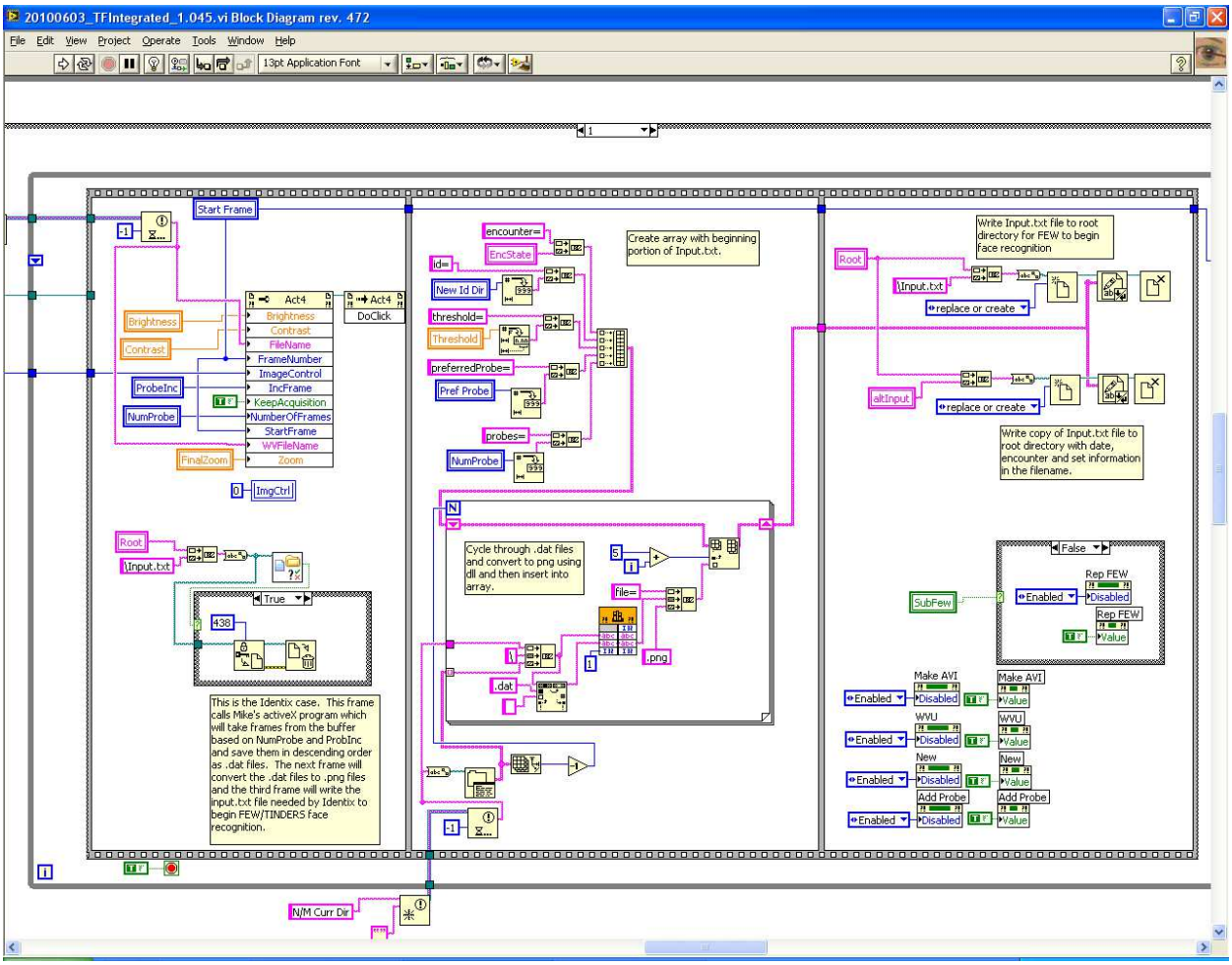


**Figure 76 Populate System Face Examiner**

## 6.3 Speckle Metric – Matlab Code

```
clear all

cd C:/Users/Roberto/Desktop/wvu/Spring2011/researchproject/050411   %get image
file = uigetfile({'*.jpg;*.png','All Image Files'});                %pop up dialog
rob=imread(file);                                                   %read image file

%select a row
figure('Name','Select a Row')                                       %New figure and set dialog
title
imshow(rob)                                                         %show image
h = impoint;
%input row value
pos = getPosition(h);
posy = pos(:,2);
posint = int16(posy);
close 'Select a Row'

%conversion
r=rob(posint,:);
x64=double(r)+1;
x64_2=double(rob)+1;

%whole image metric
strd_2=std2(x64_2);
mn_2=mean2(x64_2);
metric_2=strd_2/mn_2;

%line plot
strd=std(x64_2,0,1);
mn=mean(x64_2,1);
line_plot=strd./mn;

%Filter
[b,a]=butter(10,.25,'low');                                         %Get Butterworth filter
coef's
filted=filtfilt(b,a,line_plot);                                     %filter

%Line Metric
x64f=filtfilt(b,a,x64);
strd_mt=std(x64f);
mn_mt=mean(x64f);
metric=strd_mt/mn_mt;

%plots
t1=sprintf('Selected Line Metric: %f ; Whole Image: %f',metric,metric_2);
f=sprintf('%s',file);
figure('Name',t1)
subplot('Position',[.2 .8 .62 .15])     %top subplot
plot(filted)
axis tight
title('Standard Deviation/Mean by Columns')
subplot('Position',[-.54 0.08 2.1 .65])      %bottom subplot
imshow(rob)
x=[0 640];
y=[posint posint];
line(x,y,'Color','r','LineWidth',3)
xlabel(f)
```

## 6.4 WVU Data Collection

### 6.4.1 WVHTC Foundation Participant Contact Information Form


***Participant Contact Information***

**TINDERS ID Number:** _____

**Participant Name:** _____

**Participant Phone:** _____

**Participant e-mail:** _____

### 6.4.2 WVU Consent and Information Form


**CONSENT AND INFORMATION FORM**

TINDERS OMR ICF

**Principal Investigator:** Lemoff-WVHTCF, Brian
**Department:** Other Location
**Tracking Number:** H-20948

**Study Title:**

Tactical Imager for Night/Day Extended Range Surveillance (TINDERS)

**Co-Investigator(s):**

Dr. Brian Lemoff, Mr. Robert Martin, Ms. Christina Canonizado, Mr. William McCormick,Dr. Mikhail Sluch, Mr. Robert Ice, Mr. Brian Miller, Dr. Mary Ann Harrison, Mr. Fredric Bernal, Dr. Ayman Abaza, Dr. Hai-Shan Wu, Mr. Kristopher Kafka, Dr. Jeremy Dawson, Mr. Nathan Kalka, Dr. Simona Crihalmeanu, Dr. Thirimachos Bourlai, Dr. Bojan Cukic, Jessica Berry, Amanda Holbert, Jason Ice, Srimoyee Ray, Christopher Robison, Patrick Noll, Brandon Shaw, Chloe Snyder, Nnamdi Osia, Cameron Whitelam, Arvind Jagannathan, Kyle Smith, Michael Lyons, Neeru Nerang, Alicia Harmon, Katie Karmazyn, John Cordonier, Amber Goodwin, Lucas Rider, Jerin Young

**Sponsor**

Office of Naval Research (ONR) and National Institute of Justice (NIJ)

**Contact Persons**

In the event you experience any side effects or injury related to this research, you should contact Dr. Brian Lemoff at 304/333-6442. (After hours contact Dr. Brian Lemoff at 304/376-0962.)
If you have any questions, concerns, or complaints about this research, you can contact Dr. Brian Lemoff at 304/333-6442

For information regarding your rights as a research subject, you may contact the Office of

Research Compliance at 304/293-7073.

### Introduction

You, _____, have been asked to participate in this research study, which has been explained to you by _____. This study is being conducted by the West Virginia High Technology Consortium Foundation (WVHTCF) and WVU as part of the "Tactical Imager for Night/Day Extended Range Surveillance" (TINDERS) project to fulfill a contract with the Office of Naval Research (ONR), and part of the CITeR Co-Design Initiative, funded by the National Institute of Justice.

### Purposes of the Study

The purpose of the TINDERS project is to develop an infrared imaging system capable of tracking, imaging, and identifying people from a great distance. The data collected in this project will be used to develop infrared facial recognition and tracking algorithms, to validate facial recognition software, and to evaluate full system performance. A total of approximately 300 subjects are expected to participate in this study.

### Description of Procedures

For this study, you will be asked to schedule a 60-minute appointment at the WVU Engineering Science Building. During this appointment, you will be photographed with both visible and infrared cameras. Both still and video images may be recorded. Images may be taken at multiple angles and multiple zoom levels. In addition, you may be asked to stand at different locations, walk in different directions, and make specified movements while being imaged by an experimental infrared camera system. Infrared photography may be performed under different levels of lighting ranging from complete darkness to full daylight. Infrared photography will involve shining an invisible and eye-safe infrared light on your face.

### Risks and Discomforts

There are no known or expected risks from participating in this study.

## Alternatives

You do not have to participate in this study.

At the present time, there are no other alternatives studies in which you may participate.

## Benefits

You may not receive any direct benefit from this study. The knowledge gained from this study may eventually benefit others by enabling a new form of long-distance, night-time video surveillance technology. Such a technology would benefit the military, law enforcement, and private security services by allowing them to image and identify personnel at night at a long distance.

## Financial Considerations

In consideration for participation in this project, you will receive $40 worth of gift cards. These gift cards will be given to you at the conclusion of your appointment.

## Confidentiality

Any information about you that is obtained as a result of your participation in this research will be kept as confidential as legally possible. You will be assigned a unique ID number when you enroll in the project. All imagery, analysis, and associated data will make reference to this ID number, and your name will not be used. Anonymous still images, video images, analysis, and associated data will be used only by members of the research team, which may include the Office of Naval Research or other government agency, subcontractors and other external collaborating researchers. Unless you sign a separate release, all video and still imagery will be kept as confidential by WVHTC Foundation unless the data is subpoenaed by court order, inspected by the government customer, government agencies or regulatory authority or otherwise legally required by appropriate authorities. You may sign a separate release to permit your images to be used in presentations, publications, and other avenues of public disclosure.

## Voluntary Participation

Participation in this study is voluntary. You are free to withdraw your consent to participate in this study at any time. Refusal to participate or withdrawal will involve no penalty to you. In the event new information becomes available that may affect your willingness to participate in this study, this information will be given to you so that you can make an informed decision about whether or not to continue your participation. You have been given the opportunity to ask questions about the research, and you have received answers concerning areas you did not understand.

Upon signing this form, you will receive a copy.

I willingly consent to participate in this research.

| Signature of Subject or Subjects Legal Representative | Printed Name | Date | Time |
|---|---|---|---|

The participant has had the opportunity to have questions addressed. The participant willingly agrees to be in the study.

| Signature of Investigator or Co-Investigator | Printed Name | Date | Time |
|---|---|---|---|

### 6.4.3 WVHTC Foundation Consent to Public Release Form

WVHTC FOUNDATION | beyond expectations

**Consent to Public Release of**
**Photographic and Video Images**

I, _____, have been asked to participate in a research project, the Tactical Imager for Night/Day Extended Range Surveillance ("TINDERS"), facilitated by WVHTC Foundation, a non-profit corporation that utilizes original visible and infrared photographic and video images to advance the state of the art in facial recognition technology. By participating in the TINDERS project, I understand my body and facial photographic and video images will become available to project investigators, and with this release form, I further authorize the release of those images for future public disclosure, media release and/or analytical purposes by WVHTC Foundation, government agencies or other entities working with the images.

Accordingly, by signing below, I hereby grant the WVHTC Foundation the right to use my physical body and facial video or photographic image, whether or not recorded on or transferred to videotape, in TINDERS-related public disclosure, for media, research and/or analytical purposes.

Name (Please Print) Witness

_____ _____

_____ _____

Signature Signature

Date_____ Date_____

1000 Technology Drive • Suite 1000 • Fairmont, WV 26554 • 877-363-5482 • Local: 304-366-2577 • Fax: 304-366-2699 www.wvhtf.org

_____ _____

Initials Date

### 6.4.4 WVU Data Collection Sample Imagery

**Figure 77 WVU Data Collection Visible Spectrum Imagery**

**Figure 78 WVU Data Collection Visible Spectrum Imagery**


**Figure 79 WVU Data Collection SWIR Imagery**

## 6.5 System Video

The System video format does not conform to an industry standard. Accordingly, a Matlab GUI was developed to load a System video file, step frame-by-frame, select a frame to save, select a region to set the automatic contrast adjustment around, and save with a unique filename. Section 6.5.1 has the Matlab code for this and Figure 80 is a screenshot of this GUI. Once each SWIR probe image is extracted from the video, they are then submitted to the System Face Examiner for matching. Here, the scores are recorded in a spreadsheet and then converted to text format. Another Matlab script can then be utilized to generate the CMC curves discussed in Section 4.4.2. The Matlab code for this can be found in Section 6.5.2.

### 6.5.1 Matlab Code For System Video Frame Extraction

```
function tinders
% This GUI allows the user to step frame by frame through a System video
% file.  The user can then save the desired file.  The user must input two
% bounding box points to set the automatic contrast adjustment.

f = figure('Visible','off','Position',[360,500,650,485]);

%Use for file in other directory
%    FileSpec = 'E:\tinders study\*.tdv';
%    [fl,pth,ind]=uigetfile(FileSpec);

   % Use for file in working directory
   [fl,pth,ind]=uigetfile('*.tinders-video');
   sz=dir(fl);
   frames=1798;
%    frames=floor(sz.bytes/(512*640)/2);  %Use to auto detect frame amount

   subj=1401;                                              %Subject Number
   dist='70';                                              %used in filename
   name='1401';                                            %used in filename

   %  Construct the components.
   slid = uicontrol('Style','slider',...
          'Callback',{@frameslider_Callback},...
          'Max',frames-1,'Min',0,...
          'Position',[35,10,300,25],...
          'SliderStep',[.0005 .001]);                      %slider
   savebutt = uicontrol('Style','pushbutton','String','SAVE',...
          'Position',[545,220,70,25],...
          'Callback',{@savebutt_Callback});                %save button
   infoprint = sprintf('Subject # %s at %s m',subj,dist);%display info
   info = uicontrol('Style','text','String',infoprint,...
       'Position',[200,2,175,15]);
   ha = axes('Units','Pixels','Position',[35,40,500,450]);
   set([f,slid,ha,savebutt],...
   'Units','normalized');
   banner=imread('C:\tinders\paper\tinders banner.jpg');
   imshow(banner);               %display initial 'TINDERS!' banner
   % Assign the GUI a name to appear in the window title.
   set(f,'Name','Faceness File Selection')
   % Move the GUI to the center of the screen.
   movegui(f,'center')
   % Make the GUI visible.
   set(f,'Visible','on');


   function frameslider_Callback(hObject,eventdata,handles)
    x = get(hObject,'Value');                   %get slider value
    x = round(x);
    F=TDVread_decomp_offset(fl,x);              %read frame at slider value
    timestamp=now;
```

```
    filenm=sprintf('%s %f_LowDef.png',name,timestamp);  %create filename

    %if distance is greater than 150m, must zoom
    if dist > 150
    rect=[(320-(320/(dist/150))) (256-(256/(dist/150))) 640/(dist/150) 512/(dist/150)];
    crop=imcrop(F,rect);
    zoom=imresize(crop,dist/150);
    zoom_cont=tinders_cont(zoom,.55,.05);   %contrast adj
    imshow(zoom_cont(1:512,1:640),[]);
else
    f_cont=tinders_cont(F,.55,.05);
    imshow(F,[0 4095])
    end
      handles=guihandles(hObject);          %take care of slider
      handles.x=x;
      guidata(hObject,handles);             %set value to handles
   end

   function savebutt_Callback(hObject,eventdata,handles)
     handles=guidata(gcbo);                 %recall slider value
     x=handles.x;
    [blah fl_length]=size(fl);
    F=TDVread_decomp_offset(fl,x);          %read frame number at slider value

    %if distance is greater than 150m, must zoom
if dist > 150
    rect=[(320-(320/(dist/150))) (256-(256/(dist/150))) 640/(dist/150) 512/(dist/150)];
    crop=imcrop(F,rect);
    zoom=imresize(crop,dist/150);
    timestamp=now;
    filenm=sprintf('%s %sm %f_LowDef.png',name,dist,timestamp);
    filenm_high=sprintf('%s %sm %f_HighDef.png',name,dist,timestamp);
    zoom_cont=tinders_cont_save(zoom,.96,.01);  %contrast adj
    zoom_cont(zoom_cont>=256)=255;
    imwrite(uint8(zoom_cont(1:512,1:640)),filenm,'BitDepth',8);
    imwrite(F,filenm_high,'BitDepth',16);
else
    timestamp=now;
    filenm=sprintf('%s %sm %f_LowDef.png',name,dist,timestamp);
    filenm_high=sprintf('%s %sm %f_HighDef.png',name,dist,timestamp);
    f_cont=tinders_cont_save(F,.96,.01);    %contrast adj
    f_cont(f_cont>=256)=255;
    imwrite(uint8(f_cont),filenm,'BitDepth',8);
    imwrite(F,filenm_high,'BitDepth',16);
end
   end
 end
```

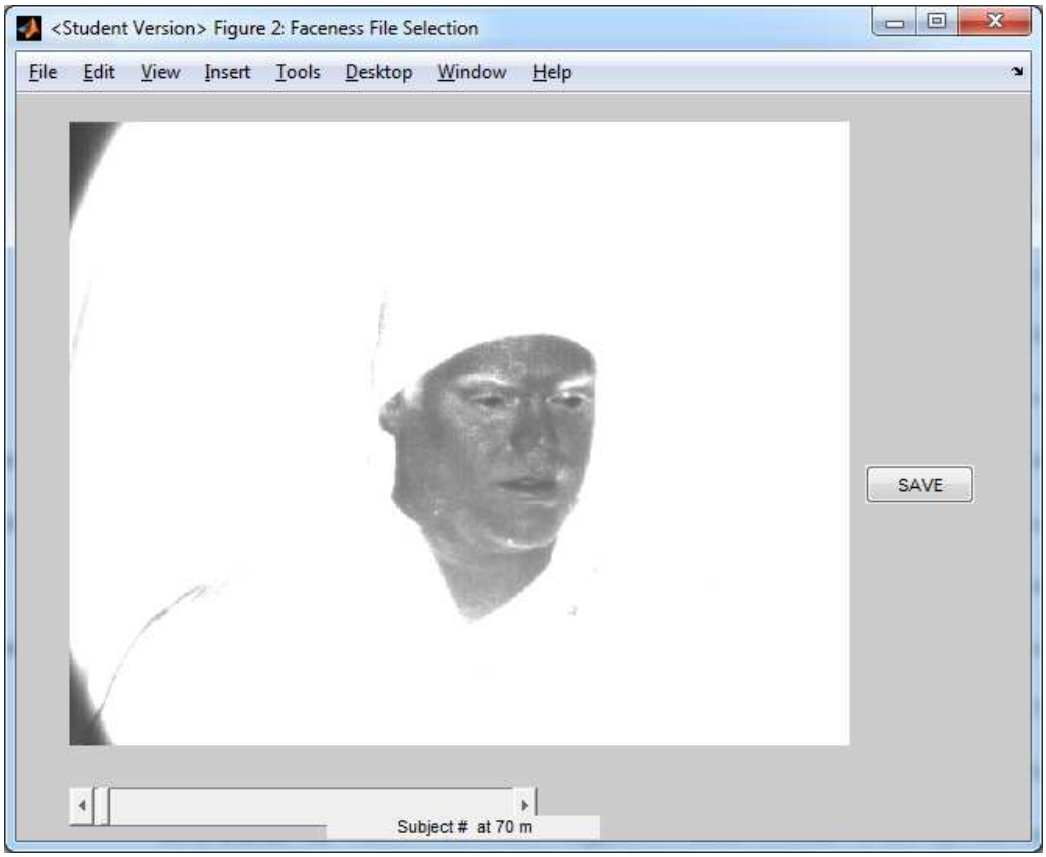


**Figure 80 System Video Frame Tool**

**This GUI allows the user to cycle through a System video file frame-by-frame and save a single image.**

### 6.5.2 Matlab Code For CMC Generation

```
clear all

% open text file where column 1 is subject #, 2 is max rank, 5 is vote rank
fid = fopen('A17.txt');
C = textscan(fid, '%f %f %f %f %f %f %f');  %build C from text file
fclose(fid);

%pick max = C{2}, vote = C{5}
clear x
c=C{2};         %read specific column of C depending on if max or vote scoring
[m,n]=size(c);
x=zeros(1,m+1);

% Build Histogram
for i=2:35
h=find(c==i-1);
hs=size(h);
x(i)=hs(1);
end
% Cumulative Match Characteristic (a running summation)
for i=1:m+1
   T(i)=sum(x(1:i));
end

norm=T/m;
plot(0:1:m,norm,'-*g','linewidth',3)
hold on
axis([0 m 0 1])
grid on
```

```
title('Cumulative Match Characteristic at 160m')
xlabel('Rank')
ylabel('Probability of Match')
```

# 7 Bibliography

[1] http://www.sensorsinc.com/images.html

[2] http://www.intechopen.com/books/advanced-biometric-technologies/normalization-of-infrared-facial-images-under-variant-ambient-temperatures

[3] Lemoff, B., Martin, R., Sluch, M., Kalka, K., Dolby, A., Ice, R. (2014). Automated, Long-Range, Night/Day, Active-SWIR Face Recognition System. *Proceedings SPIE 9070, Infrared Technology and Applications XL.*

[4] Martin, R., Sluch, M., Kalka, K., Dolby, A., Ice, R., Lemoff, B. (2014). Fusion-Based Approach for Long-Range Night-Time Facial Recognition. *Proceedings SPIE 9090, Automated Target Recognition XXIV.*

[5] Lemoff, B., Martin, R., Sluch, M., Kalka, K., McCormick, W., Ice, R. (2013). Long-Range Night/Day Human Identification Using Active-SWIR Imaging. *Proceedings SPIE 8704, Infrared Technology and Applications XXXIX.*

[6] Lemoff, B., Martin, R., Sluch, M., Kalka, K., McCormick, W., Ice, R. (2013). Automated Night/Day Standoff Detection, Tracking, and Identification of Personnel for Installation Protection. *Proceedings SPIE 8711, Sensors, and Command, Control, Communications, and Intelligence (C3I) Technologies for Homeland Security and Homeland Defense XII.*

[7] Martin, R., Sluch, M., Kalka, K., Ice, R., Lemoff, B. (2013). Active-SWIR Signatures for Long-Range Night/Day Human Detection and Identification. *Proceedings SPIE 8711, Active and Passive Signatures IV.*

[8] Saleh, B. E. A., Teich, M. C. (2007) *Fundamentals of Photonics.* Hoboken, New Jersey: John Wiley & Sons, Inc..

[9] http://www.thorlabs.com/thorcat/TTN/50-1550A-AutoCADPDF.pdf

[10] Pan, Z., Healey, G., Prasad, M., Tromberg, B. (2003). Face Recognition in Hyperspectral Images. *IEEE Transactions on Pattern Analysis and Machine Intelligence,* 25(12), 1552-1560.

[11] Bourlai, T., Kalka, N., Ross, A., Cukic, B., Hornak, L. (2010). Cross-spectral Face Verification in the Short Wave Infrared (SWIR) Band. *International Conference on Pattern Recognition.* 1343-1347.

[12] Kalka, N., Bourlai, T., Cukic, B., Hornak, L. (2011). Cross-spectral face recognition in heterogeneous environments: A case study on matching visible to short-wave infrared imagery. *IEEE International Joint Conference on Biometrics Compendium.* 1-8.

[13] Chang, H., Koschan, A., Abidi, M., Kong, S., Won, C. H. (2008). Multispectral Visible and Infrared Imaging for Face Recognition. *Computer Vision and Pattern Recognition Workshops.* 1-6.

[14]http://www.morphotrust.com/IdentitySolutions/ForFederalAgencies/Officer360/Investigator360/ABIS/FaceExaminerWorkstation.aspx

[15] http://encyclopedia2.thefreedictionary.com/speckle

[16] Iwai, T., Asakura, T. (1996). Speckle Reduction in Coherent Information Processing. *Procedings of the IEEE*, 84(5), 765-781.

[17] http://www.light-speed-tech.com/documents/FiberShaker.pdf

[18] http://en.wikipedia.org/wiki/Laser_safety

[19] IEC 60825-1, *International Standard,* (2007). Geneva, Switzerland.

[20] http://www.autodesk.com/products/inventor/overview

[21] Joshi, K. R., Kamathe, R. S. (2008). SDI: New Metric for Quantification of Speckle Noise in Ultrasound Imaging. *Workshop on Multimedia Signal Processing.* 122-126.

[22] http://oequest.com/getproduct/19413/cat/1722/page/1

[23] Chaplin, Martin. "Water Absorption Spectrum." Water Structure and Science. Creative Commons Attribution, 7 March 2013. Web. 24 October 2014. <http://www.lsbu.ac.uk/water/vibrat.html>